

AUGMENTED CUCKER-SMALE FLOCKING MODEL
WITH COLLISION AVOIDANCE, FINITE-TIME
CONTROL AND CHORUS-LINE EFFECTS

A THESIS SUBMITTED TO AUCKLAND UNIVERSITY OF TECHNOLOGY
IN PARTIAL FULFILMENT OF THE REQUIREMENTS FOR THE DEGREE OF
DOCTOR OF PHILOSOPHY

Supervisors

Professor Edmund M-K Lai

Associate Professor Tom Moir

June 2019

By

Jing Ma

School of Engineering, Computer and Mathematical Sciences

Declaration

I hereby declare that this submission is my own work and that, to the best of my knowledge and belief, it contains no material previously published or written by another person nor material which to a substantial extent has been accepted for the qualification of any other degree or diploma of a university or other institution of higher learning.

Signature of student

Acknowledgements

I sincerely thank my supervisor, Professor Edmund Lai, for his tremendous inspiration and support over the past four years. He stimulated my passion in research and supervised me to successfully achieved my research dream. Under his supervision, I learned not only how to conduct research but also how to communicate scientific ideas. I wish to express my gratitude and indebtedness to him for his helpful guidance and follow up of my work during its development.

I would like to thank my co-supervisor, Associated professor Tom Moir for his encouragement and patience. I appreciate Professor Wai Kiang (Albert) Yeap for inspiring me and teaching me valuable lessons in critical thinking. I also thank Dr Farhaan Mirza for his valuable comments and suggestions on my PhD journey, which subsequently led to fruitful research outcomes. Dr Khalid Arif gave insightful suggestions during my time at Massey University.

I also express my warmest thanks to Bumjun Kim, Saide Lo and Brian Gonzales for their support during my time at AUT. Many thanks must also go to Dianne Cook and Gang Cao who made my first year much more enjoyable.

Furthermore, I am pleased to thank my fellow students at AUT Tower 404 for their friendship and many meaningful conversations: Aminu Bello Usman, Chamari Kithulgoda, Reza Moosavi Mohseni, Su Shu, Maojun Wang, Wenwang Pang, Nawal Chanane, Herman Masindano Wandabwa and Khavee Botangen.

Finally, I am also fortunate to have the most supportive family. They always encouraged me to be "strong" and to get things done.

Abstract

Cucker-Smale model is a velocity alignment model that has been used to study the emerging behaviour of flocking of multiple self-propelled agents. It has been studied from many different perspectives. In this thesis, several issues that will impact deployment of this model to real physical agents such as robots are studied.

The first issue relates to whether the Cucker-Smale model is actually a flocking model. A technical definition of flocking that involves velocity alignment and a concept introduced here called flock diameter is first proposed. While the original Cucker-Smale model can produce velocity alignment, it has been shown to be inadequate in controlling the flock diameter. There is also no guarantee that collisions among agents will not occur. A new augmented Cucker-Smale model is proposed that can potentially be used to control the flock diameter and to prevent agent collisions. This augmented model is based on the use of cohesive and repulsive forces and is simpler in form compared with similar models in the literature. A bounded symmetric cohesion and repulsion function is also proposed to be used with this model. Its boundedness allows it to be implemented in real systems and therefore more practical than unbounded repulsive forces proposed in existing literature.

The second issue relates to how fast the Cucker-Smale system could achieve flocking from a random initial configuration. In order to derive an upper bound on the flocking time, finite-time control is applied to the augmented Cucker-Smale model. We are able to mathematically prove that this finite-time controlled model converges both

asymptotically and in a finite time. Simulation confirmed that the results are correct although this bound is not tight. It has also been discovered that the finite-time control parameters should be at the lower end of the allowable range in order to obtain the best flocking times.

The third issue is to do with the fact that the clocks of physical agents are typically not synchronized. A block-sequential approach, rather than random delay used in existing literature, is used to model the fact that each agent's state is updated or computed at regular time intervals according to its own clock. Simulations show that asynchronicity does increase the flocking time in a significant way. Furthermore, results seem to suggest that this added time is relatively immune to the degree of asynchronicity as the size of the flock becomes larger.

The fourth issue is related to the uncertainty in estimating a neighbour's velocity and the round-off errors in computation. These are modelled as additive noise to the update equation of the model. It is confirmed that a small amount of noise reduces the velocity alignment time. However, large noise could destabilize the system.

The remaining two issues are associated with perturbation to the flocking state. They are related to a leader-follower Cucker-Smale system where there is a leader agent and the rest of the agents use the Cucker-Smale update method to align with the leader. In the context of human-swarm or human-flock interaction, we need to know how often could a human operator issue change-of-direction commands to the flock without it becoming dispersed. Our study shows that the realignment time could be used as a design guide for neglect benevolence. If change-of-direction commands are issued too frequently, the cohesiveness of the flock will be destroyed. The second is based on an observed phenomenon known as the chorus-line effect. It is also a sudden change in direction initiated by one or a few birds. But the speed by which the rest of the flock follows this change appears like to speeding propagating wave. Previous research on the chorus-line effect that has been observed in bird flocks used the wave propagation

approach. However, this approach could not be transformed into an agent-based model for implementation. An adaptation of the Cucker-Smale model, called the CS-CL model, to incorporate the chorus-line effect is proposed for the first time. Simulations show that realignment times could be reduced using this model.

Publications

Flock Diameter Control in a Collision-Avoiding Cucker-Smale Flocking Model

J. Ma and E. M.-K. Lai, Advances in Swarm Intelligence. ICSI 2017. Lecture Notes in Computer Science, Vol. 10385. Springer, 2017, pp.31–39. DOI:[10.1007/978-3-319-61824-1](https://doi.org/10.1007/978-3-319-61824-1)

Cucker-Smale Flocking Under Asynchronous Update Dynamics

J. Ma and E. M.-K. Lai, Proceedings of International Conference on Agents (ICA), 2017, pp.50-54. DOI:[10.1109/AGENTS.2017.8015300](https://doi.org/10.1109/AGENTS.2017.8015300)

Finite-time Flocking Control of A Swarm of Cucker-Smale Agents with Collision Avoidance

Proceedings of 24th International Conference on Mechatronics and Machine Vision in Practice (M2VIP), 2017, 6 pages. *Best Paper Award*. DOI:[10.1109/M2VIP.2017.8211507](https://doi.org/10.1109/M2VIP.2017.8211507)

CS-CL: A Flocking Model That Incorporates the Bio-inspired Chorus-Line Effect

J. Ma, E. M.-K. Lai and W. W. Pang, Proceedings of IEEE International Joint Conference on Neural Networks (IJCNN), 2018, 6 pages. DOI:[10.1109/IJCNN.2018.8489207](https://doi.org/10.1109/IJCNN.2018.8489207)

Incorporating Chorus Line Effect into A Cucker-Smale System for Fast Manoeuvre Tracking

J. Ma and E. M.-K. Lai, Proceedings of the 17th International Conference on Autonomous Agents and MultiAgent Systems(AAMAS), 2018, pp.2007-2009.

On the Timing of Operator Commands for the Navigation of Robot Swarms

J. Ma, E. M.-K. Lai and J. Ren, Proceedings of 15th IEEE International Conference on Control, Automation, Robotics and Vision (ICARCV), 2018, pp.1634-1639. DOI:[10.1109/ICARCV.2018.8581236](https://doi.org/10.1109/ICARCV.2018.8581236)

Contents

Declaration	2
Acknowledgements	4
Abstract	5
Publications	9
1 Introduction	16
1.1 Background and Motivation	16
1.2 Aims and Objectives	20
1.3 Original Contributions	22
1.4 Organization of Thesis	24
2 Review of Flocking Models and Flocking Control	25
2.1 Flocking Phenomena in Nature	25
2.2 Basic Flocking Models	26
2.2.1 Boids Model	26
2.2.2 Vicsek Model	27
2.2.3 Cucker-Smale Model	30
2.2.4 Couzin Model	35
2.3 Flocking Control	37
2.3.1 Leader-follower and Leaderless Flocking Control	38
2.3.2 Time-constrained Flocking Control	42
2.4 Summary	44
3 Cohesion and Collision Avoidance	46
3.1 Some Definitions	47
3.2 Flocking With the Original Cucker-Smale Model	49
3.2.1 Effect of Communication Rate on Alignment Time	51
3.2.2 Need for Cohesion	52
3.2.3 Need for Repulsion	59
3.3 An Augmented Cucker-Smale Model	62
3.3.1 Unbounded Repulsion and Bounded Cohesion Forces	63
3.3.2 Unbounded Cohesive and Bounded Repulsive Forces	65

3.3.3	Symmetric Bounded Cohesive and Repulsive Forces	66
3.4	Summary	68
4	Finite-time Flocking Control	71
4.1	Preliminaries	71
4.2	Main Results	74
4.2.1	Asymptotic Convergence	74
4.2.2	Finite-time Convergence	77
4.2.3	Flock Diameter	81
4.3	Simulation	83
4.3.1	Flocking Time and Flock Diameter	84
4.3.2	Effects of Control Parameters	86
4.4	Summary	88
5	Asynchronous Update Dynamics	90
5.1	Methodology	91
5.2	Simulation Results	93
5.2.1	Synchronous Updates With Different Initial Speeds	94
5.2.2	Asynchronous Updates with Original Cucker-Smale Model	94
5.2.3	Asynchronous Updates with Augmented Cucker-Smale Model	96
5.3	Summary	97
6	Perturbations to the System	99
6.1	Effects of Noise on Alignment Time	99
6.2	Timing of Operator Commands	101
6.2.1	Model of Human-Swarm Interaction	104
6.2.2	Operator Control	105
6.2.3	Leader-follower Flocking	105
6.2.4	Neglect Benevolence	106
6.2.5	Simulation Design and Results	107
6.3	Chorus-Line Effect	114
6.3.1	The CS-CL Model	115
6.3.2	Performance Evaluation	117
6.4	Summary	125
7	Conclusions	126
7.1	Summary of Contributions	126
7.1.1	Concept of Flock Diameter	126
7.1.2	Augmented Cucker-Smale Model	127
7.1.3	Bounded Cohesive and Repulsive Forces	127
7.1.4	Finite-time Control of the Augmented Cucker-Smale Model	127
7.1.5	Effects of Asynchronous Updates	128
7.1.6	Noise	128
7.1.7	Neglect Benevolence	128

7.1.8	Cucker-Smale Model with Chorus-line Effect	129
7.2	Future Directions of Research	129
References		131
Appendices		146
A	Proof of Lemmas	147
A.1	Proof of Lemma 4.3	147
A.2	Proof of Lemma 4.2	148

List of Tables

3.1	Alignment Times	51
3.2	Alignment Times for Different Values of β	52
3.3	Flock Diameter for Different Values of β and Flock Size	53
3.4	Flock Diameter with Different Cohesive Force Coefficients (k)	58
3.5	Minimum Distance between Any Two Agents	60
3.6	Distances between Any Two Agents	62
3.7	Distances between agents after 10 seconds	62
3.8	Flock Diameter for Different Values of d_1 with $M = 1$	67
3.9	Flock Diameter for Different Values of M	68
4.1	Agents Flock Diameter when Finite-time Control Applied	86
4.2	Flocking Times with Different Values of the Parameters	86
4.3	Flocking Times with Different $\theta = 0.5$	88
5.1	Alignment Time with Asynchronous Updates	96
5.2	Flock Diameter with Asynchronous Updates	96
5.3	Flock diameters in synchronous and asynchronous updates	96
6.1	Maximum inter-robot distance at: initial stage (I), after realignment with leader's heading change of $\pi/6$ (II).	109
6.2	Inter-robot distance at instants of change of leader's direction for six robots	110
6.3	Inter-robot distance at instants of change of leader's direction for 21 robots.	112

List of Figures

2.1	Three different zones in the Couzin model	35
3.1	Average Velocity versus Time	48
3.2	Alignment Time of the Original Cucker-Smale Model	50
3.3	Alignment Time with Two Different Values of $\beta \leq 0.5$	53
3.4	Average Velocity with Two Different Values of $\beta > 0.5$	54
3.5	An Example of Cohesive Force Function	56
3.6	Flock Diameter for Different Cohesive Force Coefficients	57
3.7	Flock Diameters for $k = 0$	58
3.8	Flock Diameters for $k = 1$	59
3.9	An Example of Repulsive Force Function	60
3.10	Average Velocity with Unbounded Repulsive Force	61
3.11	The Unbounded Repulsive and Bounded Cohesive Force Function	64
3.12	Symmetric Cohesive and Repulsive Force Functions	67
3.13	Flocking Time in Different Parameters	69
4.1	Flocking Time With and Without Finite-time Control for the Augmented Cucker-Smale System	84
4.2	Upper Bound on Flocking Time vs Simulated Time for the Finite-time Controlled Augmented Cucker-Smale System	85
4.3	Finite Flocking time with Different Parameters	87
4.4	Finite Flocking time in Different M	88
5.1	Block-sequential Updates in an Asynchronous Dynamic System	92
5.2	Subgroups in Asynchronous Dynamic System	92
5.3	Alignment Time with Synchronous Update for the Original Cucker-Smale Model	95
5.4	Velocity Alignment Time with Asynchronous Updating for Original Cucker-Smale Model	97
5.5	Flocking Times for Synchronous and Asynchronous Updates with Augmented Cucker-Smale Model	98
6.1	Alignment Time with Different Noise	101
6.2	Human-Swarm Interaction Control System	104
6.3	Realignment Time for Heading Change of $\pi/6$	108

6.4	Effect on the average velocity of 11 robots with periodic leader heading changes	111
6.5	Effect on the average velocity of 51 robots with periodic leader heading changes	113
6.6	Illustration of realignment with the chorus-line effect	116
6.7	Observing range of chorus-line effect	118
6.8	Comparison of Realignment Times for CS and CS-CL Models	119
6.9	Realignment Times with Different Amount of Heading Change	120
6.10	Realignment Times with Different Relaxation Times	120
6.11	Progression of Heading Changes of Individual Agents with CS-CL Model for $N = 5$	121
6.12	Progression of Heading Changes of Individual Agents with CS Model for $N = 5$	122
6.13	Computed and Simulated Finite Realignment Times	123
6.14	Comparisons of Simulated Realignment Times	124
6.15	Progression of Heading Changes of Individual Agents with Finite-time Controlled Cucker-Smale Model with $N = 5$	124

Chapter 1

Introduction

The subject matter of this thesis is the emergent collective behaviour known as flocking of a group of autonomous agents. The main motivation of this research is to move the study of this phenomena from purely theoretical modelling toward practice. Therefore the aims and objectives of this research project are related to extending a popular flocking model in directions that make it realizable.

1.1 Background and Motivation

The collective and cooperative behaviours of living things large and small, such as birds, fish, ants, bees, locusts, wildebeest, and even bacteria are often observed in nature [1–3]. They do so to gain certain advantages which are important to their survival. These include enhancing their ability to avoid predators, to find food, to explore an unknown space, and to lift and move objects much heavier than their individual weight. It has been shown that a coordinated group of agents, also referred to as a swarm, with limited individual abilities can potentially accomplish more complex tasks which an individual cannot achieve [4].

It is interesting to note that a number of these emergent collective behaviours are

the result of self-organization based only on each agent's local interactions without centralized coordination or control. In [5], the author discussed how dissimilar oscillators become synchronized through interactions between an agent and its neighbours. This effect is exhibited in the various physical, biological, and chemical systems. Furthermore, the agents involved typically possess very limited processing and sensing abilities such as fireflies and bacteria. Inspired by these phenomena, the study of the emerging behaviour of swarm systems has become an active area of research in recent years [6–8].

The idea of using local interactions to perform coordinated motion or accomplish coordinated tasks for a large number of robots with limited capabilities is a very attractive one [9, 10]. The lack of centralized control makes it possible to overcome the communication bottleneck when a massive number of robots are deployed. With distributed and decentralized control, the system becomes more flexible, scalable and robust to individual malfunction. Potential applications include disaster rescue missions [11, 12], space exploration [13, 14], mining [15], agricultural foraging, and military tasks [16, 17]. In the early 2000's, the European Commission, under its Future and Emerging Technologies program, funded a large research project called SWARM-BOTS. Its aim was to study new approaches to the design and implementation of self-organizing and self-assembling insect-like robots and to study how it could adapt to their two-dimensional environments [18, 19]. This project was succeeded by the Swarmanoid project which extended the study to three-dimensional environments [20]. Other major projects include the Engineering Swarm Intelligence Systems (E-SWARM) project which was funded by the European Research Council for a period of five years from 2010 [21, 22].

Flocking is one of the most fundamental forms of collective self-organized swarm behaviour [23]. It occurs when a large number of autonomous agents move together in the same direction, at the same speed and maintains a cohesive formation. Each agent

adjusts its own velocity by observing and estimating the relative positions and velocities of the agents in its neighbourhood. In some systems, this type of local information could be obtained through explicit peer-to-peer or broadcast communication between nearby agents. In order to achieve flocking for a group of man-made agents, the underlying laws that govern this behaviour need to be understood. The first researchers who studied flocking from a theoretical perspective are physicists. Vicsek *et al.* [1] studied inter-agent velocity alignments in a particle system moving at constant speed and came up with a set of discrete-time update equations for the direction of motion and position for each agent. Toner *et al.* [24] presented a quantitative continuum approach, and Shimoyama *et al.* [25] introduced deterministic kinetic equations of motions for interacting elements which describe various collective behaviours using a network with all-to-all links. These and further investigations have led to the development of several models of flocking. The four most significant ones – boids, Vicsek, Cucker-Smale, and Couzin models, are reviewed in Section 2.2. These models allow us to study the parameters that govern this behaviour and are the basis of most of the research in this area.

Among the four flocking models mentioned above, the Cucker-Smale and Vicsek models have attracted the most attention. The Cucker-Smale has the advantage that it is a continuous-time model and therefore a wider range of mathematical tools are available for its analysis. Cucker and Smale proved mathematically that their flocking model can achieve velocity alignment of the agents unconditionally based only on a parameter in the interaction function between agents [26]. The fact that the flocking state can be reached independent of the initial configuration is significant. However, there are two main issues if one is to implement this model on real physical agents such as robots. The first one relates to the fact that the Cucker-Smale model is strictly speaking a velocity consensus model rather than a flocking model. This is because there is no built-in mechanism in the model to keep the agents moving close to each

other as a flock should. Furthermore, there is nothing in the model that will prevent the agents from colliding with each other. Some research works have focused on revising the original Cucker-Smale model to provide collision avoidance and cohesion among agents [27–30]. But these schemes typically involve functions that are unbounded in magnitude. Therefore they are not realizable in practice. An augmented Cucker-Smale model that only make use of finite bounded functions is needed.

The second issue is the time it takes to achieve velocity alignment. The underlying synchronization problem can be solved by a type of distributed algorithms known as consensus algorithms. It has received considerable research efforts and various consensus algorithms have been developed for different scenarios [31–34]. Most of them have been proven to converge to an agreement asymptotically [31]. The Cucker-Smale model is no exception although in practice we know that if the system converges, it converges within a finite amount of time. In many real-world applications, we often need to know how long it takes in the worst case for the system to achieve flocking. In other words, an upper bound on the flocking time under some mild conditions is required. A control mechanism known as finite-time control has recently been developed [35, 36]. It has been applied to the original Cucker-Smale model. However, how it may work with an augmented Cucker-Smale model with cohesion and collision avoidance remains unknown.

Another issue regarding the implementation of Cucker-Smale model based robotic systems is that the robots do not share a common clock. Consequently, they do not update their states at the same time. Since simulation studies typically compute these updates at the same simulation time, how this will affect flocking and the flocking time will need to be determined. An analysis on this issue for a modified Vicsek model has been conducted in [37]. For the Cucker-Smale model, a slightly different problem related to intermittent communication between agents was studied in [38]. The effect of time delay for the Cucker-Smale model is analyzed in [39]. These studies typically

assume that the time delay is governed by some random distribution. However, for real implementations, it is often the case that the updates are computed regularly for each agent except that their clocks are not synchronized. So it is different from having a randomly distributed update time. The effects of unsynchronized clock will also need to be studied for the augmented Cucker-Smale model with finite-time control discussed above.

All leaderless flocking models adjust an individual agent's velocity by averaging those in its neighbourhood. If one of the agents suddenly make a big change in its velocity, it will slowly be brought back to alignment through this averaging process. But there could be valid reasons for this sudden change in direction. For example, one of the members of the flock may sense danger from a predator and wants to escape. In nature, it has been observed that the rest of the flock reacts to this kind of sudden change in direction in a manner that is faster than the normal alignment process. This has become known as the chorus-line hypothesis [40,41]. Some effort has been made in modelling this phenomenon in terms of propagating speed waves [42]. But if this type of action is to be built into the behaviour of the flock, then a distributed model similar to the flocking model will need to be developed.

1.2 Aims and Objectives

The main aim of this research is to study some of the issues that would enable the Cucker-Smale flocking model to be deployed to real physical agents such as autonomous robots. The Cucker-Smale model is chosen because it is a continuous-time model that allows a wider range of mathematical tools to be employed in its analysis. In view of the main aim of this research, seven objectives that are associated with four issues have been identified.

The first issue relates to whether the Cucker-Smale model is actually a flocking

model. It is important that the concept of flocking be precisely defined mathematically. Intuitively this definition will need to consist of two elements - the alignment of velocities of the agents and the closeness these agents move together. The *first objective* of this research is therefore to establish this definition and study if the Cucker-Smale model as originally proposed is able to cause a group of agents to flock. If it cannot, then it has to be modified in such a way that it can. With the agents moving closely to each other, it is also important that they do not collide with each other. Existing works have proposed to include a bonding force and a repulsive force into the Cucker-Smale model. The *second objective* is to propose an effective yet simple modification to the original Cucker-Smale model – an augmented Cucker-Smale model, so that the agents can flock closely without colliding.

The second issue relates to how fast the Cucker-Smale system could achieve flocking from a random initial configuration. The agents in an original Cucker-Smale model has been proven to flock asymptotically, i.e. in a reasonably long time, under some conditions on the interaction between agents. However, in practical deployment, one would need to control the system so that the flocking state could be reached as quickly as possible. It will also be useful to establish an upper bound on the time it takes to reach that state. Finite-time control has been applied previously to the original Cucker-Smale model for this purpose. The *third objective* of this research is to mathematically establish that the augmented Cucker-Smale model proposed converges to the flocking state under finite-time control. In conjunction with this, an upper bound on the time to flocking should be derived.

The third issue is to do with the fact that the clocks of physical agents will normally not be synchronized. This means that they do not compute their velocity updates at the same time as is normally assumed in simulations. The *fourth objective* is therefore to study the effect this asynchronicity has on the flocking time of a Cucker-Smale system.

So far, the velocities and positions of the agents are assumed to be perfectly known.

In a real system, this will not be the case. Perturbations in the values of position and velocity can be modelled as additive noise. The *fifth objective* is to determine the effects of additive noise on the flocking system.

Two further kinds of perturbations to a flocking system of agents will be considered in the context of leader-follower flocking. Both perturbations relates to a sudden change in direction of the leader. One particular scenario is that an operator may issue change-of-direction commands to a leader of a flock. This change of direction can be considered a perturbation to the flock with the rest of the flock, which implements a Cucker-Smale-like system, attempting to realign with the leader. The *sixth objective* of this research is to answer the question of how frequently could these commands be issued to the leader without losing the coherence of the flock. Finally, an interesting form of leader-follower situation relates to what is known as the chorus-line effect that has been observed in nature and briefly described in the previous section. The *seventh objective* of this research is to propose, for the first time, a model based on Cucker-Smale that can achieve this effect.

1.3 Original Contributions

Original research contributions have been made according to the seven objectives of this research. They are listed below.

- A mathematical definition of flocking in terms of velocity alignment and “flock diameter” is proposed. The original Cucker-Smale model is shown to be unable to control the flock diameter and therefore it can only be considered an alignment model.
- An augmented Cucker-Smale model is proposed that incorporates both cohesion and collision avoidance properties. It has been shown through simulations that

cohesion and collision avoidance could be achieved using finite cohesive and repulsive forces. In particular, a symmetrical finite force function has been proposed and its effectiveness has been established.

- Asymptotic and finite-time convergence of a finite-time controlled augmented Cucker-Smale model has been mathematically proven. An upper bound to the flocking time is derived. Simulations have shown that flocking does occur within this bound.
- Asynchronous update of the state of the agents has been studied using a block-sequential method. It has been found that asynchronous update poses no penalty on the flocking time for large groups even though the final flock diameters are slightly larger.
- The effects of additive noise, rather than multiplicative noise, on the Cucker-Smale model has been established. It has been found that small amount of additive noise enables flocking time to be reduced but flocking will not happen if more noise is present.
- In a leader-follower system where the leader receives commands to change directions from a human operator, in order for the flock to remain coherent, it has been found that the time interval between these commands must be longer than the realignment time. For a finite-time controlled augmented Cucker-Smale model, the upper bound on the flocking time could be used as a guide.
- A new model, called CS-CL model, is proposed which incorporates the chorus-line effect into the Cucker-Smale model for fast manoeuvres of the flock. Even though the chorus-line effect has been studied in terms of wave propagation before, this is the first agent-based model that has been proposed. Simulations indicate that this model shortens the reflocking time.

1.4 Organization of Thesis

The rest of the thesis is organized as follows. Chapter 2 reviews the three most popular flocking models and the approaches to both leaderless and leader-follower flocking control. In particular, finite-time control is reviewed in this context. Chapter 3 addresses the first issue described in Section 1.2. An augmented Cucker-Smale system is proposed that enables the flock to move cohesively and closely while avoiding collision. The effectiveness of some cohesive and repulsive force functions are examined. Chapter 4 is concerned with finite-time control of the augmented Cucker-Smale model. The convergence of this model is mathematically proven and an upper bound to the flocking time is derived. Chapter 5 examines the effects of asynchronous state update on the Cucker-Smale system and addresses the third issue described in Section 1.2. Chapter 6 covers three aspects of perturbations to the Cucker-Smale system related to the last three objectives of research described in Section 1.2. A new Cucker-Smale model with chorus-line effects is proposed. Finally, Chapter 7 concludes this thesis with a summary of its original contributions and discuss their significance. Several directions of further research are also suggested.

Chapter 2

Review of Flocking Models and Flocking Control

2.1 Flocking Phenomena in Nature

Flocking is a typical example of collective behaviour that is ubiquitous in nature. It is a phenomenon where a large number of autonomous agents, using only limited information in its immediate neighbourhood and simple rules, organize into an ordered synchronous motion. Examples include flocking of birds, schooling of fish, herding of quadrupeds and swarming of bacteria. This flocking phenomenon is being investigated from the viewpoints of biology, physics [1], control theory [43, 44], and applied mathematics [26]. This is due to its potential applications in many engineering areas including mobile sensor networks, cooperative robots and formation flying spacecrafts. Moreover, flocking is a framework within which one can study, for instance, the convergence or consensus of multi-agent systems [37, 45, 46], trajectory tracking in networked systems [47–49], and the formation control of vehicles [50, 51].

2.2 Basic Flocking Models

2.2.1 Boids Model

In 1986, Reynolds [52] created a computer program that tried to simulate the flocking of birds. He called the objects in his simulation “boids”, which stands for “bird-oid objects”. The behaviour of each boid is governed by three rules – cohesion, alignment and separation. The cohesion rule keeps the boids flying close enough to each other to form a flock. The alignment rule helps the boids maintain a speed and direction of movement that is consistent with the rest of the flock. The separation provides a repulsion of the neighbouring boids that helps prevent them from colliding with each other when they are close.

Inspired by the computer simulation of boids, Welsby [53] employed helium balloons (called blimps) to try to achieve aggregation behaviour. However, it falls short of flocking due to the limitations of the blimps. Crowther and Riviere [54] used only the cohesion and alignment rules to generate flocking behaviour of unmanned air vehicles (UAVs) by simulation. The difference between their simulation and Reynolds’ is that the vehicles are modelled by a nonlinear aerodynamic model of flight so their velocities could not change instantaneously. Researchers at the NASA Dryden Flight Research Centre demonstrated the coordination of two unmanned aircrafts using Reynolds’ flocking rules in 2005 [55]. A few years later, in 2011, Hauert [49] implemented boids rules to achieve flocking with ten small fixed-wing robots in outdoor environments. The robots are equipped with WiFi for communication and Global Positioning System (GPS) to determine position and log flight trajectories.

The original boid flocks have no leader and therefore the ultimate direction of flight is dependent on the consensus of the boids through the flocking rules. One extension introduced in [56] is to allow boids at the border of flock to become leaders. A force

called the change of leadership in the alignment rule defines the chance of becoming leader. If certain conditions are satisfied, the leader boid shoots-off from the flocking direction and the others will follow it.

An interesting application of the boids model is found in [57]. Here the emergent behaviour is used in the visualization of time-varying data. Similar data are made to flock close to each other while dissimilar data will repel. This allows the interests of a group of people to be visualized in a three-dimensional virtual world.

Owing to the simplicity of the rules, the boids model is easy to implement as a computer program. However, it is not a mathematical model, and therefore not amenable to be analysed mathematically. In order to understand and predict the behaviour of a swarm of such autonomous agents, a mathematical model is required which will allow the relations between the parameters of the system and the macro-behaviour of the swarm to be rigorously explored.

2.2.2 Vicsek Model

In 1995, Vicsek *et al.* [1] studied the emergency of alignment in a particle system. The model they proposed, often referred to as the Vicsek model, is a discrete-time model that can be used to study swarm clustering and phase transition in dynamic non-equilibrium systems.

Details of the Vicsek model are as follows. N particles are moving in a two-dimensional plane with the same speed but in different directions or headings. The state of particle i at discrete time t is described by $\{(x_i(t), y_i(t), \theta_i(t))\}$, where $x_i(t), y_i(t) \in R$ are the coordinates of the particle on the plane, and $\theta_i(t) \in [0, 2\pi)$ is its heading. If the speed of the particles is v , then at time $t + 1$, the position of particle i becomes:

$$\begin{cases} x_i(t+1) = x_i(t) + v \cos \theta_i(t) \\ y_i(t+1) = y_i(t) + v \sin \theta_i(t) \end{cases} \quad (2.1)$$

The heading $\theta_i(t+1)$ is given by the average heading of the particles in a neighbourhood $N_i(t)$ of particle i . That is,

$$\theta_i(t+1) = \frac{\sum_{j \in N_i(t)} (\theta_j(t))}{|N_i(t)|} + w(t) \quad (2.2)$$

where $w(t)$ is random noise that is uniformly distributed in an interval $[-\vartheta/2, \vartheta/2]$ that represents the uncertainty in the heading estimations. The neighbourhood $N_i(t)$ is typically defined as the set of particles within the area bounded by a circle of radius $r > 0$ centred on particle i . Therefore, $N_i(t) = \{j | d_{ij}(t) < r\}$ where

$$d_{ij}(t) = \sqrt{(x_i(t) - x_j(t))^2 + (y_i(t) - y_j(t))^2} \quad (2.3)$$

is the Euclidean distance between particles i and j .

It has been shown that by simulation in [1], the particles will eventually move in the same direction when the density of agents is high and the noise is small. It has been found that there is a distinct phase transition from random motion to orderly alignment in velocity as a function of agent density and noise [58]. Theoretical justifications are later provided by [43] using a linearised Vicsek model under some assumptions of connectivity of the dynamic neighbour graphs. By considering discretized headings, Savkin [59] confirmed that all agents will reach consensus in the direction of motion under a slightly different connectivity assumption. In [60], counterexamples are used to show that if the speed is sufficiently slow, then consensus can still be reached even when the connectivity assumption given in [43] is not satisfied. The connectivity is ultimately controlled by the interaction radius r of the model. The smallest interaction radius where alignment can still be achieved has been established in [61]. However, it is still difficult to guarantee that the connectivity assumption is satisfied throughout the alignment process.

In a lot of research on the Vicsek model, the assumption is that the heading information of each agent is broadcast to those in its neighbourhood. Therefore it is reasonable that some delays in this transmission is possible. It has been observed via simulations that the Vicsek model is sensitive to communication delays in that large delays can prevent the system from achieving alignment [62]. The authors also derived, for both the delayed linear and nonlinear Vicsek models, that the initial headings of agents could not exceed some limit in order to guarantee alignment. Chen *et al.* [46] studied the convergence rate of discrete-time multi-agent systems with a switching topology and time-varying delays. Applying their results to the Vicsek model with time delays showed that convergence can be reached if the initial topology is connected.

Noise also plays an important role in the Vicsek model. As mentioned before, while a small amount of noise is acceptable, convergence in the state of the agents becomes impossible if the noise is too large. Stochastic approximation is a common approach that has been used for studying this type of problems [63, 64]. It usually demands some uniform connectivity properties. In [45], a distributed consensus protocol is designed by combining probability limit theory and algebraic graph theory that is robust to communication noise under some assumptions of the connectivity graph. A modified time-delayed Vicsek model was considered in [37] where two consensus criteria could be attained without the need for the connectivity assumption. More recently, the critical connectivity requirement is studied with evolving topologies and measurement or communication noise [65].

The Vicsek model is a simple dynamical model that can be used for the study of consensus and alignment. But unlike the boids model, it does not have control over the cohesiveness of the agents. The agents in the system may be heading in the same direction, but they are not flocking if they are travelling far apart from each other. Furthermore, the agents are assumed to have the same speed which is generally not the

case with most applications. It is also basically a discrete-time model. A continuous-time model will allow a wider range of mathematical tools to be used for its analysis so that more insights could be obtained.

2.2.3 Cucker-Smale Model

A model for flocking that is very similar to the Vicsek model was proposed by Cucker and Smale [26] in 2007. The state equations of this dynamical model for N agents are given by:

$$\begin{cases} \dot{p}_i = v_i \\ \dot{v}_i = \frac{1}{N} \sum_{j=1}^N (\|p_j - p_i\|) (v_j - v_i) \end{cases} \quad (2.4)$$

where $1 \leq i \leq N$ and the position and velocity of agent i are denoted by p_i and v_i respectively.

This model differs from the Vicsek model in three respects. Firstly, the Cucker-Smale model is a continuous-time model. Obviously it could be turned into a discrete-time one by discretizing the time variable. Secondly, it does not assume that the speed of the agents are identical; the velocity vectors v_i and v_j for $i \neq j$ do not necessarily have the same magnitude, i.e. $|v_i| \neq |v_j|$. This makes the Cucker-Smale model less restrictive. Thirdly, the acceleration or the change in velocity of agent i is proportional to a weighted sum of the difference between v_i and v_j for those agents $j \neq i$. The function ψ quantifies the influence of agent j on agent i . Known as the communication rate function, it is a symmetrical, positive decreasing function of the Euclidean distance between the agents. Therefore, it is a more general model compared with the Vicsek model. That is, the Cucker-Smale model can be transformed into a Vicsek model by discretizing the time, constraining the agents to move at a constant speed, and defining a suitable communication rate function.

In [26], the authors proved that flocking will be achieved unconditionally with

$$\psi(\|p_j - p_i\|) = \frac{1}{(1 + \|p_j - p_i\|^2)^\beta} \quad (2.5)$$

and when $\beta < \frac{1}{2}$. For $\beta \geq \frac{1}{2}$ flocking could only be guaranteed under some conditions on the initial positions and velocities of agents. The critical condition of $\beta = 0.5$ is later proven to be unconditionally convergent in [66] by using a new approach that constructs a Lyapunov functional explicitly. Since the communication rate function (2.5) is symmetrical with respect to i and j , the interaction graph is undirected. A more general proof is given in [67] for general digraphs which can be applied to leader-following as well as leaderless flocking.

Although there were initial criticisms related to the all-to-all interaction of the communication rate function (2.5), more and more researchers have been attracted to the study of this continuous-time model from various perspectives. One of these considers flocks of a very large number of agents. When N is very large, it may not be useful to keep track of the state of each individual agent. An approach similar to thermodynamics could be used to study the macroscopic behaviour such as flocking. A kinetic and hydrodynamic model derived from the Cucker-Smale model has been proposed in [68]. The authors proved that this model produces flocking behaviour. An alternative approach in [69] derives the kinetic Cucker-Smale model starting from a Boltzmann-type equation. It has also been demonstrated that the velocities converge with this model.

Another perspective is to consider how to steer a system towards consensus in velocity by applying optimal control theory. Optimal consensus control which applies an ad-hoc computational methodology was presented in [70]. A centralized forcing term is used to induce consensus on an initial configuration that would either diverge or accelerate towards convergence. Through mean-field approximation, stochastic optimal

control can be introduced to this problem [71, 72]. Most of the literature on stochastic control is focused primarily on the solution of McKean-Vlasov type of optimal control problems. Rigorous justification that the McKean-Vlasov optimal control problem is consistent with the limit of optimal controls for stochastic finite agent models has been proved in [73]. Other models of sparse mean-field optimal control have been considered [74–76]. More recently, [77] derives the existence of optimal controls in a measure-theoretical setting as the natural limit of finite agent optimal control without any assumption on the regularity of control competitors. In particular, it proves the consistency of mean-field optimal control with the corresponding underlying finite agent ones.

whereas the updating of system state of the discrete-time model is more realistic. Thus the study of convergence from the discrete-time Cucker–Smale model to the continuous-time model was in [78], where an asymptotic flocking estimate for the discrete model using the Lyapunov functional approach is presented. Combining asymptotic flocking estimate and uniform stability to derive a uniform-in-time convergence from the discrete Cucker-Smale model to the continuous model, as time-step tends to zero.

Noisy versions of the Cucker-Smale model has also been studied. Given the similarity between the Cucker-Smale and the Vicsek model, it is not surprising that the agents in the noisy version of the Cucker-Smale model behaves similar to those in the Vicsek model. In [79], it was shown that a phase transition occurs when the noise intensity increases. When the level of noise is high enough, the agents will fail to align. Cucker and Mordecki [80], studied the flocking of the Cucker-Smale system with noise. They proved mathematically that “near-flocking” could be achieved in a finite amount of time with finite non-zero probability in Gaussian noise. Further studies of the noisy Cucker-Smale system show that the ability of the agents to align is highly dependent on the structure and on the power (variance) of the noise [81]. Multiplicative white noise

was studied in [82], where the authors proved that flocking occurs when the intensity of the noise is sufficiently small.

Time delays that into account that information transfer between agents take time, or alternatively that the agents needs time to estimate and respond to velocity changes in its neighbourhood. In [83], a Cucker-Smale model with noise and delay was studied and sufficient conditions expressed in terms of noise intensity and delay length was derived for flocking. A discrete-time Cucker-Smale-type flocking system with a fixed communication time-delay was studied in [39]. Asymptotic flocking of four agents was demonstrated where normalized communication weights were used to model agent interaction. Cucker-Smale model with a time-variant delay and symmetric and nonsymmetric communication weights was considered in [84]. Convergence to alignment is proved if the time-delay is below a certain threshold which is dependent on the coupling strength, the communication weight and a bound on the time rate of change of the time-delay function.

Similar to the Vicsek model, the Cucker-Smale model is strictly an alignment model rather than a flocking model. A tighter spatial configuration could be achieved by introducing additional interaction terms between agents. These terms are sometimes referred to as inter-particle bonding forces. Such an augmented Cucker-Smale model is proposed in [85] that enables the agents to flock together. However, the geometric centre of the system has to maintain a straight trajectory. A global coordination method is used in [86] to track a given trajectory.

Complementary to the cohesive force is the repulsive force, which is needed to prevent the agents from colliding with each other when they are being drawn towards one another. Cucker and Dong [27, 28] added a repelling force which would act whenever a pair of agents become closer than a pre-defined threshold distance. The strength of this force increases exponentially as the distance between two agents is decreased. While an unbounded repulsive force will ensure that there will absolutely

be no collision between agents, it is impossible to implement in practice. Furthermore, this force is often so large that two agents which are sufficiently close to each other will accelerate away from each other so fast that flocking would not happen. Motivated by the aggregation techniques proposed in [87], a model with bounded cohesive force and bounded repulsive force is proposed in [88]. While the effects of this boundedness have been investigated theoretically, further work is needed to see how the system behaves when practical cohesive and repulsive force functions are used.

Apart from studying the effects of additional forces on the Cucker-Smale system, investigations of the inter-agent communication functions have also been conducted. In [29], a global existence theory for the Cucker-Smale flocking model with a singular communication weight function and inter-particle bonding force was established. This theory says that for some well-chosen initial configurations, the agents in the original Cucker-Smale model will not collide without introducing additional collision avoidance mechanisms. However, in practice, it is impossible to guarantee that the initial configuration possess these “well-chosen” properties. Further results with singular communication weights have been reported more recently [30, 89, 90]. Singular communication rate weights of the form

$$\psi(s) = s^{-\alpha} \quad \text{for } \alpha > 0 \quad (2.6)$$

is considered. For $\alpha \geq 1$, it has been shown that the Cucker-Smale agents indeed cannot collide as long as the initial position of two particles are not the same. Furthermore, in the case of $\alpha \geq 2$, a further investigation of the Cucker-Smale model with expanded singularity i.e. with weight

$$\psi_\delta(s) = (s - \delta)^{-\alpha} \quad \text{for } \alpha > 0, \quad \delta \geq 0 \quad (2.7)$$

For this expanded model a uniform with respect to the number of particles estimate that controls the δ -distance between particles. In case of $\delta = 0$ it reduces to the estimate of collision avoidance [30]. A critical value of the exponent α in the communication weights leading to global regularity of solutions or finite-time collision between agents has also been established. While these theoretical results are interesting, a singular communication function implies that its value becomes infinitely large at some point, making it impossible to implement in practice.

2.2.4 Couzin Model

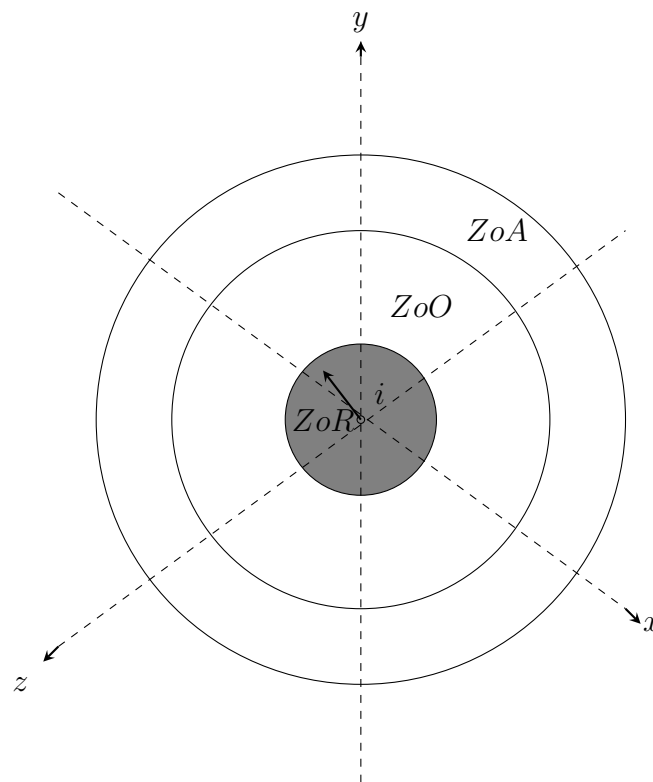


Figure 2.1: Three different zones in the Couzin model

The Couzin model [4] arised from modelling the behaviour of animal groups. It is a self-organizing model that is similar to the Boids model but has been extended to incorporate extra features in three-dimensional space. For each individual agent in

this model, three spherical zones are defined around it. They are known as repulsion, orientation, and attraction zones as shown in Figure 2.1. An agent is located in the heart of three concentric spherical zones. In the inner zone which is called the zone of repulsion (ZoR), repulsive force helps to keep other agents away. In the intermediate zone – the zone of orientation (ZoO), the direction of motion of the agent takes on the average of its neighbours in this zone. This leads to alignment of their velocities. In the outer zone of attraction (ZoA), the agents are drawn towards each other. The agents possess a couple of features which makes them more realistic. Firstly, they have a blind spot behind them so that they cannot “see” the agents that are behind them. Secondly, they have a fixed maximum turning rate. With the additional complexity, it can produce four distinct types of grouping of different shape, alignment, and cohesion. They include swarming, toroidal milling, and dynamic parallel groups. Therefore, compared with the previous three models, it is more practical and allows one to study a few more collective motions other than linear velocity alignment. It is, however, a qualitative model and is not amenable to mathematical analysis.

Some variations of the Couzin model have also been proposed. In [91], a velocity-adaptive Couzin model is proposed where the speed could be adjusted. In this case, speed control is used to affect the convergence rate of the swarm. A fuzzy-rule-based adaptive Couzin model has also been proposed for a changing environment [92]. Here, each agent updates its position according to some pre-assigned fuzzy membership functions in three sensing zones. An improved adaptive-velocity self-organizing model as a prospective candidate in order to enhance accelerate convergence was proposed in [93]. Convergence performance is assessed in terms of group polarization, convergence ratio and convergence time.

2.3 Flocking Control

Flocking control is concerned with using control engineering method to cause a swarm of agents to achieve some form of collective flocking behaviours. One of these desired behaviours that is of practical importance is for the agents to move in a formation. formation control. According to [94, 95], the term “formation” refers to the fact that a specific geometric pattern, known as formation shape, is formed by the agents and this shape is maintained while moving. Other types of behaviours include obstacle avoidance movements [44, 96] and target tracking [97, 98].

Broadly speaking, research in flocking control can be classified into two categories – leaderless and leader-follower. Leaderless flocks are similar to those modelled by Vicsek and Cucker-Smale where consensus in velocity is reached without an agent acting as a leader. In this case, flocking control has to be built into the dynamics of the agents. With leader-follower, the rest of the flock follows the direction of motion of the leader. There exists a number variations depending on whether there is a single leader or there are multiple leaders. Leaders could also be fixed or they could change. These aspects of flocking control is reviewed in Section 2.3.1.

Various types of constraints that reflect practical situations have also been considered in conjunction with traditional centralized and decentralized control methods [99]. For physical agents such as robots, the non-holonomic constraint is appropriate since they cannot change direction or speed instantaneously [100]. Input constraints are often considered since the amplitude of the control input to the system has limits [101]. Another practical consideration that is very important is time constraint. The question here relates to how quickly the agents can become aligned again after some disturbance or perturbation to the flock. Two main control techniques, known as finite-time and fixed-time control, have been applied. Time-constrained control is reviewed in Section 2.3.2.

2.3.1 Leader-follower and Leaderless Flocking Control

2.3.1.1 Leaderless Flocking Control

The flocking models such as Vicsek and Cucker-Smale reviewed earlier are leaderless. The flocking velocity is the average of the initial velocities of the agents in that flock, if it converges. For the Cucker-Smale model, essentially the control to flocking is by adjusting the parameter β in the communication rate function. It is therefore interesting that a leaderless algorithm, proposed in [102], is able to align the agents without the explicit knowledge of the velocity headings of each agent's neighbours. The time derivative of the perceived centre of the centre of mass is generated for each agent, which is used for alignment.

Similar to leader-follower flocking, leaderless flocking has also been studied through consensus algorithms. While research in distributed consensus algorithms have been focussed on linear single and double-integrator systems, a number of works on leaderless consensus have extended to more general nonlinear systems. Such distributed nonlinear systems are usually formulated as networked Lagrangian systems. For example, a controller based on potential functions is proposed in [103] for networked Lagrangian systems to achieve leaderless flocking. In [104], three distributed leaderless consensus algorithms are proposed for networked Lagrangian systems under an undirected graph.

Leaderless flocking was being applied to robotics since the 1990s [105, 106]. The challenge is to translate the knowledge gained through studying point-mass agents to more realistic nonholonomic robots. Leaderless flocking for a group of such robots is investigated in [107]. A Lyapunov-like function and graph theory are employed for convergence analysis. The simulation results proved the effectiveness of the proposed distributed flocking control scheme. Behaviour-based methods have also been proposed. Typically, a set of behaviours such as “move-to-go”, “avoid-obstacle”, “follow-wal”, “avoid-robo” and “keep-formation” are pre-defined. The overall behaviour is

computed from the sum of these sub-behaviours. This approach is utilized for navigating in an unknown environment with obstacles in [108]. These robots communicate with each other through wireless broadcast communication.

Leaderless formation control is also known as virtual structure formation control. This is because the formation is treated as a single virtual structure. The structure therefore consists of a collection of agents that maintain a rigid or semi-rigid geometric relationship with each other within a frame of reference. In this approach, control is acquired in three steps. First, the desired dynamics of virtual structure are defined. Then, the motion of the virtual structure is translated into the desired motion for each agent. Finally, tracking controls for each agent are derived. In [109], a general controller strategy was developed for the virtual structure. An interesting time-invariant formation of unicycle mobile robots was studied in [95]. Several control laws including consensus, flocking, and flocking with collision avoidance, based on virtual structures, were used in this case. The robots communicate wirelessly to exchange information. The authors also proved the asymptotically stability of their system. However, only two robots have been used to demonstrate the results experimentally. Sadowska [95] designed a virtual structure controller with mutual coupling between neighbouring individual robots. They proposed two controllers – one based on a kinematic model of the mobile robot and the other on a dynamic model. However, it will be difficult to adapt this approach to time-varying formations. The computational demand on the robots is also very high.

2.3.1.2 Leader-follower Flocking Control

The leader-follower approach to flocking was introduced in [110]. Since then, many leader-follower algorithms and architectures have been investigated. The fundamental idea is to assign one agent as a leader among a group of agents. The role of the leader is to navigate and control the flock behaviour. It will have to be provided with global information, such as the desired direction or destination. The rest of agents will keep

the position and direction within a prescribed range of distance to the leader and to each other. One of the agents in the flock could act as the leader [111–114], or a virtual leader could be used [115–118]. In [44], the design of flocking algorithms is investigated. A method for constructing cost functions that keeps the flock moving in a certain shape is proposed. With suitable cost functions, the agents are able to track the path of a virtual leader in both free space and when obstacles are present. The agents in this system follows the Boid model rules for flocking. In addition, they possess information on the state of the virtual leader.

There could also be multiple leaders. Typically, they handle different responsibilities in the group for flocking. For example, in formation control, a hierarchical structure where a follower can also be a leader of other followers is commonly used. Dynamic models of relative distances and bearings between leaders and followers must be maintained. In this way, complex formations could be achieved [110, 113, 116, 117, 119–121]. Different kinds of leaders are allowed in the system studied in [122]. While a global “power” leader may set the trajectory, a “knowledge” leader may possess complementary information on the dynamics of the target. A convergent condition was established by the authors using contraction theory.

Tracking control for multi-agent consensus with an active leader is considered in [123] using a neighbour-based rule. In [31, 123, 124], some algorithms are proposed for second-order consensus and consensus tracking. It has been shown that both the real and imaginary parts of the eigenvalues of the Laplacian matrix of the adjacency graph play a key role in reaching consensus [31]. Moreover, second-order consensus in delayed directed networks can be achieved with a directed spanning tree if and only if the time delay is less than a critical value. Note that these works typically assume that the agents are linear with single or double integrator dynamics.

A special type of leader-follower dynamics arises from observed phenomena. One of these phenomena is known as the chorus-line effect. With the leaderless flocking models

such as Vicsek and Cucker-Smale, once the agents' velocities are aligned, the flock is stable under small perturbations. That is to say, if a single agent's velocity is changed, the interaction rule will keep the remainder of the flock to largely maintain its current velocity due to the averaging effect. The agent with a different velocity will eventually adjust it back to that of the rest of the flock. However, it has been observed in flocks of Dunlin that a sudden abrupt change in flight path could be initiated by a single bird or a very small number of birds [40]. These initiators could arise from any part of the flock, not necessarily at the front in the traditional leader-follower formation. This type of manoeuvre spreads through the flock in a wave. The propagation of this "manoeuvre wave" starts slowly but reaches average three times higher than if birds affect only from their neighbours [125]. This ability to react quickly to sudden manoeuvres is important for birds to respond to the movements of potential predators [126]. Since this manoeuvre wave propagates in a similar fashion to the movement in a chorus line, Potts [40] proposed the chorus-line hypothesis in 1984 for this phenomenon.

Some models have been proposed to study this phenomenon. StarDisplay [41, 127] is a computational model that has been used for studying the wave propagation speed for starling flocks. They concluded that short range interactions are all that are needed to generate the underlying wave. The propagation of density waves was derived with an pseudo-Hamiltonian based on the Vicsek model [42]. By analyzing a single dimensional model, the authors have found a line of critical damping in the parameter space. While these models are useful for studying the propagating wave of movements, they are not in a form that is compatible with current flocking models. That is, they are not rules or equations that can be implemented in each agent in order to recreate this type of phenomenon. Hence, a different type of modelling is required.

2.3.2 Time-constrained Flocking Control

Studies reviewed above on flocking and consensus typically prove asymptotic convergence of the proposed algorithms. However, many practical applications require convergence within some time constraints. For instance, a finite-time tracking control algorithm is designed and implemented in a robot to track virtual robot within a finite-time interval [128]. Some researches have emerged recently that are concerned with methods to attain flocking within a finite amount of time. These research typically apply finite-time or fixed-time control theory to swarm system [129]. Finite-time control is based on Lyapunov stability theory [35, 36] while fixed-time control arises from the theory of non-linear dynamic systems [130, 131]. When applied to flocking systems, both finite-time and fixed-time control are used to solve essentially the same problem. They are able to drive the system to reach the alignment or equilibrium stable state within a finite amount of time starting from an arbitrary initial state.

2.3.2.1 Finite-time Control

It has been known that bang-bang control can be used to drive a feedback control system to its equilibrium point in a time-optimal manner [132]. However, this kind of discontinuous control law would cause problems such as chattering [133]. This motivated the design of time-optimal continuous and bounded controllers. In [35], the proposed first and second order dynamic controllers have been shown to reach equilibrium within a finite time, as opposed to asymptotic convergence of conventional controllers. These controllers are referred to as finite-time controllers. Finite-time control theory was later established more rigorously by [36]. Most significantly, by using Lyapunov stability theory, the authors were able to derive an upper bound for the convergence time.

Finite-time control for single integrator dynamics is considered in [134]. A number of finite-time consensus algorithms were subsequently proposed for multi-agent consensus problems with second-order dynamics [135–137] as well as nonlinear dynamics [138–140]. In addition, a new approach to finite-time adaptive stabilization of higher-order uncertain nonlinear system has been studied in [141]. In this work, a novel control strategy that combines sign function with adaptive techniques is able to handle uncertainty and nonlinear growth rates. The convergence time can be adjusted through the design parameter. Consensus with fixed and switching undirected topology was considered in [50]. The authors showed that when a particular type of nonlinear inter-agent interaction was used, consensus can be reached in finite time. A terminal sliding model control based finite-time consensus tracking algorithm was considered in [142] for agents with a fixed topology. Another distributed finite-time consensus protocol was presented in [143]. Moreover, the relationship between the convergence time and the communication topology was also investigated. It showed that shorter convergence time could be obtained when the parameters are adjusted according to the state of the agents. The work that addressed finite-time flocking directly are found in [144, 145]. They studied the convergence time based on the Cucker-Smale model with a continuous non-Lipschitz velocity update protocol. The main result are that convergence time decreases as the number of agents increases.

2.3.2.2 Fixed-time Control

The concept of fixed-time stability is first proposed in [130]. The main result of [130] is that if dynamical system globally fixed-time stable, then there is an upper bound on the time to reach the equilibrium state. The fixed-time consensus of a first-order system was addressed in [146, 147] where a fixed-time nonlinear control protocol has been designed to achieve consensus within a prescribed time. Fixed-time consensus tracking based on double-integrator dynamics with a directed topology was investigated in [48].

The objective is to design a control protocol that solves a fixed-time consensus problem for any given initial states if it solves a finite-time consensus problem and the settling time is bounded. Further fixed-time algorithms can also be found in [131, 147].

For leader-follower control, a distributed control protocol was proposed in [148] to guarantee that each follower tracks a single virtual leader within a prescribed time. Formation control in fixed-time was considered in [130, 146]. Here, a control protocol was proposed which will cause the agents to be spread out with equal distance from each other. The fixed-time consensus of multi-agent systems with high-order integrator dynamics where the leader was available not to all followers but to only a portion of them was addressed in [149].

The advantage of fixed-time control is that the upper bound of the convergence or settling time is dependent only on some design parameters and the network connectivity. In contrast with finite-time control where the convergence time is dependent on the initial condition of the group of agents. However, the upper bound derived for fixed-time control can be quite conservative. But finite-time controllers arise from time-optimal designs and therefore is capable of providing faster convergence. In [150], both finite-time and fixed-time algorithms have been designed for leader-follower consensus. Their results indicate that the finite-time controller converges faster.

2.4 Summary

This literature review on flocking models and flocking control highlighted a number of research gaps. In particular, a Cucker-Smale model augmented with cohesive and collision avoidance mechanisms that are bounded in magnitude and therefore physically implemented is needed. The application of finite-time control on this augmented model will enable it to reach the flocking state in a time-optimal manner. Along the line of practical implementation of the system, the effects of unsynchronized update time

of the agents in the system will need to be studied. Furthermore, it is interesting to see if a distributed model based on Cucker-Smale can be implemented to achieve the chorus-line effect. These are the subject matters of the following four chapters.

Chapter 3

Cohesion and Collision Avoidance

It has been pointed out in Section 2.2.3 that the agents in the original Cucker-Smale flocking model has been proven to converge to a common velocity asymptotically under some initial conditions and when the communication rate parameter β is less than $\frac{1}{2}$ [26, 151]. However, in practice, an understanding of the dynamics of this process is important. In this chapter, the original Cucker-Smale model is studied in terms of two measures. The first one is the *time* it takes a group of agents to have their velocities aligned with each other. The second measure is the *spread* of the flock which we called the flock diameter. From the simulation results, it is established that the Cucker-Smale model needs to be augmented with a cohesive term in order to stay within specified flock diameter limits. This cohesive term has to be counter-balanced by a collision avoidance term so that the agents will not be drawn so close to each other that they collide. An augmented Cucker-Smale model which contains these two terms are proposed. The behaviours of this model under unbounded and bounded repulsive functions together with bounded cohesive functions are then studied through simulation.

3.1 Some Definitions

With a group of agents, flocking is a state at which the velocity of every agent is the same as that of the rest. When that happens, the magnitude of the (vector) sum of the velocities will be the same as the sum of the magnitudes of the velocities. Mathematically, for a group of N agents,

$$\left| \sum_{i=1}^N v_i \right| = \sum_{i=1}^N |v_i| \quad (3.1)$$

where v_i represents the velocity of agent i . Thus a useful indicator of whether velocity alignment has occurred is the *normalized average velocity* v_a which is defined as [1]

$$v_a = \frac{\left| \sum_{i=1}^N v_i \right|}{\sum_{i=1}^N |v_i|} \quad (3.2)$$

This gives rise to the following definition of alignment.

Definition 3.1. *A group of autonomous agents are said to be aligned when their normalized average velocity is unity, i.e. $v_a = 1$.*

On the other hand, if the velocities are completely random, then $v_a \approx 0$.

In practice, exact alignment is very difficult, if not impossible to achieve. This is especially true when the computations are performed digitally with finite precision. Therefore a more practical criterion for alignment is when the velocity of every agent is close enough to the rest. This gives rise to a definition for *practical alignment*.

Definition 3.2. *A group of N autonomous agents are said to be practically aligned if*

$$|v_i - v_j| \leq \delta \quad (3.3)$$

for all $i, j \in [1, N], i \neq j$, and for an arbitrarily small $\delta > 0$.

The above condition is equivalent to

$$|1 - v_a| < \delta' \quad (3.4)$$

for some arbitrarily small $\delta' > 0$. Figure 3.1 shows how the average velocity changes as a group of Cucker-Smale agents align their velocities, starting with random directions initially.

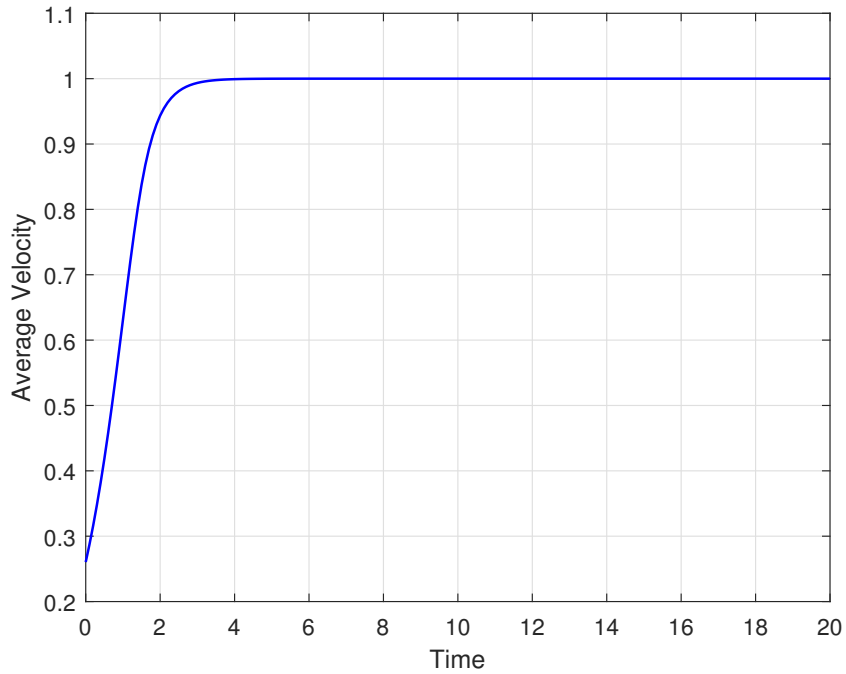


Figure 3.1: Average Velocity versus Time

An important measure of comparison for a flocking model is the minimum time it takes a group of agents with random initial velocities to achieve alignment. This time is referred to as the *alignment time* in this thesis. More formally,

Definition 3.3. *The alignment time T_f is defined as the maximum lower bound of the time it takes a group of autonomous agents to reach alignment from a random initial state, i.e.*

$$T_f = \inf \{T : |1 - v_a| < \delta'\} \quad (3.5)$$

for some arbitrarily small $\delta' > 0$.

While velocity alignment alone has been used in many research publications as the sole criterion that constitutes flocking, the general concept of flocking requires that the agents are moving in reasonably close proximity to each other. In order to measure the spread of a flock, the idea of a "flock diameter" is introduced in this thesis. It is defined as the largest distance between two agents in a flock.

Definition 3.4. For a group of N agents, its flock diameter is defined as $\sup \|p_i - p_j\|$ for all $i, j \in [1, N], i \neq j$.

The flock diameter is usually measured after alignment is achieved.

The criteria for flocking can now be stated in terms of alignment time and flock diameter.

Definition 3.5. A group of N autonomous agents is said to be flocking if the following conditions are satisfied:

1. $|1 - v_a| < \delta$ for some arbitrarily small $\delta > 0$; and
2. $0 < \sup_{t \geq T_f} |p_i - p_j| < \epsilon$ for some suitable finite value of ϵ and where T_f denotes the alignment time

for all $1 \leq i, j \leq N$.

3.2 Flocking With the Original Cucker-Smale Model

The original Cucker-Smale model (2.4) shall first be characterized in terms of the alignment time and the flock diameter through computer simulation. The simulations are conducted under the following conditions:

- The agents move in an infinitely large two-dimensional space. This means that they will be able to move freely without encountering any boundaries or obstacles.

- Each agent moves at a constant speed of 0.5 units of distance per unit time. For convenience, distances and time shall be dimensionless.
- The initial direction of movement of each agent is chosen uniformly randomly in the range $[0, 2\pi)$.
- The initial positions of the agents are randomly spread out in a square of 10 units in distance.
- The communication rate function (2.5) is used unless stated otherwise.

Each simulation is repeated 20 times with different random initial velocities and positions. The simulation program is written in MATLAB®.

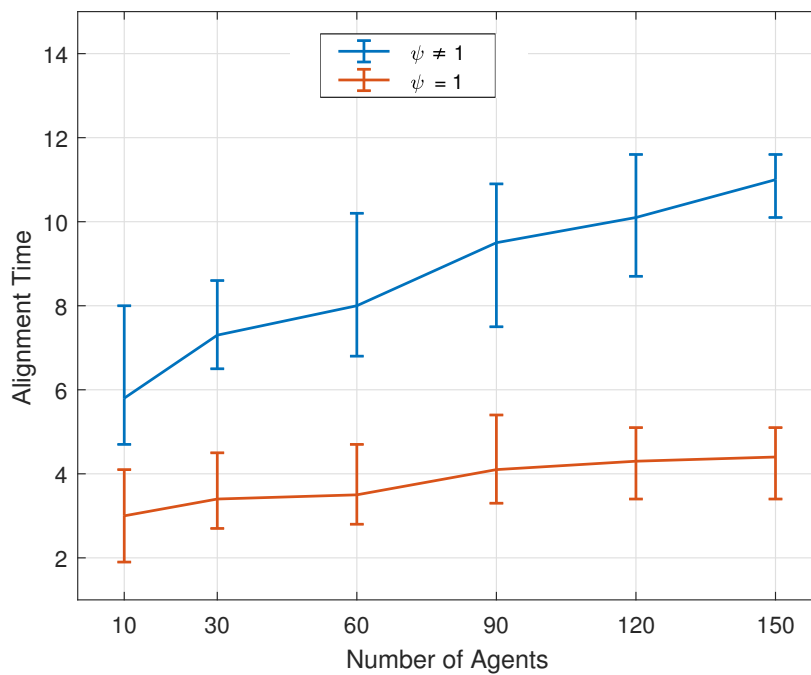


Figure 3.2: Alignment Time of the Original Cucker-Smale Model

Figure 3.2 shows the alignment time for flock sizes between 10 and 150. The system is considered to be in an aligned state when $v_a \geq 0.99$, i.e. $\delta = 0.01$ in Definition 3.5. Two sets of results are shown in Figure 3.2. One is based on setting the communication

Table 3.1: Alignment Times

Number of Agents	$N = 10$	$N = 30$	$N = 60$	$N = 90$	$N = 120$	$N = 150$
$\psi = 1$	3.0	3.4	3.5	4.1	4.3	4.4
$\psi \neq 1$	5.8	7.3	8.0	9.5	10.1	11.0
Ratio	1.93	2.15	2.29	2.32	2.35	2.5

rate parameter β to 0.25 to guarantee convergence. The other is based on a constant communication rate of 1. In both cases, the average flocking time increases with the number of agents although the one with the exponential communication rate increases more substantially. For instance, 150 agents require 11 units of time to align for non-constant communication rate while it takes only 4.4 with constant communication rate. This is approximately 2.5 times longer. This is reasonable as a constant communication rate implies that those agents that are far away have the same effects as those that are close by. The numerical values of Figure 3.2 are shown in Table 3.1 for the sake of clarity.

3.2.1 Effect of Communication Rate on Alignment Time

The only variable parameter for a communication rate function ψ in the form of (2.5) is β . It has been proven that when $\beta < 1/2$, flocking will emerge unconditionally. If $\beta \geq 1/2$, then flocking could only be guaranteed under some conditions on the initial positions and velocities of agents. This is verified through simulations with the value of β set to 0.25, 0.5, 1 and 2, respectively.

Figure 3.3 shows that alignment times for various flock sizes are reduced for smaller values of β . This is because as $\beta \rightarrow 0$, $\psi \rightarrow 1$. Combining these results with those in Figure 3.2 tells us that for $0 \leq \beta \leq 0.5$, the smaller the value of β , the shorter the alignment time. Note that the same alignment criterion of $v_a < 0.99$ is used here.

Table 3.2 shows the numerical values of the alignment times. In this table, the two columns labelled "ratio" indicates the ratio of the alignment time with respect to the

Table 3.2: Alignment Times for Different Values of β

Number of Agents	$\beta = 0$	$\beta = 0.25$		$\beta = 0.5$	
		<i>Time</i>	<i>Ratio</i>	<i>Time</i>	<i>Ratio</i>
$N = 10$	2.1	5.8	2.76	17.7	8.43
$N = 30$	3.0	7.3	2.35	20.6	6.87
$N = 60$	3.5	8.0	2.29	23.5	6.71
$N = 90$	3.9	9.5	2.44	27.7	7.10
$N = 120$	4.2	10.1	2.40	31.2	7.43
$N = 150$	4.7	11.0	2.34	32.5	6.91

time for $\beta = 0$. For $\beta = 0.25$, the alignment times are 2.39 to 2.76 times higher than when $\beta = 0$. Increasing β to 0.5 causes the alignment time ratios increase to between 6.71 and 8.43.

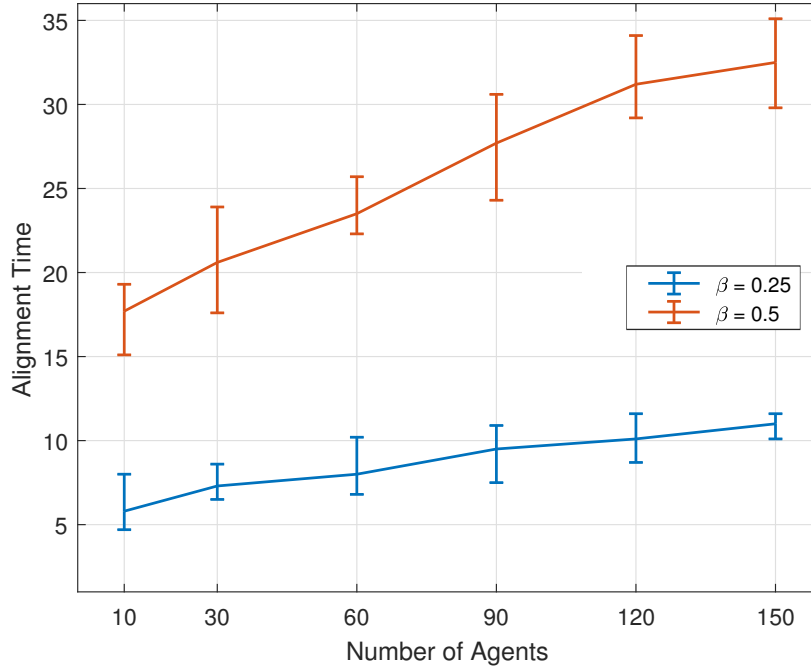
For $\beta = 1$ and $\beta = 2$, alignment could not be achieved. Figure 3.4 shows the average velocities after 200 units of time. As the average velocities are lower as the number of agents is increased, the system is further and further away from alignment.

These simulation results confirm that the theory is correct – that the Cucker-Smale agents align their velocities if $\beta \leq 0.5$. What is more important to note is that if the system converges, it converges within a finite amount of time.

3.2.2 Need for Cohesion

In previous studies such as [66,85], flocking is assumed to be achieved when the velocity is aligned and the flock diameter could be very large, as long as it is finite. To the best of this author’s knowledge, none of the previous research on Cucker-Smale model has examined the spatial spread of agents after velocity alignment is achieved. But this “flock diameter”, i.e. the furthest distance between any two agents, is an important measure to indicate if the flock is cohesive.

The flock diameters of the simulations in the previous section are tabulated in Table 3.3. This table shows the flock diameter at the beginning of the simulation and

Figure 3.3: Alignment Time with Two Different Values of $\beta \leq 0.5$ Table 3.3: Flock Diameter for Different Values of β and Flock Size

Number of Agents	$\beta = 0.25$		$\beta = 0.5$		$\beta = 1$		$\beta = 2$	
	Initial	Final	Initial	Final	Initial	Final	Initial	Final
$N = 10$	11.3196	14.0798	10.3390	12.6331	10.8185	29.0401	11.0188	51.9447
$N = 30$	11.9164	14.1906	11.2782	14.4087	11.2474	34.2011	11.1460	53.2011
$N = 60$	12.0834	14.2012	12.4845	16.0345	11.447	38.6777	11.3876	58.1573
$N = 90$	12.7376	14.3327	12.2157	17.0923	12.5726	40.6656	12.5086	57.4189
$N = 120$	12.9657	14.2625	12.7819	17.4862	12.829	41.3899	12.9865	58.9723
$N = 150$	13.3539	14.3980	12.9339	17.6586	13.2012	41.6228	12.9339	60.4273

when the velocities are aligned. In the cases where alignment could not be achieved (i.e. $\beta = 1$ and $\beta = 2$), the values shown are the furthest distances after 200 units of time. It is obvious that they are large as the agents are not flocking and are moving away from each other. For $\beta = 0.25$ and $\beta = 0.5$, alignment is reached. However, the diameters of the aligned flock are still larger than their respective initial values. This indicates that the flock moved apart before reaching consensus on the velocity. If the speed of the agents are higher, then one would expect the final flock diameter to be larger.

Remark 3.1. *The results in Section 3.2.2 illustrate that the Cucker-Smale system is*

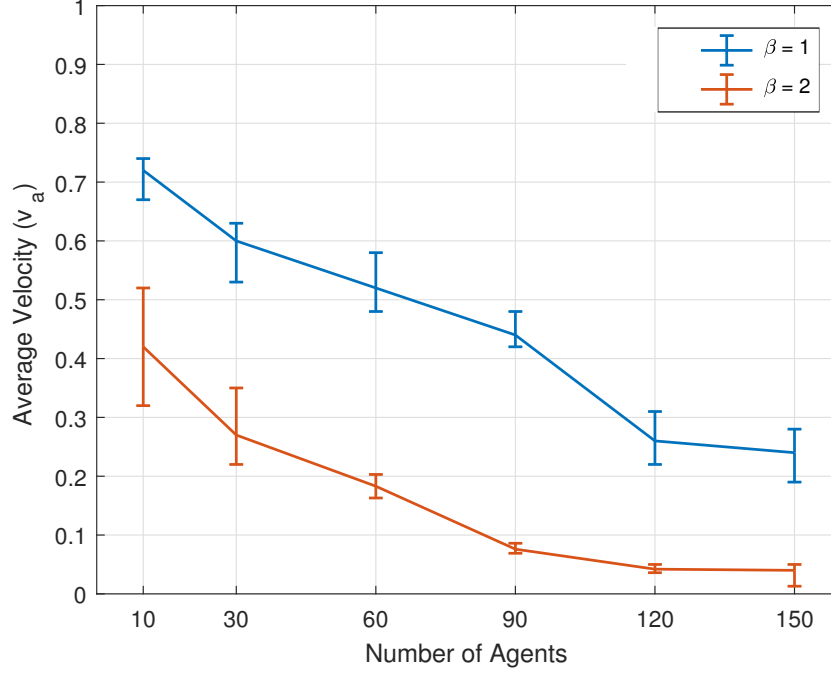


Figure 3.4: Average Velocity with Two Different Values of $\beta > 0.5$

essentially a velocity alignment model. There is no built-in mechanism within this model to keep the agents in a spatially tighter configuration. Thus it is impossible to guarantee flocking according to Definition 3.5 since the Cucker-Smale model has no control over the flock diameter.

One way to impose control of flock diameter is to introduce a cohesive force into the original Cucker-Smale model. Such an approach was proposed in [85]. This model is given by

$$\begin{cases} \dot{x}_i = v_i \\ \dot{v}_i = \frac{\lambda}{N} \sum_{j=1}^N (r_{ij}) (v_j - v_i) \\ \quad + \frac{\sigma}{N} \sum_{j=1}^N \frac{K_1}{2r_{ij}^2} \langle v_j - v_i, x_j - x_i \rangle (p_j - p_i) \\ \quad + \frac{\sigma}{N} \sum_{j=1}^N \frac{K_2}{2r_{ij}} (r_{ij} - 2R) (p_j - p_i) \end{cases} \quad (3.6)$$

where p_i and p_j are the positions of agent i and j respectively, and $r_{ij} = |p_j - p_i|$. Compared with the Cucker-Smale model (2.4), there are two extra terms in the velocity

update equation. They constitute an inter-particle (or inter-agent) bonding force between the agents. Between any two agents i and j , this component is essentially an acceleration directed along the line through the positions of these two agents, and towards each other. With suitably chosen K_1 and K_2 , the distance between these two agents will converge exponentially to $2R$. Although for more than two agents, the final inter-agent distance will not be exactly $2R$. But if R is large enough, the agents will not collide. The coupling strength of the inter-agent bonding force can be further controlled by the non-negative parameter σ . It was mathematically proven that asymptotic flocking could be achieved with this augmented Cucker-Smale model. The authors also verified that the agents indeed flock close to each other. Simulation result shows the relative distances are bounded by $4R$ in this case. The agents eventually stay in a $4R$ circle without moving, but it is not satisfied the definition of flocking status that agents move at the more or less velocity at the end. But the simulation in [85] was limited to only five agents. More importantly, the inter-agent bonding force could be very large for agents that are very far apart and is essentially unbounded.

The model given by (3.6) has two major disadvantages. First, there are five parameters ($\lambda, \sigma, K_1, K_2, R$) that need to be determined. In particular, the system works well in achieving cohesion only if σ, K_1 and K_2 are chosen well. Secondly, there is no explicit repulsive force in the system that prevents the agents from colliding.

A cohesive force $\phi(r)$ where r denotes the distance between two agents should have the following characteristics. For r less than a certain distance d_1 , this cohesive force should cease. But for $r > d_1$, $\phi(r)$ should be a monotonically non-decreasing function of r . A possible cohesive force function is given by:

$$\phi(r) = \begin{cases} 0 & r \leq d_1 \\ k * \frac{1}{1+e^{-r}} & r > d_1 \end{cases} \quad (3.7)$$

where $1/(1 + e^{-r})$ is the sigmoid function and is Lipschitz continuous. k is a constant that can be used to adjust the strength of this cohesive force. It will be referred to as the cohesive force coefficient. This function is shown in Figure 3.5. Note that ϕ remains relatively constant when $r > d_2$.

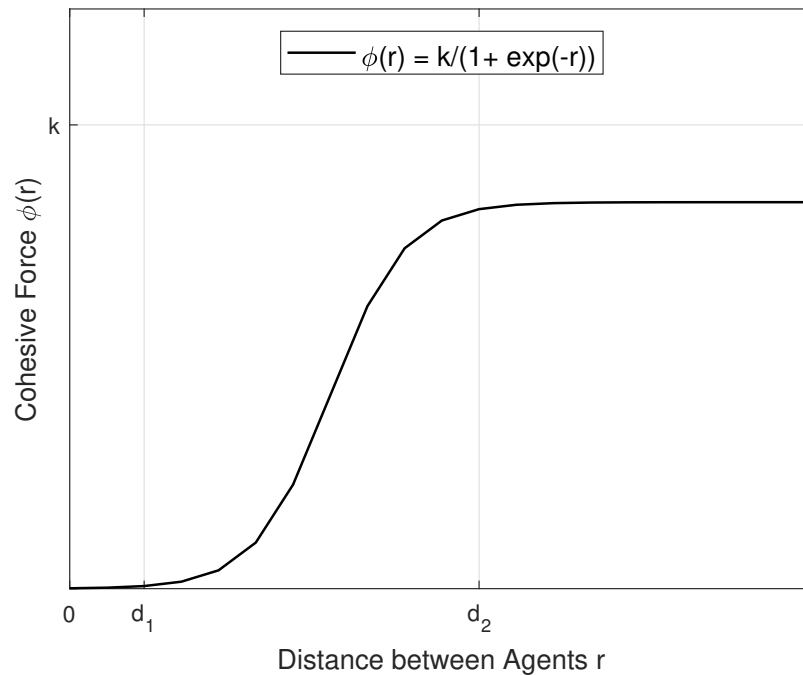


Figure 3.5: An Example of Cohesive Force Function

3.2.2.1 Effect of Cohesive Force Coefficient

We shall first examine the effects of the cohesive force coefficient k in (3.7) on the flock diameter. The values of k between 0 and 3 are examined with $k = 0$ indicating that cohesive force is not used. The size N of the flock ranges from 10 to 150. The initial field size is 10 units squared. The distances are $d_1 = 5$, $d_2 = 9$.

The results in Figure 3.6 shows that increasing the cohesive force coefficient leads to a substantial reduction in the flock diameter for all values of N . Thus flock diameter is reduced or controlled by introducing this cohesive force. It is also interesting to note

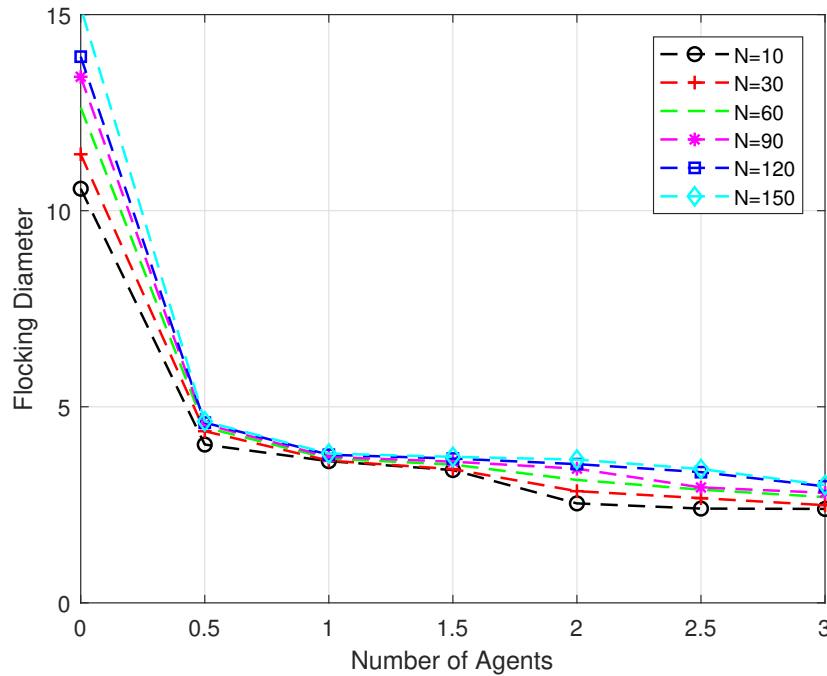


Figure 3.6: Flock Diameter for Different Cohesive Force Coefficients

that increasing the value of k from 0.5 to 3 does not lead to a very significant reduction in flock diameter.

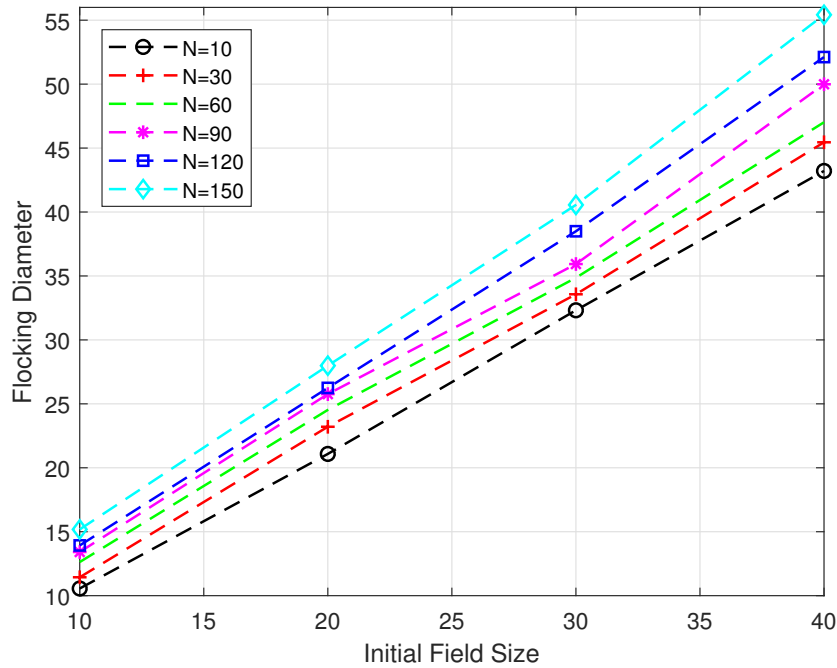
3.2.2.2 Effect of Initial Field Size

The initial field size, which reflects the initial density of the agents, may have a significant effect on the final flock diameter. In this set of simulations, the initial field size is varied while keeping other system parameters the same. The results shown in Table 3.4 confirms that increasing the initial separation of the agents does affect the final flock diameter. In the case where a cohesive force is not used ($k = 0$), the flock diameter approximate 4 times with field size increased from 10^2 to 40^2 . With the use of cohesive force, the corresponding increase is less than 2 times.

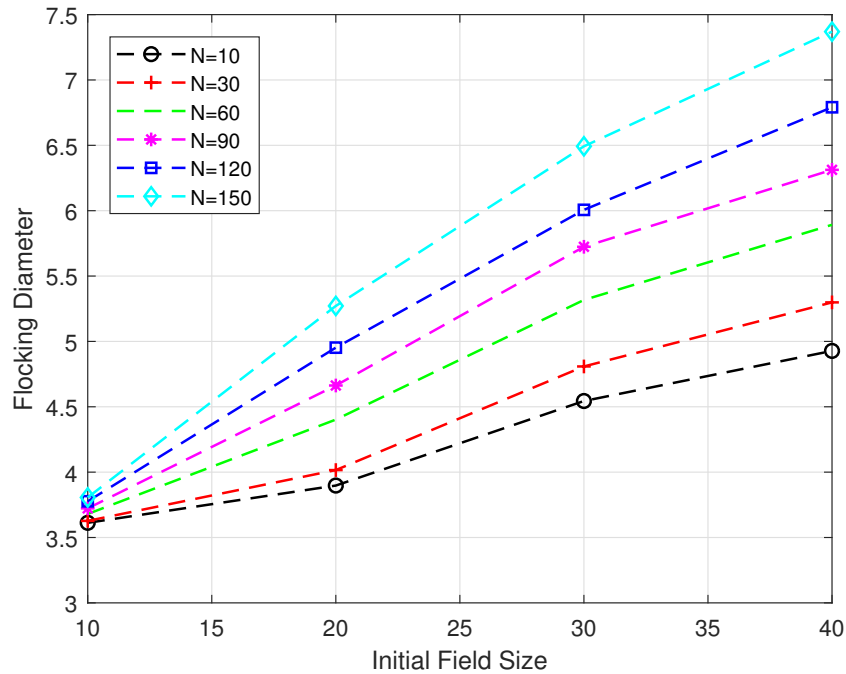
These results are also shown in graphical form in Figures 3.7 and 3.8. It is interesting to note that the increase in flock diameter without cohesive force is about linear in

Table 3.4: Flock Diameter with Different Cohesive Force Coefficients (k)

Number of Agents	Initial Field Size = 10		Initial Field Size = 20		Initial Field Size = 30		Initial Field Size = 40	
	$k = 0$	$k = 1$						
$N = 10$	10.5600	3.6125	21.0839	3.8974	32.3147	4.5441	43.2118	4.9274
$N = 30$	11.4386	3.6270	23.2078	4.0158	33.5672	4.8085	45.4526	5.2986
$N = 60$	12.6290	3.6801	24.5256	4.4020	34.8579	5.3172	47.0190	5.8921
$N = 90$	13.4146	3.7229	25.7614	4.6628	35.9309	5.7239	49.9904	6.3125
$N = 120$	13.9272	3.7770	26.2451	4.9524	38.4951	6.0064	52.1158	6.7912
$N = 150$	15.1806	3.8063	27.9868	5.2714	40.5561	6.4925	55.4223	7.3697

Figure 3.7: Flock Diameters for $k = 0$

initial field size. This is true for all values of N . Furthermore, cohesive force plays crucial effect on the final flock diameter. The value of flock diameter increases 36% when the initial field size increases from 10^2 to 40^2 with $N = 10$. As for $N = 150$, the corresponding increase is about 96%. That implies that cohesive force have more effect with a larger flock.

Figure 3.8: Flock Diameters for $k = 1$

3.2.3 Need for Repulsion

When an external cohesive force is applied, the agents may collide at the beginning stage because the initial heading is random. After they become more or less aligned in velocity, the possibility of collision will be small. Meanwhile, they also stay closer with each other since the cohesive force is applied. Table 3.5 shows the minimum distance between any two agents from the simulations in Section 3.2.2 with an initial field size of 10^2 . From this table, the smallest distance between any two agents is 0.0040. While technically the agents have not collided because they are point-masses, in reality, the physical size of the agents would likely exceed 0.004 and they would have collided. Let $d_0 > 0$ be the minimum distance between any two agents. Then for $\|p_j - p_i\| < d_0$, collision is said to have occurred.

One way to prevent collision is to introduce a repulsive force into the system equation that will cause the agents to accelerate away from each other when they become too

Table 3.5: Minimum Distance between Any Two Agents

Number of Agents	$N = 10$	$N = 30$	$N = 60$	$N = 90$	$N = 120$	$N = 150$
$k = 0$	1.0569	0.1312	0.0933	0.0212	0.0339	0.0563
$k = 1$	0.1299	0.0398	0.0567	0.0229	0.0152	0.0040
$k = 2$	0.0872	0.0050	0.0401	0.0172	0.0167	0.0141

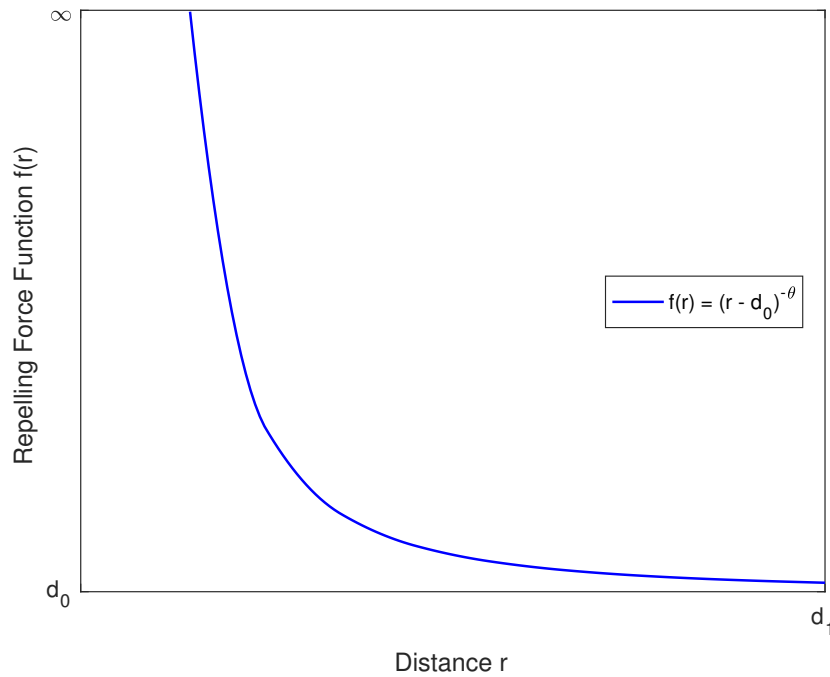


Figure 3.9: An Example of Repulsive Force Function

close. This has been suggested in [28]. The authors argued that this repulsive force function $f : (d_0, \infty] \rightarrow [0, \infty)$ should have the following properties:

1. $\int_{d_0}^{d_1} f(r) dr = \infty$, and
2. $\int_{d_1}^{\infty} f(r) dr < \infty$.

for $d_1 > d_0$. A simple exponential function

$$f(r) = (r - d_0)^{-\theta} \quad (3.8)$$

for any $\theta > 1$ is suggested in [28] as a suitable candidate. It has the required properties

and is both Lipschitz continuous and differentiable. A graph of this function is shown in Figure 3.9.

Note that the magnitude of the repulsive function (3.8) tends towards infinity as the distance r approaches d_0 . It is therefore impossible for two agents to get closer than a distance of d_0 and thus collision avoidance is guaranteed. However, the problem with this function is that it is unbounded. The first issue with an unbounded function is that it is not physically implementable. The second issue, which is equally serious, is that, if two agents happen to be too close to each other, the force applied to separate them can become so large that the agents will move away from each other with such high acceleration that flocking becomes impossible.

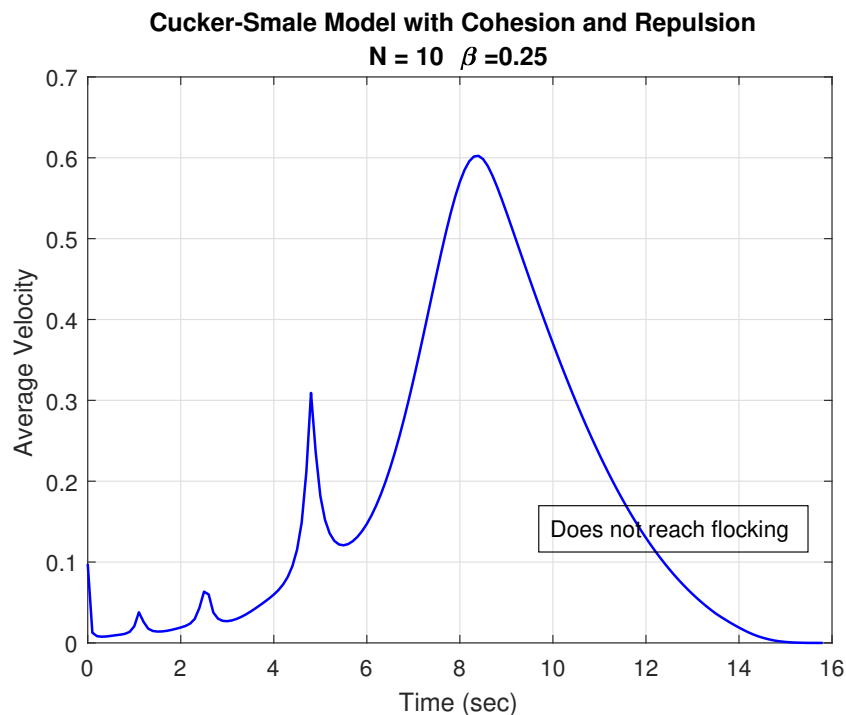


Figure 3.10: Average Velocity with Unbounded Repulsive Force

An example of divergence is shown in Figure 3.10 where 10 agents and $k = 1$ could not reach flocking with the unbounded repulsive force. The agents attempted to align their velocities and the average velocity reached a peak of 0.6. But the average velocity

Table 3.6: Distances between Any Two Agents

Agent	1	2	3	4	5	6	7	8	9	10
1	0	0.0135	19.3774	0.0214	0.1348	18.7886	0.0213	0.0130	0.0021	0.0059
2	0.0135	0	19.3784	0.0146	0.1380	18.7891	0.0110	0.0013	0.0151	0.0163
3	19.3774	19.3780	0	19.3637	19.2442	0.5890	19.3687	19.3791	19.3759	19.3718
4	0.0214	0.0146	19.3637	0	0.1249	18.7748	0.0059	0.0159	0.0217	0.0197
5	0.1348	0.1380	19.2442	0.1249	0	18.6553	0.1307	0.1389	0.1330	0.1289
6	18.7886	18.7891	0.5890	18.7748	18.6553	0	18.7798	18.7902	18.7870	18.7829
7	0.0213	0.0110	19.3687	0.0059	0.1307	18.7798	0	0.0123	0.0221	0.0212
8	0.0130	0.0013	19.3791	0.0159	0.1389	18.7902	0.0123	0	0.0147	0.0162
9	0.0021	0.0151	19.3759	0.0217	0.1330	18.7870	0.0221	0.0147	0	0.0041
10	0.0059	0.0163	19.3781	0.0197	0.1289	18.7829	0.0212	0.0162	0.0041	0

Table 3.7: Distances between agents after 10 seconds

Agent	1	2	3	4	5	6	7	8	9	10
1	0	0.0135	19.3774	0.0214	0.1348	18.7886	0.0213	0.0130	0.0021	0.0059
2	0.0135	0	19.3784	0.0146	0.1380	18.7891	0.0110	0.0013	0.0151	0.0163
3	19.3774	19.3780	0	19.3637	19.2442	0.5890	19.3687	19.3791	19.3759	19.3718
4	0.0214	0.0146	19.3637	0	0.1249	18.7748	0.0059	0.0159	0.0217	0.0197
5	0.1348	0.1380	19.2442	0.1249	0	18.6553	0.1307	0.1389	0.1330	0.1289
6	18.7886	18.7891	0.5890	18.7748	18.6553	0	18.7798	18.7902	18.7870	18.7829
7	0.0213	0.0110	19.3687	0.0059	0.1307	18.7798	0	0.0123	0.0221	0.0212
8	0.0130	0.0013	19.3791	0.0159	0.1389	18.7902	0.0123	0	0.0147	0.0162
9	0.0021	0.0151	19.3759	0.0217	0.1330	18.7870	0.0221	0.0147	0	0.0041
10	0.0059	0.0163	19.3781	0.0197	0.1289	18.7829	0.0212	0.0162	0.0041	0

started dropping from that point because two agents were getting too close to each other. The acceleration away from each other was very high. Consequently, there was no way these agents could be pulled back together. Table 3.7 shows the distance between agents after 10 seconds. The maximum distance reaches 19.3781. Thus unbounded repulsive forces are problematic.

3.3 An Augmented Cucker-Smale Model

In view of the discussions in Sections 3.2.2 and 3.2.3 above, an augmented Cucker-Smale model that explicitly incorporates cohesive and repulsive force functions is proposed. Cohesive and repulsive forces could be incorporated explicitly into the original Cucker-Smale model (2.4). This augmented Cucker-Smale model could be

expressed as:

$$\begin{cases} \dot{p}_i = v_i \\ \dot{v}_i = \frac{1}{N} \sum_{j=1}^N \psi(\|p_j - p_i\|^2) (v_j - v_i) \\ \quad + \sum_{j \neq i} f(\|p_j - p_i\|^2) (p_j - p_i) \\ \quad + \sum_{j \neq i} \phi(\|p_j - p_i\|^2) (p_j - p_i) \end{cases} \quad (3.9)$$

for $1 \leq i \leq N$. Here, ϕ and f are the cohesive and repulsive force functions respectively.

The second and third terms for \dot{v}_i in (3.9) could be combined to make the model more concise since they essentially have the same form. Hence we have

$$\begin{cases} \dot{p}_i = v_i \\ \dot{v}_i = \frac{1}{N} \sum_{j=1}^N \psi(\|p_j - p_i\|^2) (v_j - v_i) \\ \quad + \sum_{j \neq i} H(\|p_j - p_i\|^2) (p_j - p_i) \end{cases} \quad (3.10)$$

When the distance between any two agents $r = \|p_j - p_i\|$ is less than collision avoidance distance d_1 , H will act like the repulsive force function f . Otherwise, it acts like the cohesive force function ϕ .

The main advantage of this proposed model is that the cohesion and repulsion parts of the force function could be independently designed. There are an infinite number of choices for these functions. In the following sections, we shall explore the use of unbounded and bounded functions for repulsion in conjunction with a bounded sigmoidal function for cohesion.

3.3.1 Unbounded Repulsion and Bounded Cohesion Forces

The bounded cohesive force function (3.7) can be combined with the repulsive force function given by (3.8) to give us $H(r)$ which is plotted in Figure 3.11. In this case, the repulsive function is unbounded while the cohesive function is bounded. The

unbounded repulsive function will ensure that absolutely no collision will occur. The only parameters that determine the shape of H are θ and k .

Remark 3.2. While the function $H(r)$ should be continuous in r , it needs not be smooth.

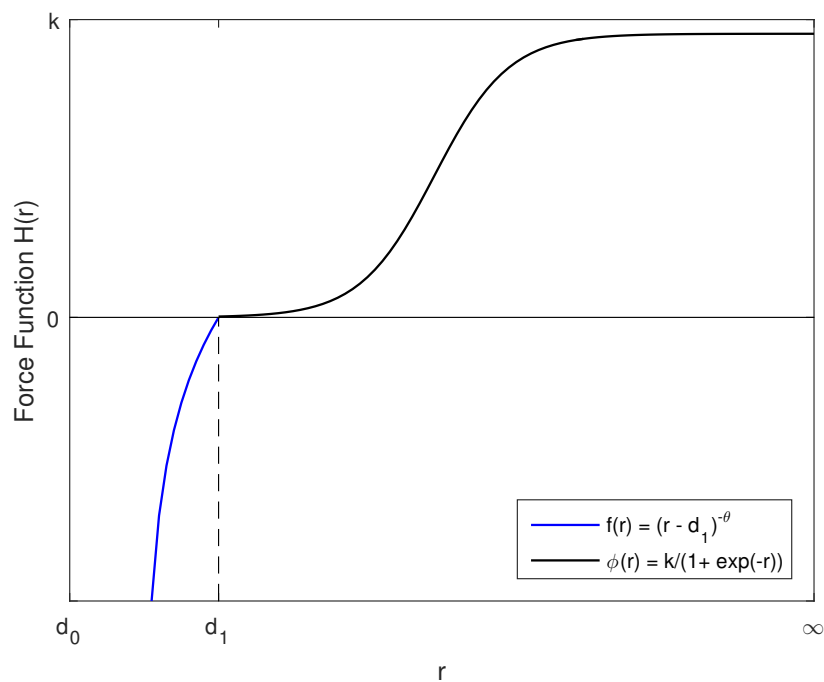


Figure 3.11: The Unbounded Repulsive and Bounded Cohesive Force Function

As demonstrated in Section 3.2.3, the system often finds it difficult to flock with unbounded repulsive forces. Therefore this function is not practical.

3.3.2 Unbounded Cohesive and Bounded Repulsive Forces

Bounded repulsive and cohesive forces were first introduced in [88] for the flocking of a second-order multi-agent system given by

$$\begin{cases} \dot{p}_i = v_i \\ \dot{v}_i = \frac{1}{N} \sum_{j=1}^N \psi(\|p_j - p_i\|) (v_j - v_i) \\ \quad + k_a \sum_{j=1}^N \frac{r_{ij} - \eta}{r_{ij}} (p_j - p_i) \\ \quad - \sum_{j=1}^N \nabla_{x_j} f(\|p_j - p_i\|) \end{cases} \quad (3.11)$$

where $k_a > 0$, $\eta > 0$, and $r_{ij} = |p_j - p_i|$. This system is based on the Cucker-Smale model with a cohesive force that is linearly proportional to the difference in position of any two agents. It also has a repulsive term which is related to the gradient of a bounded repulsive function with a bounded gradient. The authors are able to show that velocity alignment can be reached regardless of the value of β in the communication rate function (2.5). A possible bounded repulsive has been given as:

$$f(\|p_j - p_i\|) = Q * \exp(-\mu\|p_j - p_i\|^2) \quad for \quad \|p_j - p_i\| > 0, \quad (3.12)$$

where $0 < Q < \infty$ and $\mu > 0$. As long as Q is greater than the initial value of an energy function, collision will not occur.

It should be noted that even though in practice, the cohesive force is finite since r_{ij} is finite, the cohesive term $k_a \sum_{j=1}^N \frac{r_{ij} - \eta}{r_{ij}} (p_j - p_i)$ in (3.11) is still unbounded with respect to $(p_j - p_i)$.

3.3.3 Symmetric Bounded Cohesive and Repulsive Forces

Inspired by the finite repulsive force function (3.12), we propose to combine it with the bounded cohesive force function (3.7) we have considered earlier in Section 3.2.2. Furthermore, these two functions are made to be complementary to each other so that there is an equilibrium point where the two forces are equal. Thus we have the cohesive force ϕ and the repulsive force f defined by

$$\begin{cases} \phi(r) = \frac{M}{1+\exp(-k(r-d_1))} \\ f(r) = \frac{M}{1+\exp(k(r-d_1))} \end{cases} \quad (3.13)$$

where r is the distance between two agents. Figure 3.12 plots these two functions graphically. The constants M and k control the magnitude and the gradient of the cohesive and repulsive forces respectively. The equilibrium point d_1 controls the asymptotic distance between the agents. If the agents have a physical size of d_0 , then the functions could be shifted by this amount along the x -axis.

Combining ϕ and f from the equation (3.13), the function $H(r)$ in the augmented Cucker-Smale model (3.10) is given by

$$\begin{aligned} H(r) &= f(r) - \phi(r) \\ &= \frac{M}{1 + \exp(k(r - d_1))} - \frac{M}{1 + \exp(-k(r - d_1))} \end{aligned}$$

3.3.3.1 Simulation Results

Performance using the symmetric forces will now be examined. The following parameters are used in the simulations. The initial field size is 10^2 and the initial heading of the agents is randomly generated with a uniform distribution over $[0, 2\pi)$. The other parameters are: $d_0 = 0.5$, $d_2 = 9$, $\beta = 0.25$, and $k = 1$. The flock diameter results

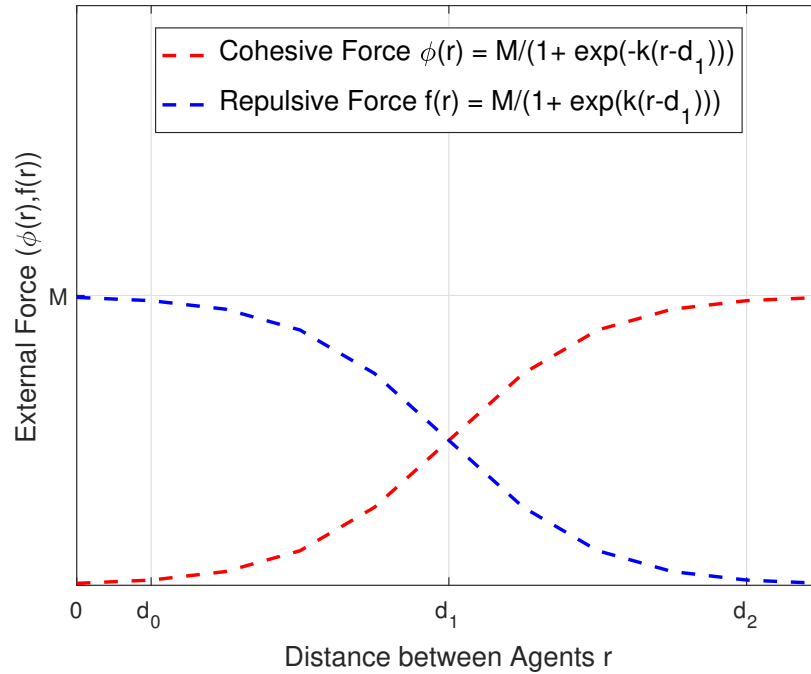


Figure 3.12: Symmetric Cohesive and Repulsive Force Functions

are shown in Tables 3.8 and 3.9. Note that in all the cases shown in these tables, the minimum distance between agents is always greater than d_0 and so collision does not occur.

Table 3.8: Flock Diameter for Different Values of d_1 with $M = 1$

Number of Agents	$d_1 = 5$			$d_1 = 7$		
	<i>Initial</i>	<i>Final</i>	<i>Min</i>	<i>Initial</i>	<i>Final</i>	<i>Min</i>
$N = 10$	10.9532	6.7375	2.1335	10.7199	9.6800	2.9211
$N = 30$	11.3565	6.7175	0.7476	12.1343	10.0644	1.3292
$N = 60$	11.9131	6.9377	0.5844	12.2132	10.1193	0.7738
$N = 90$	12.5143	6.9351	0.6799	12.4900	10.1573	0.5812
$N = 120$	12.7092	6.8539	0.5705	13.2414	10.1601	0.6036
$N = 150$	13.1360	6.8711	0.5420	13.4521	10.1209	0.5295

Table 3.8 shows the flock diameters for different values of d_1 while keeping $M = 1$. The system is able to reach flocking in all cases for $d_1 = 5$ and $d_1 = 7$. However, for $d_1 = 3$, the system reached flocking only when $N = 10$. The system will not align for larger values of N . This implies that d_1 is a crucial parameter in the augmented

Table 3.9: Flock Diameter for Different Values of M

Number of Agents	$M = 1$			$M = 2$			$M = 3$		
	<i>Initial</i>	<i>Final</i>	<i>Min</i>	<i>Initial</i>	<i>Final</i>	<i>Min</i>	<i>Initial</i>	<i>Final</i>	<i>Min</i>
$N = 10$	10.1284	6.7957	1.5387	10.5769	6.7949	1.6292	11.0122	6.8277	1.4599
$N = 30$	11.3565	6.9175	0.7246	11.3525	6.7901	0.6604	11.7821	6.8112	0.6576
$N = 60$	12.6185	6.9377	0.6482	12.3182	6.7456	0.6403	12.4106	6.7576	0.6300
$N = 90$	12.5143	6.9351	0.7148	12.8506	6.7188	0.5542	13.1648	6.7380	0.5156
$N = 120$	12.7092	6.8539	0.5905	12.9651	6.7343	0.5250	13.2626	6.7145	0.5290
$N = 150$	13.1360	6.8711	0.5030	13.0614	6.7006	0.5037	13.4879	6.7113	0.5043

Cucker-Smale model with the symmetric bounded cohesive and repulsive forces. If the d_1 is too small, the repulsive force becomes very large so that the agents are pushed away from each other. Interestingly, Table 3.9 shows that when we adjust the coefficient M , there is no obvious difference with the final flock size.

Figure 3.13 compares the flocking times of the augmented Cucker-Smale model with different parameter values. In general, agents need more time to achieve flocking with cohesive and repulsive forces. The results in Figure 3.13(a) show that when d_1 is increased, flocking time increases too. However, the flocking time decreases when the coefficient M increases the Figure 3.13 (b) shows that the flocking time decreases when the coefficient M increases.

3.4 Summary

This chapter introduced the technical definition of flocking in terms of the average velocity and flock diameter. An augmented Cucker-Smale model is proposed which adds cohesion and repulsion terms to the original Cucker-Smale model. These terms allow us to control how closely the agents are flocking while preventing them from colliding. It was shown that unbounded repulsive forces as proposed in the literature will cause problems, both in terms of the practicality of implementation and also in potentially causing the agents to diverge. A symmetrical bounded force function based

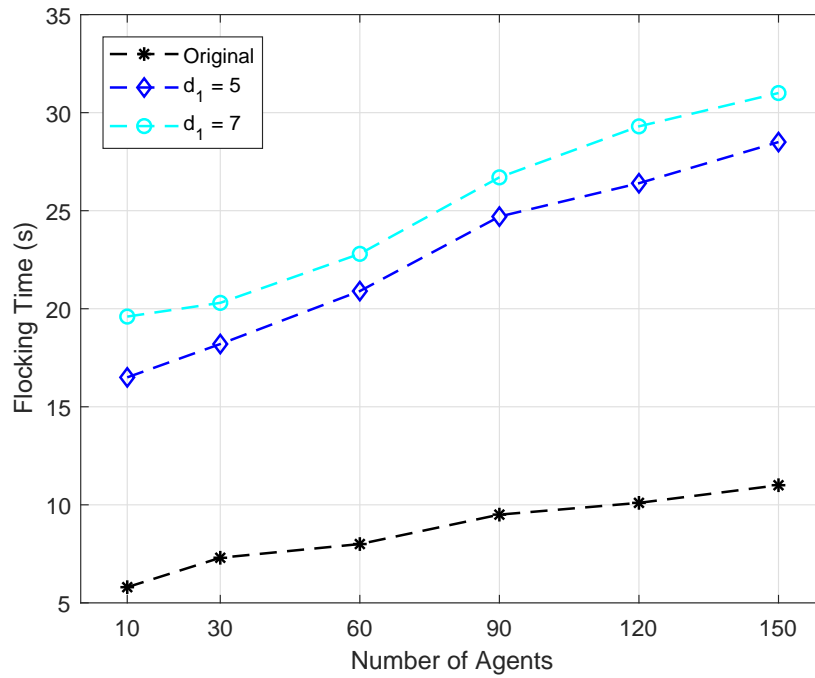
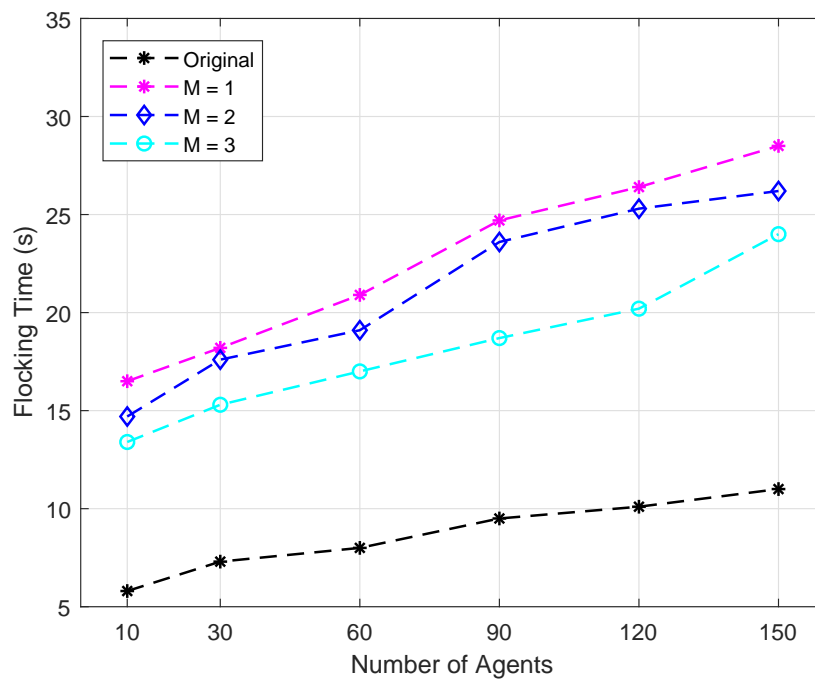
(a) Flocking Time for Different d_1 (b) Flocking Time for Different M

Figure 3.13: Flocking Time in Different Parameters

on the logistic function has been proposed. Through simulation, this function has been shown to be both functional and practical that helps to avoid collision and keeps the flock tight.

Part of the original research presented in this chapter has been published in [152].

Chapter 4

Finite-time Flocking Control

It has been shown in the previous chapter that the proposed augmented Cucker-Smale model proposed is able to achieve flocking without collision in a sufficiently long time. In practical applications, we often need the agents to flock in a time-optimal manner. This can be achieved using finite-time control. In this chapter, finite-time control is applied to augmented Cucker-Smale system. This system is proven to be asymptotically stable, and the time to flocking is derived. Simulations show that flocking can indeed be achieved within this time. The effects of the control parameters on the alignment time will also be studied.

4.1 Preliminaries

A number of non-Lipschitz continuous finite-time equations have been proposed [35]. The following one has been successfully applied to the original Cucker-Smale model [145]:

$$\operatorname{sgn}(x)^\theta = \operatorname{sign}(x)|x|^\theta \quad (4.1)$$

where

$$\operatorname{sgn}(x) = \begin{cases} 1, & x > 0 \\ 0, & x = 0 \\ -1, & x < 0 \end{cases} \quad (4.2)$$

Most significantly, by using Lyapunov stability theory, the authors were able to derive an upper bound for the settling time.

The augmented Cucker-Smale model (3.10) with a combined cohesion and repulsion force function which is proposed in Section 3.3 is given by

$$\begin{cases} \dot{p}_i = v_i \\ \dot{v}_i = \frac{1}{N} \sum_{j=1}^N \psi(\|p_j - p_i\|) (v_j - v_i) \\ \quad + \sum_{j \neq i} H(\|p_j - p_i\|) (p_j - p_i) \end{cases} \quad (4.3)$$

Applying the finite-time control law (4.1) to $(v_j - v_i)$ and $(p_j - p_i)$ in this model, we have

$$\begin{cases} \dot{p}_i = v_i \\ \dot{v}_i = \frac{1}{N} \sum_{j=1}^N \psi(\|p_j - p_i\|) \operatorname{sgn}(v_j - v_i)^\theta \\ \quad + \sum_{j \neq i} H(\|p_j - p_i\|) \operatorname{sgn}(p_j - p_i)^\alpha \end{cases} \quad (4.4)$$

for $1 \leq i \leq N$.

The following lemma is important for establishing an upper bound on the convergence time.

Lemma 4.1. *Let $\bar{p} = \frac{1}{N} \sum_{i=1}^N p_i$ and $\bar{v} = \frac{1}{N} \sum_{i=1}^N v_i$. Further, let $\hat{p}_i = p_i - \bar{p}$ and $\hat{v}_i = v_i - \bar{v}$. The system given by (4.4) is unchanged if the variables p_i and v_i are substituted by \hat{p}_i and \hat{v}_i respectively.*

Proof. It is obvious that

$$\begin{aligned} v_j - v_i &= (v_j - \bar{v}) - (v_i - \bar{v}) = \hat{v}_j - \hat{v}_i \\ p_j - p_i &= (p_j - \bar{p}) - (p_i - \bar{p}) = \hat{p}_j - \hat{p}_i \end{aligned}$$

Thus the system defined by (4.4) remains unchanged by the substitution. ■

As a result, in the subsequent proofs, we will use v_i and \hat{v}_i interchangeably. Similarly for p_i and \hat{p}_i .

Also, the total deviation from the average position and velocity is zero. That is,

$$\sum_{i=1}^N \hat{p}_i = \sum_{i=1}^N p_i - N\bar{p} = 0 \quad (4.5)$$

$$\sum_{i=1}^N \hat{v}_i = \sum_{i=1}^N v_i - N\bar{v} = 0 \quad (4.6)$$

The following lemma is first established in [135] which provides an upper bound on the convergence time in a finite-time controlled system.

Lemma 4.2. *Assume that a continuous, positive-definite function $V(t)$ satisfies the following differential inequality:*

$$\dot{V}(t) \leq -kV^\rho(t) \quad (4.7)$$

where k, ρ are constants. Then, for any given t_0 , $V(t)$ satisfies the following inequality:

$$V^{1-\rho}(t) \leq V^{1-\rho}(t_0) - k(1-\rho)(t-t_0) \quad (4.8)$$

for $t_0 \leq t \leq t_1$ and $V(t) \equiv 0, t \geq t_1$ with t_1 is given by

$$t_1 = t_0 + \frac{V(t_0)^{1-\rho}}{k(1-\rho)} \quad (4.9)$$

The following lemma was originally stated and proven in [144]. Its proof is included in Appendix A for the sake of completeness and ease of reference.

Lemma 4.3. *Suppose function ϕ satisfies $\phi(x_i, x_j) = -\phi(x_j, x_i)$, $i, j \in N, i \neq j$. Then for a group of numbers y_1, y_2, \dots, y_N ,*

$$\sum_{i=1}^N \sum_{j=1}^N y_i \phi(x_j, x_i) = -\frac{1}{2} \sum_{i=1}^N \sum_{j=1}^N (y_j - y_i) \phi(x_j - x_i) \quad (4.10)$$

The following two lemmas can be found in [153].

Lemma 4.4. *Let $a_1, a_2, \dots, a_n > 0$ and $0 < r < p$. Then*

$$\left(\sum_{i=1}^n a_i^p \right)^{1/p} \leq \left(\sum_{i=1}^n a_i^r \right)^{1/r}. \quad (4.11)$$

Lemma 4.5. *If $\xi_1, \xi_2, \dots, \xi_n \geq 0$ and $0 < p \leq 1$, then the following inequality holds:*

$$\left(\sum_{i=1}^n \xi_i \right)^p \leq \sum_{i=1}^n \xi_i^p. \quad (4.12)$$

4.2 Main Results

4.2.1 Asymptotic Convergence

Since not all finite-time controlled systems are asymptotically stable, the first result is to establish that (4.4) is asymptotically convergent.

Theorem 4.6 (Asymptotic Convergence). *The velocities of the agents in the finite-time controlled augmented Cucker-Smale model defined by (4.4) converges asymptotically to the same velocity.*

Proof. Consider the non-negative function given by

$$V(t) = \sum_{i=1}^N v_i^2(t) + \frac{1}{N} \sum_{i=1}^N \sum_{j \neq i} \int_0^{p_j - p_i} H(\|p_j - p_i\|) \operatorname{sgn}(p_j - p_i)^\alpha dt \quad (4.13)$$

Proving the asymptotic convergence of velocity is the same as proving that $\dot{V}(t)$ is always less than zero.

Let

$$V_1(t) = \sum_{i=1}^N v_i^2(t) \quad (4.14)$$

Its derivative is given by

$$\dot{V}_1(t) = \sum_{i=1}^N 2v_i(t)\dot{v}_i(t) \quad (4.15)$$

Replacing $\dot{v}_i(t)$ by the system equation (4.4), we have

$$\begin{aligned} \dot{V}_1(t) &= 2 \sum_{i=1}^N v_i \left[\frac{1}{N} \sum_{j=1}^N \psi(\|p_j - p_i\|) \operatorname{sgn}(v_j - v_i)^\theta \right. \\ &\quad \left. + \frac{1}{N} H(\|p_j - p_i\|) \operatorname{sgn}(p_j - p_i)^\alpha \right] \\ &= \frac{2}{N} \sum_{i=1}^N \sum_{j \neq i} v_i \psi(\|p_j - p_i\|) \operatorname{sgn}(v_j - v_i)^\theta \\ &\quad + \frac{2}{N} \sum_{i=1}^N \sum_{j \neq i} v_i H(\|p_j - p_i\|) \operatorname{sgn}(p_j - p_i)^\alpha \end{aligned} \quad (4.16)$$

Applying Lemma (4.3) to the two terms on the right-hand-side of 4.16, we have

$$\begin{aligned}
& \frac{2}{N} \sum_{i=1}^N \sum_{j \neq i} v_i \psi(\|p_j - p_i\|) \operatorname{sgn}(v_j - v_i)^\theta \\
&= -\frac{1}{N} \sum_{i=1}^N \sum_{j \neq i} (v_j - v_i) \operatorname{sgn}(v_j - v_i)^\theta \psi(\|p_j - p_i\|) \\
&= -\frac{1}{N} \sum_{i=1}^N \sum_{j \neq i} (v_j - v_i) \operatorname{sign}(v_j - v_i) |v_j - v_i|^\theta \psi(\|p_j - p_i\|) \\
&= -\frac{1}{N} \sum_{i=1}^N \sum_{j \neq i} |v_j - v_i|^{\theta+1} \psi(\|p_j - p_i\|)
\end{aligned}$$

since $(v_j - v_i) \operatorname{sign}(v_j - v_i) = |v_j - v_i|$, and

$$\begin{aligned}
& \frac{2}{N} \sum_{i=1}^N \sum_{j \neq i} v_i H(\|p_j - p_i\|) \operatorname{sgn}(p_j - p_i)^\alpha \\
&= -\frac{1}{N} \sum_{i=1}^N \sum_{j \neq i} (v_j - v_i) \operatorname{sgn}(p_j - p_i)^\alpha H(\|p_j - p_i\|)
\end{aligned}$$

Let

$$V_2(t) = \frac{1}{N} \sum_{i=1}^N \sum_{j \neq i} \int_0^{p_j - p_i} H(\|p_j - p_i\|) \operatorname{sgn}(p_j - p_i)^\alpha dt \quad (4.17)$$

Then,

$$\begin{aligned}
\dot{V}_2(t) &= \frac{1}{N} \sum_{i=1}^N \sum_{j \neq i} H(\|p_j - p_i\|) \operatorname{sgn}(p_j - p_i)^\alpha [\dot{p}_j - \dot{p}_i] \\
&= \frac{1}{N} \sum_{i=1}^N \sum_{j \neq i} H(\|p_j - p_i\|) \operatorname{sgn}(p_j - p_i)^\alpha (v_j - v_i)
\end{aligned} \quad (4.18)$$

Since $V(t) = V_1(t) + V_2(t)$, we have

$$\dot{V}(t) = \dot{V}_1(t) + \dot{V}_2(t) \quad (4.19)$$

$$\begin{aligned} &= -\frac{1}{N} \sum_{i=1}^N \sum_{j \neq i}^N |v_j - v_i|^{\theta+1} \psi(\|p_j - p_i\|) \\ &\quad - \frac{1}{N} \sum_{i=1}^N \sum_{j \neq i}^N (v_j - v_i) \operatorname{sgn}(p_j - p_i)^\alpha H(\|p_j - p_i\|) \\ &\quad + \frac{1}{N} \sum_{i=1}^N \sum_{j \neq i}^N H(\|p_j - p_i\|) \operatorname{sgn}(p_j - p_i)^\alpha (v_j - v_i) \end{aligned} \quad (4.20)$$

The last two terms of (4.20) cancel each other. Hence, given that the communication rate function ψ is non-negative,

$$\begin{aligned} \dot{V}(t) &= -\frac{1}{N} \sum_{i=1}^N \sum_{j \neq i}^N |v_j - v_i|^{\theta+1} \psi(\|p_j - p_i\|) \\ &\leq 0 \end{aligned}$$

Since $V(t) \geq 0$ and the $\dot{V}(t) \leq 0$, the Cucker-Smale finite-time system is asymptotically stable. ■

4.2.2 Finite-time Convergence

Theorem 4.7 (Finite-time Convergence). *The velocities of the autonomous agents in the system given by (4.4) converges to the same velocity in a finite amount of time given by*

$$T_f \leq C_f N^{-\frac{\gamma-1}{2}} \quad (4.21)$$

where

$$C_f = \frac{2W(0)^{\frac{1-\gamma}{2}}}{(\psi^* + M)(1-\gamma)(\sqrt{2})^{\gamma-1}} \quad (4.22)$$

$$\gamma = \min(\theta, \alpha) \quad (4.23)$$

$$W(t) = \sum_{i=1}^N \|v_i(t)\|^2 \quad (4.24)$$

under the following conditions:

1. There exists $\psi^* > 0$ such that $\inf_{s \geq 0} \psi(s) \geq \psi^*$.
2. There exists a constant M such that $H(\|p_j - p_i\|^2) \geq M$ for all $i \neq j$ and $t \in [0, T_f)$.

Proof. Let $W(t) = \sum_{i=1}^N v_i^2(t)$. Then we have

$$\begin{aligned} \dot{W}(t) &= \sum_{i=1}^N 2v_i(t)\dot{v}_i(t) \\ &= \frac{2}{N} \sum_{i=1}^N \sum_{j \neq i} v_i \psi(\|p_j - p_i\|) \operatorname{sgn}(v_j - v_i)^\theta \\ &\quad + \frac{2}{N} \sum_{i=1}^N \sum_{j \neq i} v_i H(\|p_j - p_i\|) \operatorname{sgn}(p_j - p_i)^\alpha \end{aligned} \quad (4.25)$$

Denote the two terms of $\dot{W}(t)$ above by $\dot{W}_0(t)$ and $\dot{W}_1(t)$ respectively. Using Lemma 4.3,

we have,

$$\begin{aligned} \dot{W}_0(t) &= \frac{2}{N} \sum_{i=1}^N \sum_{j \neq i} v_i \psi(\|p_j - p_i\|) \operatorname{sgn}(v_j - v_i)^\theta \\ &= -\frac{1}{N} \sum_{i=1}^N \sum_{j \neq i} \psi(\|p_j - p_i\|) (v_j - v_i) \operatorname{sgn}(v_j - v_i)^\theta \\ &= -\frac{1}{N} \sum_{i=1}^N \sum_{j \neq i} \psi(\|p_j - p_i\|) (v_j - v_i) \operatorname{sign}(v_j - v_i) |v_j - v_i|^\theta \\ &= -\frac{1}{N} \sum_{i=1}^N \sum_{j \neq i} \psi(\|p_j - p_i\|) |v_j - v_i|^{\theta+1} \end{aligned} \quad (4.26)$$

since $(v_j - v_i)\text{sign}(v_j - v_i) = |v_j - v_i|$. Under the condition that $\inf_{s \geq 0} \psi(s) \geq \psi^*$,

$$\begin{aligned} \dot{W}_0(t) &\leq -\frac{1}{N} \sum_{i=1}^N \sum_{j \neq i}^N \psi^* |v_j - v_i|^{\theta+1} \\ &= -\frac{1}{N} \sum_{i=1}^N \sum_{j \neq i}^N \psi^* (|v_j - v_i|^2)^{\frac{\theta+1}{2}} \end{aligned} \quad (4.27)$$

Given (4.6), we can establish that

$$\begin{aligned} \sum_{i=1}^N \sum_{j=1}^N |v_i - v_j|^2 &= N \sum_{i=1}^N \sum_{j=1}^N (v_i^2 + v_j^2 - 2|v_i||v_j|) \\ &= N \sum_{i=1}^N v_i^2 + N \sum_{j=1}^N v_j^2 - 2 \sum_{i=1}^N |v_i| \sum_{j=1}^N |v_j| \\ &= 2NW(t) \end{aligned} \quad (4.28)$$

Using (4.28) and Lemma 4.5, (4.27) becomes

$$\begin{aligned} \dot{W}_0(t) &\leq -\frac{1}{N} \psi^* \sum_{i=1}^N \sum_{j \neq i}^N (|v_j - v_i|^2)^{\frac{\theta+1}{2}} \\ &\leq -\frac{1}{N} \psi^* \left(\sum_{i=1}^N \sum_{j \neq i}^N |v_j - v_i|^2 \right)^{\frac{\theta+1}{2}} \\ &= -\frac{1}{N} \psi^* (2N)^{\frac{\theta+1}{2}} W(t)^{\frac{\theta+1}{2}} \end{aligned}$$

Now for the second term of $\dot{W}(t)$ in (4.25), we have

$$\begin{aligned} \dot{W}_1(t) &= \frac{2}{N} \sum_{i=1}^N \sum_{j \neq i}^N v_i H(\|p_j - p_i\|) \text{sgn}(p_j - p_i)^\alpha \\ &= -\frac{1}{N} \sum_{i=1}^N \sum_{j \neq i}^N (v_j - v_i) H(\|p_j - p_i\|) \text{sgn}(p_j - p_i)^\alpha \\ &= -\frac{1}{N} \sum_{i=1}^N \sum_{j \neq i}^N (v_j - v_i) H(\|p_j - p_i\|) \text{sign}(p_j - p_i)^\alpha |p_j - p_i|^\alpha \end{aligned}$$

If there exists a constant M such that, for all $i \neq j$ and $t \in [0, T_f)$, $H(\|p_j - p_i\|) \geq M$,

then

$$\begin{aligned}
\dot{W}_1(t) &\leq -\frac{M}{N} \sum_{i=1}^N \sum_{j \neq i}^N (v_j - v_i) \operatorname{sgn}(p_j - p_i)^\alpha \\
&= -\frac{M}{N} \sum_{i=1}^N \sum_{j \neq i}^N (v_j - v_i) \operatorname{sign}(p_j - p_i) |p_j - p_i|^\alpha \\
&\leq -\frac{M}{N} \sum_{i=1}^N \sum_{j \neq i}^N (v_j - v_i) |p_j - p_i|^\alpha \\
&= -\frac{M}{N} \sum_{i=1}^N \sum_{j \neq i}^N (v_j - v_i) \left| \int_0^{T_f} v_j(t) dt - \int_0^{T_f} v_i(t) dt \right|^\alpha \\
&= -\frac{M}{N} \sum_{i=1}^N \sum_{j \neq i}^N (v_j - v_i) |(v_j(t) - v_i(t)) + (v_i(0) - v_j(0))|^\alpha
\end{aligned}$$

Since $0 < \alpha < 1$, we can use Lemma 4.5, and the fact that $|(v_i(0) - v_j(0))|$ is a constant for a given initial configuration to obtain

$$\begin{aligned}
\dot{W}_1(t) &= -\frac{1}{N} M \sum_{i=1}^N \sum_{j \neq i}^N (v_j - v_i) |(v_j(t) - v_i(t)) + (v_i(0) - v_j(0))|^\alpha \\
&\leq -\frac{M}{N} \sum_{i=1}^N \sum_{j \neq i}^N (v_j - v_i) (|v_j(t) - v_i(t)|^\alpha + |v_i(0) - v_j(0)|^\alpha) \\
&\leq -\frac{M}{N} \sum_{i=1}^N \sum_{j \neq i}^N (v_j - v_i) |v_j(t) - v_i(t)|^\alpha \\
&\leq -\frac{M}{N} \sum_{i=1}^N \sum_{j \neq i}^N |v_j - v_i|^{\alpha+1} \\
&= -\frac{M}{N} \sum_{i=1}^N \sum_{j \neq i}^N (|v_j - v_i|^2)^{\frac{\alpha+1}{2}}
\end{aligned}$$

With (4.28) and Lemma 4.5, we get

$$\begin{aligned}
\dot{W}_1(t) &\leq -\frac{M}{N} \left(\sum_{i=1}^N \sum_{j \neq i}^N (|v_j - v_i|^2) \right)^{\frac{\alpha+1}{2}} \\
&= -\frac{1}{N} M (2N)^{\frac{\alpha+1}{2}} W(t)^{\frac{\alpha+1}{2}}
\end{aligned}$$

Thus,

$$\begin{aligned}
\dot{W}(t) &= \dot{W}_0(t) + \dot{W}_1(t) \\
&\leq -\frac{1}{N}\psi^*(2N)^{\frac{\theta+1}{2}}W(t)^{\frac{\theta+1}{2}} - \frac{1}{N}M(2N)^{\frac{\alpha+1}{2}}W(t)^{\frac{\alpha+1}{2}} \\
&\leq -\frac{1}{N}\psi^*(2N)^{\frac{\gamma+1}{2}}W(t)^{\frac{\gamma+1}{2}} - \frac{1}{N}M(2N)^{\frac{\gamma+1}{2}}W(t)^{\frac{\gamma+1}{2}} \\
&= -\frac{(2N)^{\frac{\gamma+1}{2}}}{N}(\psi^* + M)W(t)^{\frac{\gamma+1}{2}}
\end{aligned}$$

where $\gamma = \min(\theta, \alpha)$.

Applying Lemma 4.2 with $t_0 = 0$ and $\rho = \frac{\gamma+1}{2}$, we have

$$T_f = C_f N^{-\frac{\gamma-1}{2}}$$

where

$$C_f = \frac{2W(0)^{\frac{1-\gamma}{2}}}{(\psi^* + M)(1-\gamma)(\sqrt{2})^{\gamma+1}}$$

Hence the theorem is proved. ■

Remark 4.8. Note that T_f increases as N increases since $0 < \gamma < 1$. This is in line with the results obtained using the augmented Cucker-Smale model in Chapter 3. However, this is in contrast with existing results for finite-time flocking based on the original Cucker-Smale model where the alignment time decreases as the size of the flock increases. It is reasonable to attribute this effect to the inclusion of collision avoidance in the system.

4.2.3 Flock Diameter

In addition to alignment of velocity, flocking requires that the flock diameter be finite.

Theorem 4.9. For the finite-time controlled augmented Cucker-Smale model given by (4.4), the flock diameter is finite for $t \geq T_f$ where T_f is given by Theorem 4.7.

Proof. Let $P(t) = \sum_{i=1}^N p_i^2$. Then by (4.5) and similar to (4.28), we have

$$\sum_{i=1}^N \sum_{j=1}^N N |p_i - p_j|^2 = 2NP(t)$$

Proving that the flock diameter is finite is equivalent to proving that

$$\sup_{0 \leq t \leq \infty} P(t) < \infty \quad (4.29)$$

Now,

$$\begin{aligned} \dot{P}(t) &= \sum_{i=1}^N 2p_i \cdot \dot{p}_i \\ &= 2 \sum_{i=1}^N p_i \cdot v_i \\ &\leq 2 \left(\sum_{i=1}^N \|p_i\| \right) \left(\sum_{i=1}^N \|v_i\| \right) \\ &\leq 2P^{\frac{1}{2}}(t)W^{\frac{1}{2}}(t) \end{aligned}$$

Assume that $P(t) \leq \Gamma(t)$, where $\Gamma(t)$ for all t with the initial condition $\Gamma(0) = P(0) = \|p(0)\|^2$. Using the comparison theorem of differential equations, we can solve the differential equation

$$\dot{\Gamma}(t) = 2\Gamma^{\frac{1}{2}}(t)W^{\frac{1}{2}}(t)$$

Let $z(t) = \Gamma^{\frac{1}{2}}(t)$, this differential equation becomes

$$\begin{aligned} 2z(t)\dot{z}(t) &= 2z(t)W^{\frac{1}{2}}(t) \\ \implies \dot{z}(t) &= W^{\frac{1}{2}}(t) \end{aligned}$$

Hence,

$$\Gamma^{\frac{1}{2}}(t) = \Gamma^{\frac{1}{2}}(0) + \int_0^t W^{\frac{1}{2}}(s)ds$$

This gives us

$$P^{\frac{1}{2}}(t) \leq P^{\frac{1}{2}}(0) + \int_0^t W^{\frac{1}{2}}(s) ds$$

Since $W(t) \equiv 0$ for $t > T_f$, we only need to integrate $W(t)$ up to $t = T_f$

$$\begin{aligned} P^{\frac{1}{2}}(t) &\leq P^{\frac{1}{2}}(0) + \int_0^{T_f} W^{\frac{1}{2}}(s) ds \\ &\leq P^{\frac{1}{2}}(0) + T_f W(0) \end{aligned}$$

since $W(t) \leq W(0)$. Thus $P^{\frac{1}{2}}(t) < \infty$ and the flock diameter is finite for $t > T_f$. ■

4.3 Simulation

The alignment time given by (4.24) in Theorem 4.7 will be compared with computer simulation results. For convenience, distances and time shall be dimensionless. Each agent moves with the same speed of 0.5 per unit time but initially in a random direction. The initial direction is uniformly random in $[0, 2\pi)$. The agents are initially randomly positioned in a squared field of size 10^2 . We consider agents moving in an infinitely large two-dimensional space. Consequently, they will not encounter any boundaries. The initial direction is uniformly random in $[0, 2\pi)$.

The communication rate function ψ is given by $\psi(\|p_j - p_i\|) = \frac{1}{(1 + \|p_j - p_i\|^2)^\beta}$. Note that in previous publications in the finite-time control of Cucker-Smale models such as [145], a constant communication rate function of $\psi = 1$ is often used. The symmetric bounded cohesive and repulsive force function (3.13) proposed in Section 3.3.3 is used. The distances d_1 and d_0 for the repulsive force are set at 5 and 0.5, respectively. The distance for cohesive force is set to $d_2 = 9$. The parameters of the force functions, M and k , are fixed at 1. The sampling interval is 0.1.

The system is considered to be in a flocking state when $v_a \geq 0.99$. The flock diameter is measured when this condition occurs. Each simulation scenario is repeated 20 times

with different random initial values. The results presented are the average values.

4.3.1 Flocking Time and Flock Diameter

First, we shall verify that the upper bound on the alignment time derived in Theorem 4.7 is correct using simulation. Apart from the parameters specified above, the remaining ones used in this part of the simulation are: $\theta = 1/2$, $\alpha = 1/2$, and $\psi^* = 1$.

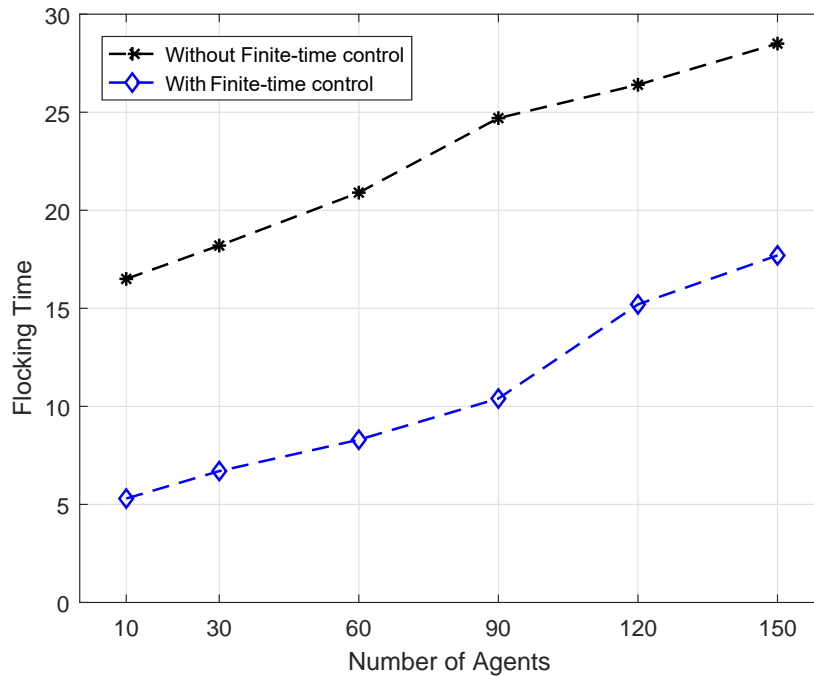


Figure 4.1: Flocking Time With and Without Finite-time Control for the Augmented Cucker-Smale System

Figure 4.1 compares the flocking times for the augmented Cucker-Smale model with and without finite-time control. It shows that finite-time control is able to significantly reduce the flocking time. Without using finite-time control, the flocking time increases substantially as N increases. For instance, with $N = 150$, the flocking time is approximately 28 without finite-time control. This is compared with around 16.5 for $N = 10$. The same trend applies when using finite-time control. For $N = 150$, the flocking time is around 17.5 with finite-time control while it is just over 5 for $N = 10$.

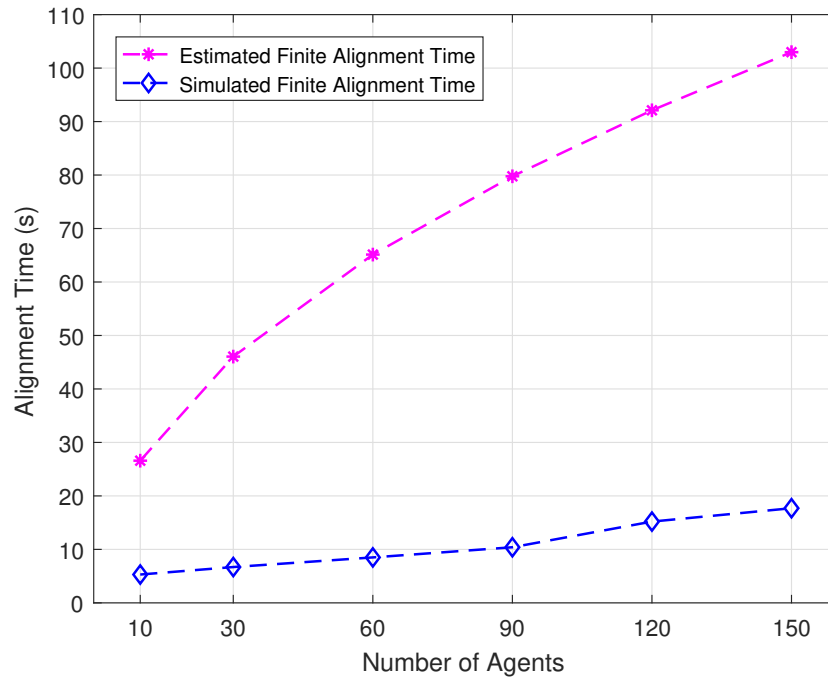


Figure 4.2: Upper Bound on Flocking Time vs Simulated Time for the Finite-time Controlled Augmented Cucker-Smale System

Although the finite-time control has a significant effect in reducing flocking time, the difference is much larger for smaller groups of agents.

Figure 4.2 shows the flocking time according to (4.24) versus the simulated results. This graph indicates that the actual flocking time is definitely below the upper bound. However, this upper bound is obviously not tight.

Table 4.1 shows the flock diameters after the agent velocities are aligned when the $M = 1$. The final flock diameters are larger than their initial values. This indicates that finite-time control has no effects on the flock diameter even though the augmented Cucker-Smale system has cohesive force in place. A possible explanation is that with finite-time control, the agents are able to their velocities very quickly. Thus they do not have as much time to get closer to each other before velocity alignment occurs. These results also show that no collision has occurred.

Most importantly, these results confirm that Theorems 4.6 and 4.9 are correct.

Table 4.1: Agents Flock Diameter when Finite-time Control Applied

Flock Diameter	N = 10	N = 30	N = 60	N = 90	N = 120	N = 150
Initial Diameter	8.4860	11.5569	11.9851	12.2654	12.7526	12.8742
Final Diameter	10.6749	12.2958	12.7181	14.5671	16.4856	18.3058
Minimum Distance	1.0783	0.7192	0.5838	0.6927	0.6510	0.5057

4.3.2 Effects of Control Parameters

Next, the effects of the control parameters θ , α , and M on the flocking time is considered. First, let $\theta = \alpha$. Figure 4.3(a) shows the change in flocking time for three different values of θ and α .

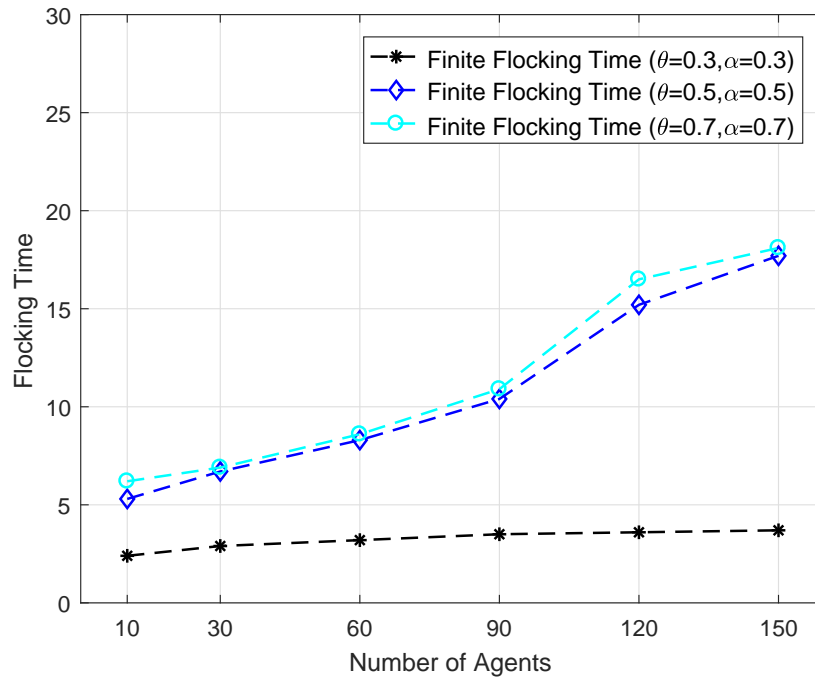
The shortest flocking time is obtained when $\theta = \alpha = 0.3$, the smallest of the three values considered. What is more important, the increase in flocking time is minimal between a flock size $N = 10$ to $N = 150$. To be more specific, with 10 agents take 2.4 to flock when the parameters are at 0.3. While with 150 agents take 3.7 to flock when the parameters are at 0.3. However, when the parameters are 0.7, then 10 agents and 150 agents take 6.2 and 18.1 to flock, respectively. Using larger values of these parameters has a more pronounced effect on the flocking times of larger flocks.

Table 4.2: Flocking Times with Different Values of the Parameters

Flock Diameter	N = 10	N = 30	N = 60	N = 90	N = 120	N = 150
$\beta = \alpha = 0.3$	2.4	2.9	3.2	3.5	3.6	3.7
$\beta = \alpha = 0.5$	5.3	6.7	8.3	10.4	15.2	17.7
$\beta = \alpha = 0.7$	6.2	6.9	8.6	10.9	16.5	18.1

In the second sets of simulation, the value of θ kept constant at 0.5, but with α increasing from 0.3 to 0.7. However, in comparison to the Figure 4.3(a), the group of agents flock in shorter time when $\theta = 0.5$ and $\alpha = 0.3$ in Figure 4.3(b), which implies α has a crucial role for finite flocking time.

Finally, we consider the effects of strength of the cohesive and repulsive function. With $\theta = \alpha = 0.5$, the value $M = 1, 2, 3$ is varied. The alignment time results are shown



(a) Flocking Time with Different Values of the Parameters

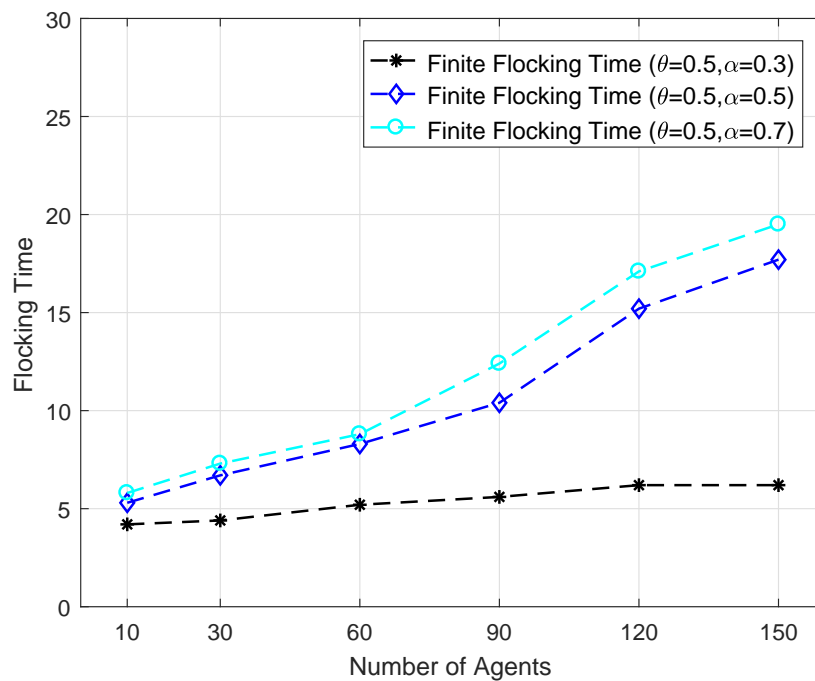
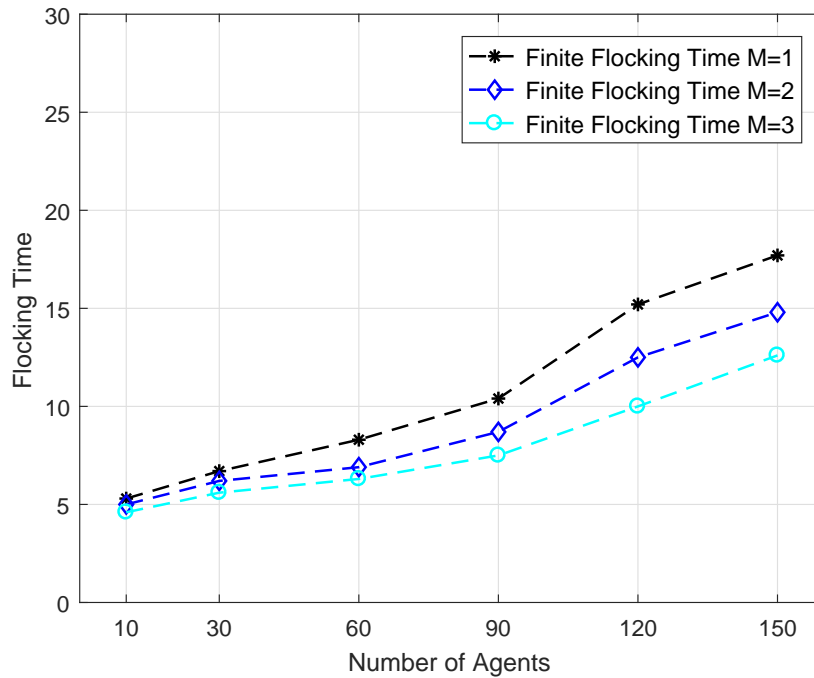
(b) Flocking Time with Different $\theta = 0.5$

Figure 4.3: Finite Flocking time with Different Parameters

Table 4.3: Flocking Times with Different $\theta = 0.5$

Flock Diameter		N = 10	N = 30	N = 60	N = 90	N = 120	N = 150
$\beta = 0.5$	$\alpha = 0.3$	4.2	4.4	5.2	5.6	6.2	6.2
$\beta = 0.5$	$\alpha = 0.5$	5.3	6.7	8.3	10.4	15.2	17.7
$\beta = 0.5$	$\alpha = 0.7$	5.8	7.3	8.8	12.4	17.1	19.5

in Figure 4.4. We expect M to have relatively small effect on the flocking time and this is confirmed by the results. Overall, the simulation results proved that the flocking force using finite time control makes a big portion of contribution to the flocking time.

Figure 4.4: Finite Flocking time in Different M

4.4 Summary

In this chapter, finite time control is applied to the augmented Cucker-Smale model developed in Chapter 3. It has been proved mathematically that this controlled model is able to converge both asymptotically and in finite-time. An upper bound on the finite

flocking time is also obtained. Furthermore, we also proved that after the velocities are aligned, the flock diameter will also be finite. In other words, the flocking state can be reached in finite-time. These mathematical results are verified by computer simulations. Simulation results also showed that shorter alignment times can be achieved when smaller values of the finite-time control parameters are used.

Part of the research presented in this chapter has been published in [137].

Chapter 5

Asynchronous Update Dynamics

Most of the researches on flocking and consensus have been assumed that the agents either update their states continuously for continuous-time models or at the same time instants for discrete-time models. If a flocking model is to be implemented on real physical agents, it is most likely that a discrete-time version of the model is used. This means that each agent computes updates to its velocity at uniformly spaced time instants. However, the clocks of the agents are typically not synchronized. Therefore, the velocity update are not computed at the same time for all agents.

The convergence of asynchronous consensus was first reported in [154] and then in [155]. De Castro *et al.* [156] studied the asynchronous consensus problem for discrete-time multi-agent systems with a fixed communication topology. In 2005, Fang *et al.* [157] studied the consensus of asynchronous discrete-time multi-agent systems, with various communication patterns. Asynchronous consensus control for a continuous-time multi-agent system with switching topology is investigated in [38]. The continuous-time system was transformed into its equivalent discrete-time system, and a distributed consensus algorithm was proposed to address problems such as time-varying communication delays. In [158], an asynchronous Vicsek model has been studied where each agent independently updates its heading at times determined by its own clock but

these times are not evenly spaced.

In the above-mentioned works, it is typically assumed that asynchronicity arises due to randomly varying communication delays. Therefore, the update time instants for each agent are irregularly spaced. If the update time is governed by an agent's own clock, then apart from a very small amount of clock jitter, the update instants are evenly spaced in time. In this chapter, the effect of this type of asynchronous update on the Cucker-Smale model is investigated through computer simulation.

5.1 Methodology

In previous simulations, the velocity of agent i is updated at uniformly spaced discrete times $t = t_1, t_2, \dots, t_k, t_{k+1}, \dots$. For example, with the original Cucker-Smale model, the change in velocity at time step t_{k+1} will be computed by

$$\Delta v_i(t_{k+1}) = \frac{1}{N} \sum_{j=1}^N a_{ij}(t_k) (v_j(t_k) - v_i(t_k)), \quad (5.1)$$

where $a_{ij}(t_k) = \psi(\|p_j(t_k) - p_i(t_k)\|)$. The velocity state for all agents, i.e. $i \in 1, 2, \dots, N$, are computed at the same time instant. This basically assumes that the internal clocks of all the agents are perfectly synchronized. In order to study the effects of asynchronous update, a method to simulate various degrees of asynchronicity is needed.

Asynchronous update in dynamical systems has been studied in the context of artificial neural networks [159, 160]. Four types of update patterns have been identified. They are known as overlapping, sequential, parallel and block-sequential updates [161]. Overlapping update refers to the case where the units update in a random order. Moreover, it is possible that some units are not updated at all. If the agents update their states one after another in a pre-determined order, then we have sequential update. A variation of

this is block-sequential update. This is when the units are partitioned into a number of sets. The units in each set are updated at the same time whereas and the sets are updated sequentially. So if the number of sets is reduced to one, then this set consists of all the units, and we have parallel update which is equivalent to synchronous update.

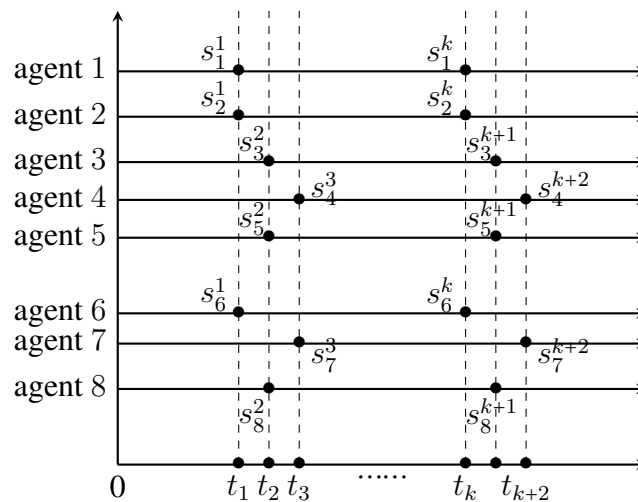


Figure 5.1: Block-sequential Updates in an Asynchronous Dynamic System

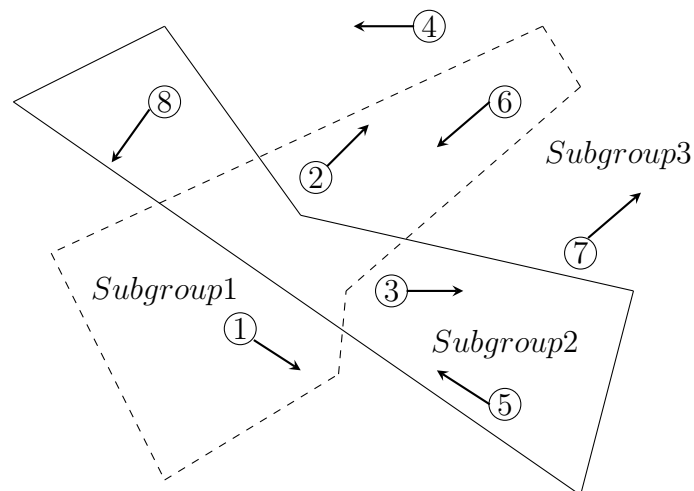


Figure 5.2: Subgroups in Asynchronous Dynamic System

In this study, the block-sequential update methodology will be adopted as it allows us to vary the extent of asynchronicity of the agents. Figure 5.1 illustrates how block-sequential updates are scheduled. In this figure, s_i denotes the state of the agent i . At

$t = t_k$, agent i updates its state to s_i^k . Thus agents 1, 2 and 6 are updated at t_1 . Agent 3, 5 and 8 are updated at t_2 . Agents 4 and agent 7 are updated at t_3 . In other words, at each time instant, only a subset of the n agents have their states updated. After one cycle of updates, the states of all n agents would have been updated. Then this cycle is repeated using the same pattern. In this example, a cycle consists of three time instants t_k, t_{k+1} and t_{k+2} . The next cycle starts from t_{k+3} .

In our simulation, agents are randomly allocated into a number of subgroups. Each of the N agents in the system randomly assigned to one of the m subgroups, with subgroup i containing $N_i > 0$ agents. Figure 5.2 shows three subgroups. Agents 1, 2, and 6 belong to subgroup 1, agents 3, 5, and 8 in subgroup 2, and agents 4 and 7 in subgroup 3. The agents in each subgroups have their states updated at the same time. Each individual agent will always has its state updated every T_p seconds. Every interval of T_p seconds is further divided into m equal time periods if there are m subgroups in the system. Those agents in subgroup i are updated at time instants $t = kT_p + \frac{iT_p}{m}$ for $k = 0, 1, 2, \dots$ and $1 < i < m$. The degree of asynchronicity is therefore determined by the number of subgroups. Thus more subgroups implies that the clocks of the agents are less synchronized.

5.2 Simulation Results

Two Cucker-Smale models will be studied. The first is the original Cucker-Smale model (2.4). The second is the augmented Cucker-Smale model with cohesive and repulsive forces (3.10). Simulations are performed using Matlab as in previous chapters. In our experiments, the agents move in an infinitely large two-dimensional space. Consequently, they will not encounter any boundary. The agents initially move in a random direction with either the same speed or different speeds. The initial heading is uniformly random in $[0, 2\pi)$. It has been shown in [26] that the flocking will be achieved

if $\beta < 1/2$. Hence, we set β to $1/4$ to ensure that flocking occurs. For convenience, distances shall be dimensionless and time is in seconds. The system is considered to be in a flocking state when the average velocity $v_a \geq 0.99$ as defined by (3.2). The initial position of the agents is randomly chosen in a square field with 10 units of length on each side. Each simulation scenario is repeated 20 times with different random initial velocities and positions for the agents. The results presented are the average values. In addition, we deploy the asynchronous update as described in the previous section for different numbers of subgroups.

5.2.1 Synchronous Updates With Different Initial Speeds

We have already obtained the synchronous update results with the original Cucker-Smale model previously in Chapter 3. In that case, all agents have the same initial speed. Now the results with different initial speeds will be established as a basis for comparisons later. An agent's speed is initialized uniformly randomly to the range of 0.5 ± 0.05 . The number of agents N varies from 10 to 150.

Figure 5.3 shows that the alignment times are slightly longer if the agents start with different speeds. This implies that it takes longer to reach consensus of both speed and heading than with heading alone. Furthermore, in both cases, the alignment time increases gradually when the number of agents increases.

5.2.2 Asynchronous Updates with Original Cucker-Smale Model

We shall study the effect of asynchronous updates on the alignment time. The block-sequential update method described above is used with the number of subgroups varying from 2 to 10. With different number of subgroups, we can vary the degree of asynchronicity.

Table 5.1 shows that the alignment time results both when the agents start with the

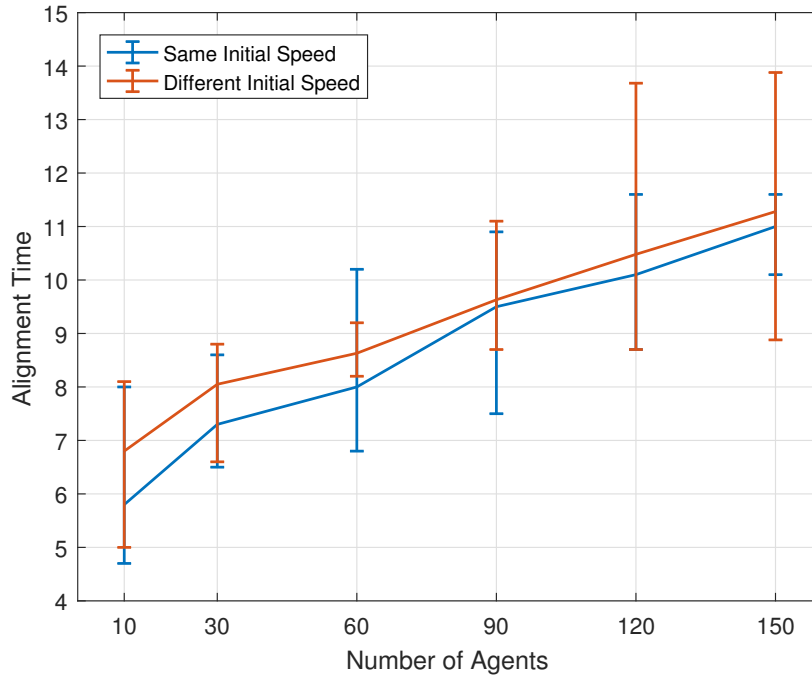


Figure 5.3: Alignment Time with Synchronous Update for the Original Cucker-Smale Model

same speed or with different speeds. For the first case, all agents move with the speed of 0.5. In the second case, the initial speeds are randomly chosen to be in the range 0.5 ± 0.05 . The alignment times with the same initial speed is also plotted in Figure 5.4. These results show that asynchronous update does impose a penalty on the alignment time. For $N = 10$, completely asynchronous update needs about 8 units of time to align when compared with synchronous update at 5.8, an increase of 38%. As expected, the alignment times with different initial speeds follows a similar trend as those with the same initial speed as N increases.

Although asynchronous updates increase the alignment time, the flock diameter has not been affected in original Cucker-Smale system. This is shown in Table 5.2 where the number of subgroups is 4. Note that collisions occur in this case since the original Cucker-Smale model is used.

Table 5.1: Alignment Time with Asynchronous Updates

Number of Subgroups	2		4		6		8		10	
	Same	Different								
$N = 10$	6.2	6.8	6.8	7.6	7.2	7.6	7.5	7.6	7.7	8.0
$N = 30$	7.8	7.1	8.3	8.3	8.4	8.4	8.6	9.0	8.7	9.4
$N = 60$	8.3	8.5	8.6	9.2	9.2	9.4	9.3	9.7	9.7	10.0
$N = 90$	9.0	9.2	9.9	9.9	10.1	9.9	10.2	10.2	10.2	10.4
$N = 120$	10.2	10.3	10.4	10.5	10.7	10.8	11.0	11.1	11.3	11.5
$N = 150$	11.2	10.8	11.3	11.3	11.5	11.5	11.5	11.7	11.7	11.8

Table 5.2: Flock Diameter with Asynchronous Updates

Number of Agents	$N = 10$	$N = 30$	$N = 60$	$N = 90$	$N = 120$	$N = 150$
<i>Initial</i>	11.2030	11.6962	11.6656	12.7101	12.3594	12.6899
<i>Final</i>	11.4961	10.9191	11.7545	13.7658	13.1735	13.6587
<i>Min</i>	0.9222	0.2798	0.1221	0.2789	0.0299	0.0896

5.2.3 Asynchronous Updates with Augmented Cucker-Smale Model

We then apply the asynchronous updates methodology to the augmented Cucker-Smale system. The symmetric function is used to avoid collision and maintain cohesion, with $d_1 = 5$ and $M = 1$. The agents move with the same initial speed.

In Figure 5.5, the flocking times when the agents are divided into four subgroups are compared with synchronous update. As expected, asynchronous update causes the system to take extra time to flock. However, it is interesting to note that as the degree of asynchronicity is decreased as N increases, the additional time it requires to flock remain

Table 5.3: Flock diameters in synchronous and asynchronous updates

Number of Agents	<i>Synchronous</i>			<i>Asynchronous</i>		
	<i>Initial</i>	<i>Final</i>	<i>Min</i>	<i>Initial</i>	<i>Final</i>	<i>Min</i>
$N = 10$	10.9532	6.7375	2.1335	11.2243	6.7690	1.6608
$N = 30$	11.3565	6.7175	0.7476	12.9275	6.9508	0.7317
$N = 60$	11.9131	6.9377	0.5844	12.4475	6.9253	0.6045
$N = 90$	12.5143	6.9351	0.6799	12.9018	6.9411	0.6231
$N = 120$	12.7092	6.8539	0.5705	13.2148	6.9501	0.5585
$N = 150$	13.1360	6.8711	0.5420	13.3653	6.9143	0.5213

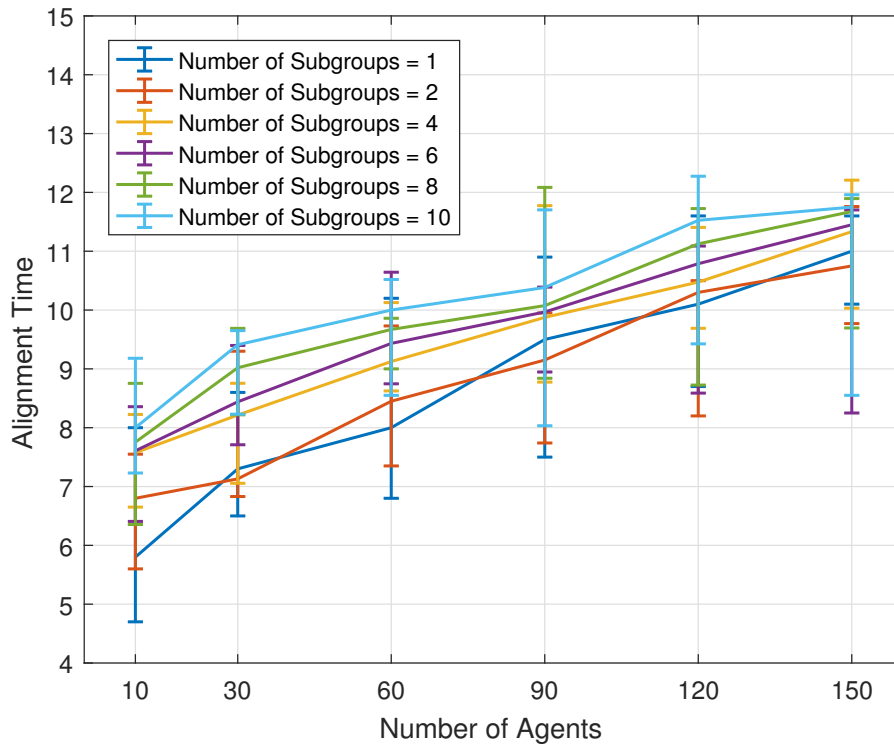


Figure 5.4: Velocity Alignment Time with Asynchronous Updating for Original Cucker-Smale Model

roughly the same, especially where $N \geq 90$. This seems to suggest that the system is relatively immune to the degree of asynchronicity when the number of agents is large.

Table 5.3 shows the flock diameters corresponding to the flocking times in Figure 5.5. There is no significant difference in the final flock diameters between two kinds of updates although they are generally larger in the asynchronous case. The final diameters are nearly half of the initial flock diameters. Also note that no collision occurred as the minimum distance between two agents are larger than 0.5.

5.3 Summary

In this chapter, we mainly studied the effects on alignment time and final flock diameter in asynchronous updates. In addition, different initial speeds have been studied to

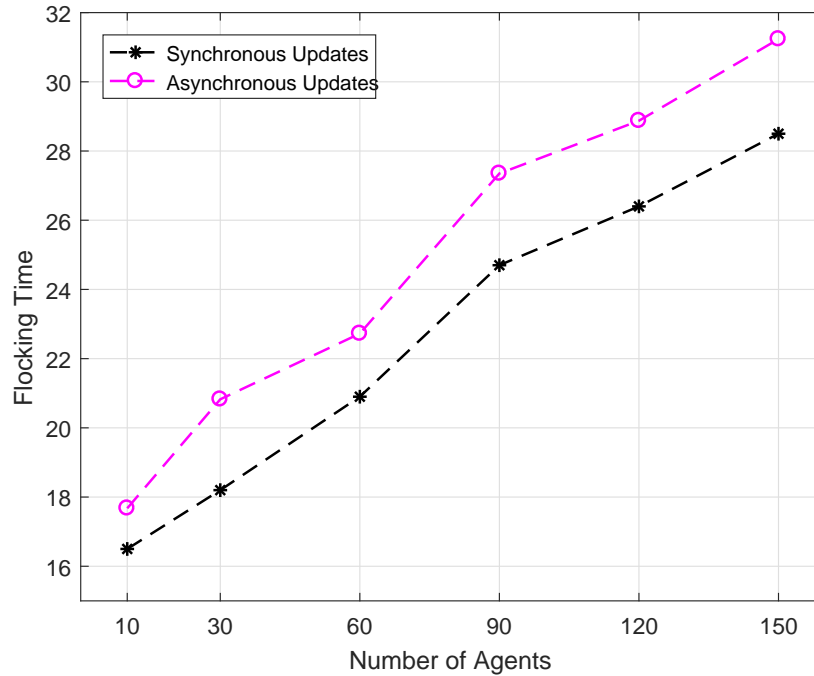


Figure 5.5: Flocking Times for Synchronous and Asynchronous Updates with Augmented Cucker-Smale Model

compare with the same initial speed in asynchronous updates. A somehow interesting result shows that there is no significant difference for alignment time with asynchronous updates, especially in a big number of group. Under asynchronous updates, the time it takes to achieve flocking is substantially increased when compared to synchronous updates. This means that in practical implementation of such systems, a longer alignment time should be taken into account. An reasonable result is that the flock diameters are slightly larger with asynchronous updates. Furthermore, the same trend is shown on the Augmented Cucker-Smale system with asynchronous updates. In summary, the different initial speed of agents and asynchronous updates increase the flocking time and flock diameter in Cucker-Smale dynamical system.

Part of the research presented in this chapter has been published in [162].

Chapter 6

Perturbations to the System

So far, variants of the original Cucker-Smale model have been studied without any form of perturbation to the ideal system. In practice, there always exist perturbations to the system, both before flocking and after flocking. In this chapter, three specific types of perturbations are investigated. The first one is noise, which is inherent in any practical system. In particular, we are interested in the effects of noise before flocking occurs. Would noise increase the alignment time or on the contrary, decrease it?

The other two types of perturbations are associated with leader-follower systems after flocking. The first is related to the question of how often we should issue change of direction commands to a leader in order that the flock maintains its cohesion. The second relates to the chorus-line effect briefly described in Section 2.3.1.2. Here, an attempt is made to model this effect as a distributed multi-agent system since this has not been done before. Such a model is proposed and its performance is evaluated.

6.1 Effects of Noise on Alignment Time

The effects of noise on the Vicsek model have been studied in [1]. The relationship between order, noise, and population density were explored. It has been found that the

self-propelled particle system exhibits a second-order phase transition from disordered to ordered motion. The system switches between ordered and disordered states an infinite number of times for any noise intensity and population density. This indicates that even small noise may break the order of the system [163].

The effects of communication noise on the leader-follower model of [44] has been reported in [164]. The noise that was considered was the noise in communicating information between the leader and its followers. Simulations show that the smaller the communication noise, the better is the performance of system in terms of achieving stable flocking. A perturbed Cucker-Smale model is studied by Ha *et al.* [165]. They considered a form of multiplicative white noise. They found sufficient conditions on the control parameters to guarantee the almost sure exponential convergence. In [83], a generalized Cucker-Smale model that incorporates multiplicative noise and reaction delay is studied. However, measurement noise and errors in estimation are most commonly modelled as additive white noise instead of multiplicative noise.

In view of the limited study of additive noise in a Cucker-Smale system, in this section, an investigation on the effects of such noise on the alignment time is presented. This additive noise models the measurement noise of the velocities of the neighbours. Thus the Cucker-Smale system equations becomes

$$\begin{cases} \dot{p}_i = v_i \\ \dot{v}_i = \frac{1}{N} \sum_{j=1}^N (\|p_j - p_i\|) (v_j - v_i) + \Delta\eta \end{cases} \quad (6.1)$$

The amount of noise $\Delta\eta$ is uniformly distributed between $[-\eta, \eta]$ where $\eta \in (0, 2\pi)$.

Simulations are performed with $\eta = \pi/6, \pi/3$, and $\pi/2$. The communicate rate function parameter β is set to $1/4$ to ensure flocking occurs. The velocities are considered to be aligned when $v_a \geq 0.99$.

Figure 6.1 shows the time to alignment for several different flock sizes. It is

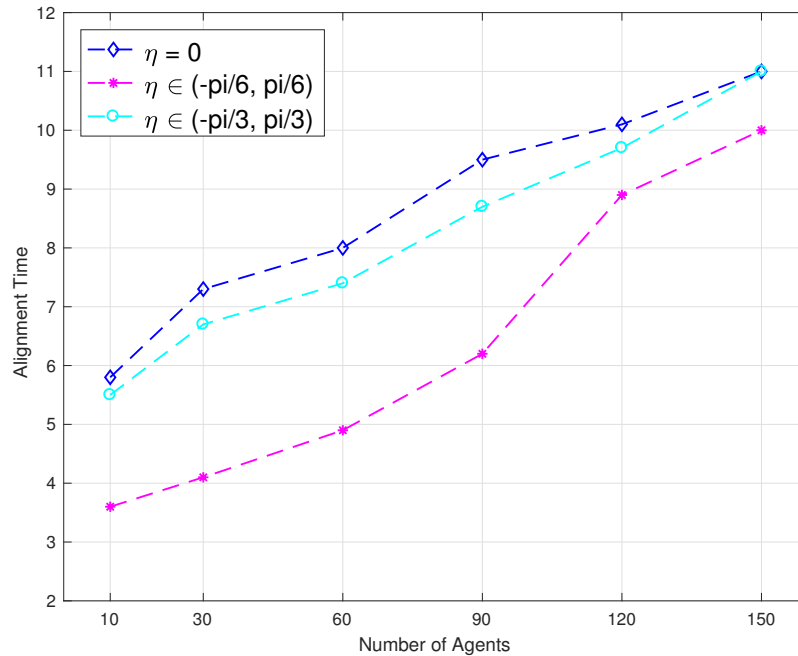


Figure 6.1: Alignment Time with Different Noise

interesting to note that in comparison with having no noise, the agents would take a shorter time to flock with added noise. The best results are obtained when a small amount of noise, i.e. $\eta = \pi/6$, is used. In this case, the alignment time is reduced significantly, especially when the group is small. With 10 agents, the alignment time is reduced by 38% compared to having no noise. Increasing the noise to $\eta = \pi/3$ causes the alignment time to be much closer to when $\eta = 0$. Further increasing the noise to $\eta = \pi/2$, the agents are no longer able to flock. Thus a small amount of noise is useful in reducing alignment time. But large amount of noise would destabilize the system.

6.2 Timing of Operator Commands

The multi-agent systems that have been considered so far are autonomous. That is, they do not involve any external control. While it is important and useful to understand the behaviours of such autonomous systems, real deployments will often involve some

interaction with human operators. Several research studies have reported that a human operator can be beneficial for navigation and to mitigate some of the shortcomings of autonomous robotic swarms [166–168]. However, research on the control of human operated dynamic swarm systems is still in the early stages [169].

Owing to the large number of robots involved, control of a robot swarm must rely on both intrinsic and extrinsic methods. Intrinsic control laws are used to govern each robot's behaviour with regard to local interaction with neighbouring robots. For instance, flocking is a collective behaviour which can be achieved using the three basic rules of separation, alignment and cohesion. The Vicsek model [1] and the Cucker-Smale model [26] define such rules and are the most popular models. Using these models of simple local interaction, a swarm of robots can achieve flocking without any external control under some general conditions. It is possible to control the time to achieve flocking and the spread of the robots by adjusting the control law and its parameters as discussed in previous chapters.

Extrinsic control is necessary to achieve more complex tasks collectively [167]. This relatively new area of study is known as human-swarm interaction (HSI). It has been studied from a number of different perspectives. The study of [170] is an early investigation of HSI. In this study, human users represent themselves in the swarm using their "avatars". This means that the humans can select a robot and take control of it. They use a computer to observe the swarm distribution and their behaviour, and can select any of the robots within the swarm as their avatar at a time. It aims to show that HSI interface is fairly easy to learn and that user-guided swarms are more efficient in achieving the goals. In [171], a distributed human-swarm interaction scheme between a human operator and a swarm of robots was proposed for the aggregation to a single cluster within a given time period. The operator issues motion commands to a single randomly selected robot. Simulation results showed that 85% aggregation of the robots could be achieved while untrained participants, with a bird's-eye view, succeeded in

aggregating 90%. A graph-based description was used in [172] for human interaction with a bio-inspired robot team (HuBIRT) based on biological principles. The robots are connected with each other locally with limited communication, and additive dynamics allow for swarming and flocking behaviours. Human operators are able to influence a small subset of robots. Performance, cohesiveness, and management properties were explored using simulations. In the HSI system studied in [173], the current state of the leader-follower swarm system is displayed on a computer screen. Based on this information, the operator predicts the future state of the swarm and determines the control parameters that need to change in order to influence its behaviour.

The effects of the frequency of human interaction on a swarm was investigated in [174]. It showed that if human commands are issued too frequently to a swarm, performance will actually degrade and will cause the robots to separate from each other. Eventually, the robots in the swarm could not reach their target positions. The concept of neglect benevolence has been proposed to capture the idea that human operators should leave the swarm alone to self-organize for a period of time before issuing the next command. Several studies have been conducted over the past few years [168, 174, 175]. However, it is still not clear how frequently could an operator send commands to the swarm without adversely affecting its coherence and integrity.

The aim of this Section is to shed some light on this issue by investigating how often could the human operator issue change of direction commands to the leader of a Cucker-Smale flock such that the flocking state is maintained. The operator controls the heading of a single leader of the flock. Initially, from a flocking state, when the heading of the leader is changed, the rest of the swarm will attempt to realign with that of the leader. With the human operator issuing change of direction commands at regular time intervals, we study the effect the length of this time interval has on the coherence of the swarm.

6.2.1 Model of Human-Swarm Interaction

The control system that involves human-swarm interaction is depicted in Figure 6.2. With a human operator, the leader of the swarm does not need to have all the information necessary to achieve a goal beforehand. The operator can observe the (partial) state of the swarm and direct it as it moves through space. As such, changes in mission goals could be conveyed as and when necessary and appropriate commands be issued to the leaders of the robot swarm. It is assumed that the rest of the robots of the swarm are pre-programmed to self-organize, eliminating the need to manipulate every single individual in the swarm. This is important for large swarms, as it is not possible for the human operator to monitor and control every individual robot in the swarm.

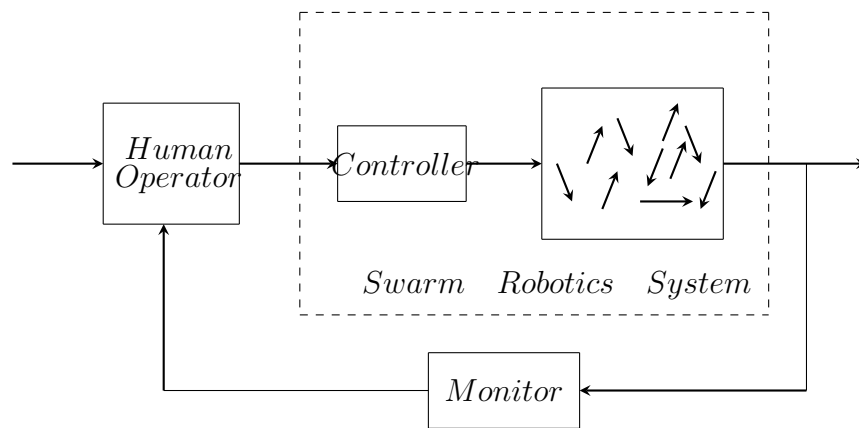


Figure 6.2: Human-Swarm Interaction Control System

The human operator sends commands to influence the rest of the swarm at certain instances in time. In [166], human operator has a device to manipulate the velocity of the robots, and a monitor displays information obtained from the robots to the operator. In other studies, the operator sets a reference describing the desired goals [176]. The system shown in Figure 6.2 is sufficiently generic to be applicable to these cases.

In this study, we assumed a single leader for the swarm. The purpose of the swarm is to maintain a flocking state, even as the leader changes direction. The robots follow the alignment rules given by the Cucker-Smale flocking model which will be described

below.

6.2.2 Operator Control

The operator can exert influence on the behaviour of a robot swarm in a number of ways [167]. They include changing parameters such as the communication rate in a Cucker-Smale model, indirect control of the swarm via environmental influences and direct control of some members of the swarm. Control can also be applied to every member of the swarm. This is known as broadcasting control. In [168], the human operator broadcasts one of three commands: stop, heading and apply-constraints, to the swarm. The robots then use a distributed consensus algorithm to flock in a common direction. In [177], partial state of the swarm is estimated through information obtained from a subset of the robots. A Bayesian classifier is then used to discern one of two behaviours – flocking in a single direction and flocking in a circle. A single parameter is adjusted to achieve flocking instead of issuing control laws. While broadcasting is an effective way to directly alter the behaviour of every robot, problems in wireless communication such as shadowing may cause some robots not receiving the broadcasted message. One way to overcome this shortcoming is to communicate only with a small number of members of the swarm and use them to influence the rest. This effectively leads to a leader-follower structure.

6.2.3 Leader-follower Flocking

The leader-follower approach to flocking was introduced in [110]. The leader is assumed to have information pertaining to the desired direction or destination. The leader could be chosen beforehand and all the followers know who the leader is [113]. A virtual leader could also be affected [117, 118]. In this case, the followers do not explicitly observe the leader; the virtual leader only exerts influence on the flock through the

swarm dynamics. Multiple leaders can also be used to guide a swarm to achieve targets. Typically, they handle different responsibilities in the group for flocking. In [44], flocking algorithms are proposed for a group of agents tracking the path of a virtual leader in both free space and when obstacles are present.

In a leader-follower swarm system, the controller shown in Figure 6.2 would represent the leaders. A human operator can guide a virtual leader to the destination. This control method has been studied in [172]. Since the leader robot is virtual, the operator continually broadcast to the swarm members to maintain influence. In addition, the case where the human operator can only communicate with a number of leader robots has also been investigated.

In [169], the effects of the location of the leader on its influence on the flock have been studied. Three locations have been chosen - at the head, an offset from the head, or the centre node of a line graph. Experimental results show that a leader located centrality is more effective. Most studies use pre-selected leaders throughout the whole task, examples include [169, 172]. However, in [178], the use of dynamically selected leaders is first studied. In this case, a human operator randomly choose a robot in the swarm at any given time to guide the rest of the swarm. It shows that dynamically selected leaders could perform well when pre-chosen leaders fail or loose communication with the operator.

6.2.4 Neglect Benevolence

In [168], the authors discovered that if the human operators issued commands to the swarm too frequently, then the performance will degrade. But if they allowed the swarm to settle in-between new commands, then it will perform better. This concept has become known as neglect benevolence. It was formally defined in [174]. In this paper, simulation results showed that when the human operator inputs were applied

too frequently, the swarm splits and only a small number of robots reached the goal of the rendezvous. On the other hand, if human input was more infrequent, the swarm converges around the destination as an entity.

How a human operator learns to adjust the amount of time between commands in order to control a group of robots to form different shapes was investigated in [175]. It is not clear if it is possible to estimate the amount of "neglect time" based on certain parameters of a swarm. We choose to use the task of navigation through a single leader robot while maintaining flocking in a Cucker-Smale swarm to obtain some bounds to this neglect time.

6.2.5 Simulation Design and Results

The aim of these computer simulations is to study the range of time for neglect benevolence for a leader-follower Cucker-Smale system. In our experiments, the robots move in a two-dimensional plane with a constant speed. There is a single designated leader and the rest of the flock are followers. However, the followers are not aware of which robot is the leader. The human operator is able to change the heading of the leader. This will be the only interaction between the operator and the swarm. We will observe whether the rest of the swarm is able to re-flock in relation to how often the leader changes direction. Ideally, the follower robots will realign with the leader's direction with every change after a certain time, which shall be referred to as the "realignment time". We shall also measure the inter-robot distance if the swarm realigns.

6.2.5.1 Realignment Time

We shall first investigate the realignment time when the leader changes its direction. The scenario is that a group of robots is initially moving at the same speed of 0.3 and the same heading. This means that they are already flocking, and thus the average velocity

$v_a = 1$ from (3.2). The heading of the leader then changes by an angle of θ and maintain its movement in this new direction. We shall consider that the robots are realigned if the average velocity v_a reaches 0.99 [137]. The communication rate parameter for the Cucker-Smale system is $\beta = 1/4$. Each simulation scenario is repeated 20 times with different random initial values. The results presented are the average values of these 20 tries.

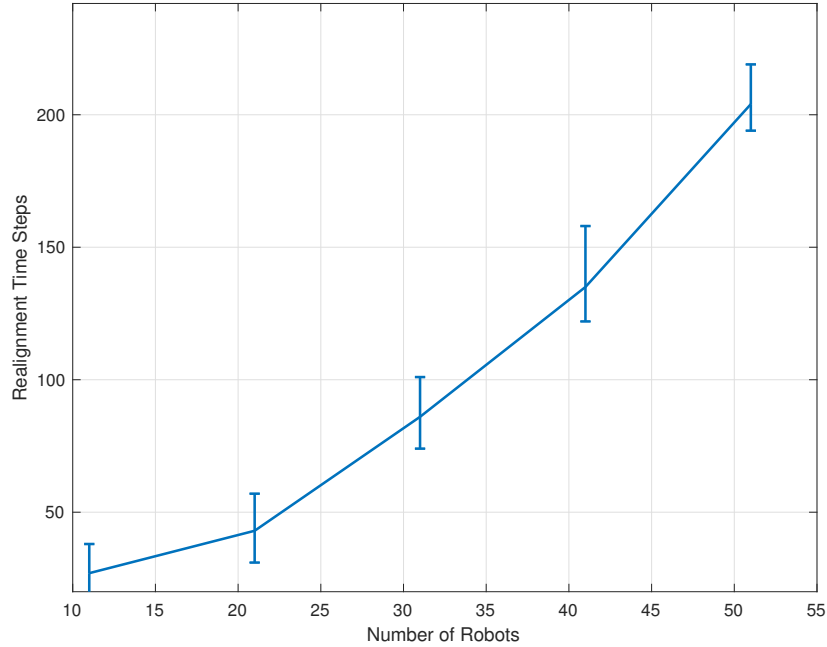


Figure 6.3: Realignment Time for Heading Change of $\pi/6$

Simulation results for $\theta = \pi/6$ is shown in Figure 6.3 for flock size N of 11, 21, 31, 41 and 51, which include 10, 20, 30, 40 and 50 follower robots respectively and a single leader robot in each case. In general, realignment time (t_r) increases linearly as the number of robots N increasing. The equation of the best fit line is given by

$$t_r = 4.46N - 39.26. \quad (6.2)$$

Table 6.1 shows the maximum inter-robot distances when at various stages of the

process. The initial stage (I) is when the robots' positions are randomly generated on the 2-D plane. Stage (II) is when the robots realigned after the leader has its heading changed by $\theta = \pi/6$. The agents initially spread out in a field with the same density $\rho = \frac{N}{s^2}$, where s is the field size, and ρ is fixed as 0.11.

Table 6.1: Maximum inter-robot distance at: initial stage (I), after realignment with leader's heading change of $\pi/6$ (II).

N	Distance (I)	Distance (II)
11	9.9120	9.9521
21	15.4267	16.7303
31	19.0403	20.4514
41	21.1121	21.2458
51	26.3142	27.9408

Table 6.1 shows that the maximum inter-robot distances slightly increases after stage (II). This is due to the fact that the original Cucker-Smale system is only an alignment model with no cohesive feature. This shows that after a few turns the flock will disperse over a larger distance if a cohesive force is not applied.

6.2.5.2 Small Robot Swarms

Next we turn our attention to the time interval between which heading change commands are issued by the human operator to the leader robot. It is reasonable to assume that the operator has to wait for some time before issuing new commands to allow the swarm to realign with the leader in the new heading. This is in accordance with the principle of neglect benevolence. What we would like to determine from these simulations is how frequent these change of heading commands could be issued without affecting the alignment of the swarm.

The simulation scenario is similar to that in Section 6.2.5.1. The difference is that multiple change of direction commands are issued at regular time intervals. In this section, we shall focus on a flock size of $N = 11$.

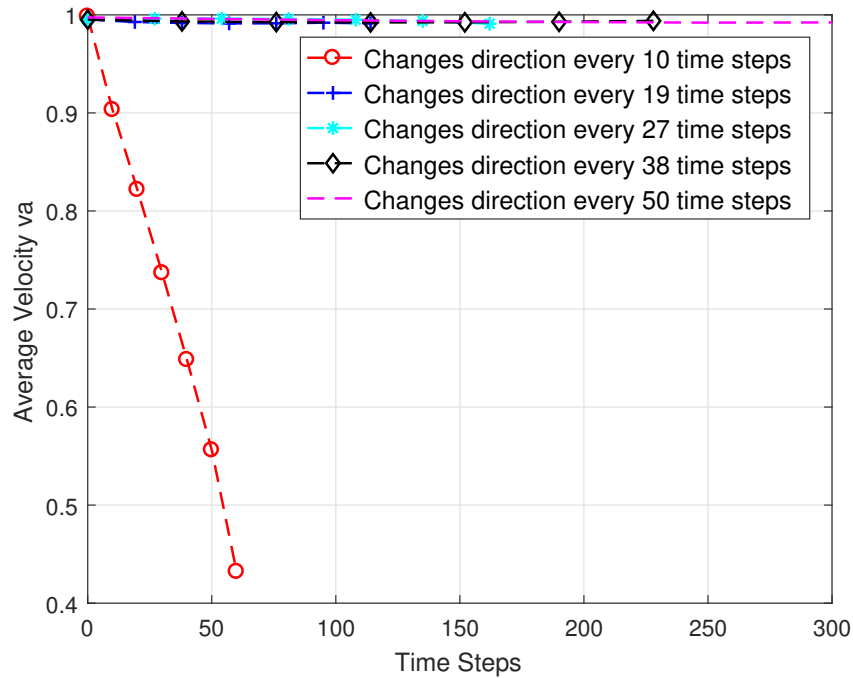
Figure 6.4 shows the average velocity (v_a) of the swarm when a new change of heading command is issued. The first change of heading command is issued at the first time step. So the first point of the curves in these graphs show the average velocity at the instant when the leader receives the second change of direction command from the operator.

From Figure 6.3, we know that the average realignment time is 27 time steps, with a minimum of 19 and a maximum of 38 time steps. We study the operator commands are issued at time intervals of 19 and 38 time steps, all the rest of robots are able to realign with the leader before the next change in heading in Figure 6.4. If the commands are issued more frequently than 19 time steps, then the group of robots is not able to realign properly as shown in Figure 6.4 (a). Moreover, the results shown that the robots realign very well when the commands of changing heading is issued in every 50 time steps because Cucker-Smale system is an alignment model. Once all robots reach the realignment state, they move more or less the same direction.

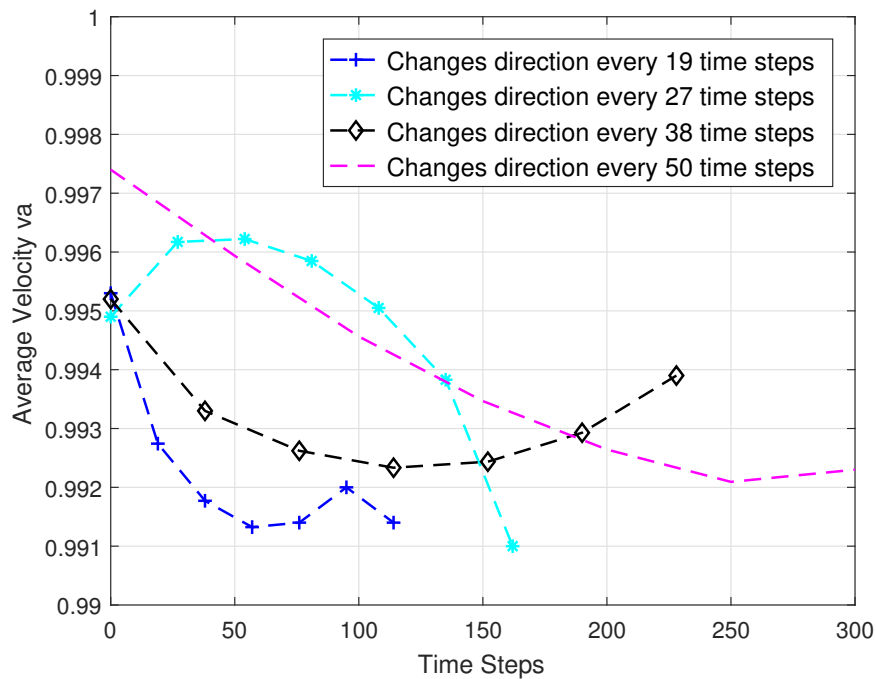
The maximum inter-robot distances at the data points in Figure 6.4 are studied as well. It is observed that this distance tends to remain the relatively more or less the same for intervals of 19, 27, 38, and 50 time steps. However, the maximum inter-robot distance reduces for intervals of 10 when the robots become less aligned after several changes of heading.

Table 6.2: Inter-robot distance at instants of change of leader's direction for six robots

<i>TimeSteps</i>	(I)	(II)	(III)	(IV)	(V)	(VI)
60	0.6774	0.5984	0.5316	0.4532	0.3343	0.2188
80	0.6696	0.4870	0.3831	0.3122	0.2084	0.1009
120	0.6477	0.4283	0.3433	0.2279	0.1397	0.0822
140	0.6843	0.4505	0.3714	0.2576	0.1867	0.1416



(a) Heading changes every 10 to 50 time steps



(b) Expanded (a): for changes every 19 to 50 time steps

Figure 6.4: Effect on the average velocity of 11 robots with periodic leader heading changes

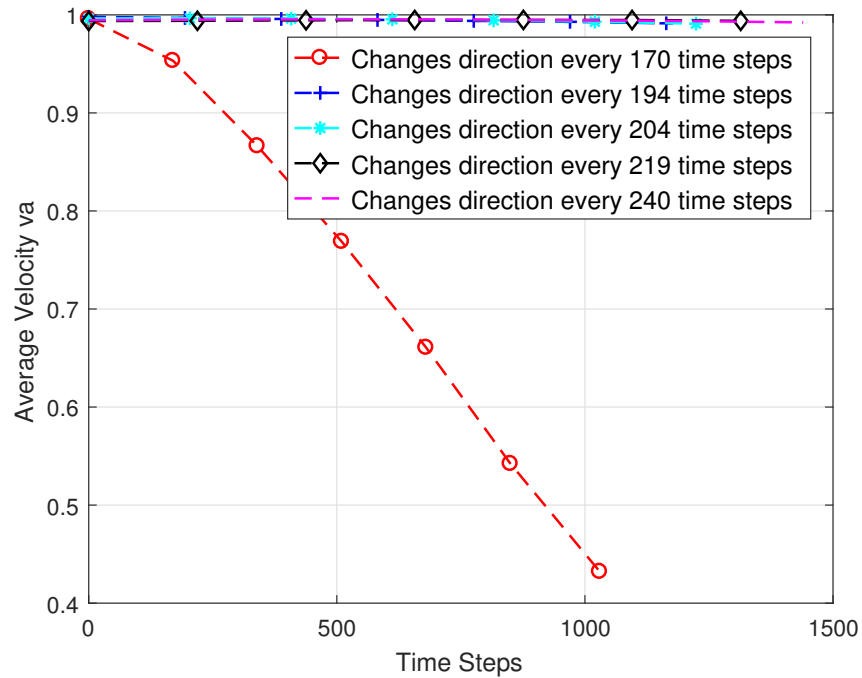
6.2.5.3 Medium Robot Swarms

The same simulations as in Section 6.2.5.2 are repeated for 50 robots with a single leader. From Figure 6.3, the realignment time of 51 robots is approximately 204 time steps within the range [194, 219]. Therefore we look at heading change intervals of 170, 194, 219 and 240 time steps. Figure 6.5 (a) shows the 51 robots status when the leader changes its direction in every different time steps. It clearly depicts that for change intervals of 170 time steps, the average velocity is not able to reach 0.99. It is also observed the inter-robot distances is finally about 16.3961 after 1030 time steps when the changes heading is issued in every 170 time steps. However, for change intervals of 194, 204, and 219 time steps, the average velocity of robotic swarm reaches alignment states with $v_a > 0.99$. Interestingly, the same happens for a change interval of 240 time steps.

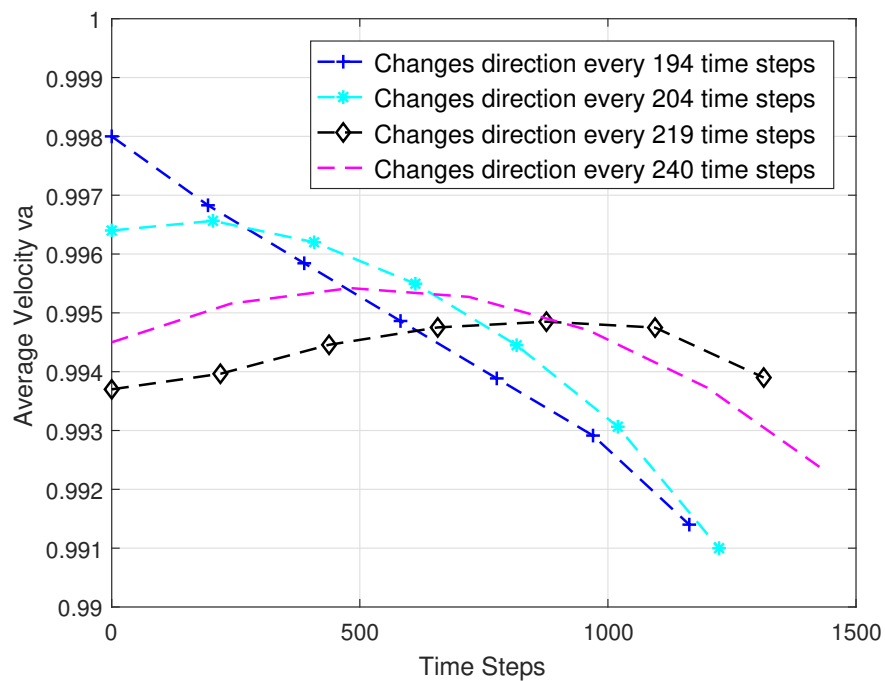
Table 6.3: Inter-robot distance at instants of change of leader's direction for 21 robots.

<i>TimeSteps</i>	(I)	(II)	(III)	(IV)	(V)	(VI)
160	0.9724	0.7162	0.5414	0.4115	0.2847	0.1704
180	0.9779	0.6377	0.5032	0.3138	0.2046	0.0837
220	0.9657	0.6241	0.4782	0.3265	0.1465	0.0594
240	0.9685	0.6378	0.4950	0.3650	0.2067	0.1040

Remark 6.1. *Even though we have only considered a single leader in this study, some useful observations can be made. The results of this study showed that a suitable amount of time should be allowed between human operator commands in order to keep the flock coherent. In general, the time interval between change of heading commands need to be longer than the minimum realignment time for the size of the swarm considered.*



(a) Heading changes every 170 to 240 time steps



(b) Expanded (a): for changes every 194 to 240 time steps

Figure 6.5: Effect on the average velocity of 51 robots with periodic leader heading changes

6.3 Chorus-Line Effect

Analysis by Potts [40] on the observations of dunlin flocks indicates that a sudden change in flight path could be initiated by only one or a few birds. When that happens, the rest of the birds will follow in a coordinated movement. This change in direction initially propagates through the flock slowly but it subsequently accelerates to a high speed. Potts' hypothesis is that the birds perceive the motion of the oncoming "manoeuvre wave" and time their own turn to match it. Thus, they behave like chorus-line dancers who anticipate the timing of an approaching leg kick. Hence he referred to it as the "chorus-line hypothesis".

The ability for flocks to react quickly to such sudden manoeuvres is important for survival. It allows them to escape by responding to the movements of a potential predator. In fact, it has been observed that the response of the group can be so fast that members can wait for their turn to react in the chorus-line and yet be able to escape from predators [126]. However, Lima and Zollner [179, 180] postulated that the coordinated chorus-line movement will only succeed if the manoeuvre wave can be reliably detected and that the absolute reaction time is short in comparison to the speed of the approaching predator. In [125], the authors found that the propagation waves in a flock originated from the position of the attacking predator and always propagate away from it.

There have been some attempts in modelling this kind of propagating manoeuvre waves in flocks. Using a computational model called StarDisplay, the authors in [41, 127] studied the underlying wave speed for starling flocks. They concluded that only short range interactions are needed to generate such an underlying wave. In [42], the propagation of density waves was derived with a pseudo-Hamiltonian based on the Vicsek model. By analysing a single dimensional model, the authors have found a line of critical damping in the parameter space. While these models are useful for studying

the propagating wave of movements, they cannot be translated into a form similar to current flocking models which are rules that each agent in the flock follows in adjusting its own velocity.

Therefore, we propose a way to incorporate the chorus-line effect into a standard Cucker-Smale model. Using this proposed model, we shall study the scenario where one of members of an aligned flock suddenly changes its direction of movement. We shall refer to this model as the Cucker-Smale model with chorus-line effect, or the “CS-CL model” for short. Through computer simulation, we analyse the time it takes for the rest of the flock to realign in this new direction. In order to put into perspective the effectiveness of using the chorus-line modification to the Cucker-Smale model, we compare it with the recently studied finite-time controlled Cucker-Smale model proposed in Chapter 4. Furthermore, we apply finite-time control to the proposed CS-CL model to see if additional gain could be obtained by combining the two techniques.

6.3.1 The CS-CL Model

Consider a group of N agents which are moving with the same velocity of \bar{v} (towards the left) as shown in Figure 6.6. The agents are numbered from 1 to N from left to right. In this state, the agents are flocking with the same velocity \bar{v} . They continue to observe the movement of their neighbours within a certain distance, where the relative velocity is monitored.

Assuming that agent 1 abruptly changes its velocity to $v_1(t)$ and maintains this new velocity. The chorus line effect dictates that agent 2 changes its velocity upon observing the change in agent 1. To be able to change the velocity to be the same as agent 1 in a time τ , an acceleration of $(v_2 - v_1)/\tau$ would be needed. τ is known as the relaxation time which is the time required for an agent to return to the realignment velocity. This is the terminology used in [181–183]. In [182, 183], a social steering force is used to

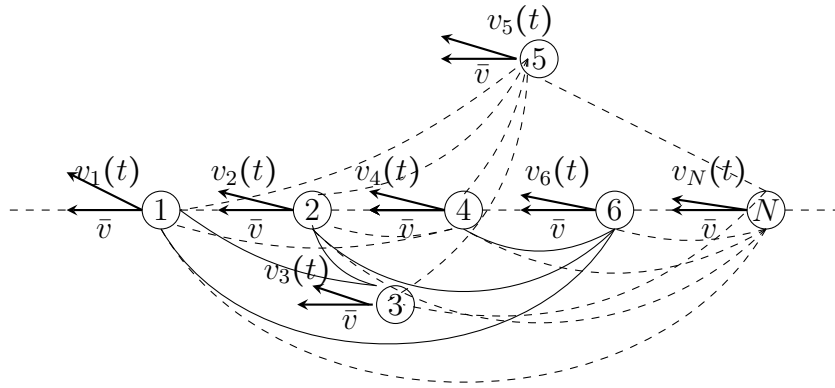


Figure 6.6: Illustration of realignment with the chorus-line effect

cause agents to slow down (e.g. to avoid collision) or to speed up (e.g. to catch up).

This steering force is given by

$$f_{speed_i} = \frac{1}{\tau} (v_0 - v_i) e_{x_i} \quad (6.3)$$

where the τ represents the relaxation time, v_0 is cruise speed and v_i is the velocity of agent i , and e_{x_i} indicates its forward direction.

The velocity of agent 3 will also change, not only because of agent 2 but also because it observed the change in agent 1, assuming it is within its monitoring distance. Thus its acceleration will be a sum of that caused by agent 1 as well as agent 2. This means that the acceleration of agent 3 will be larger than that of agent 2. Agent 4 accelerates due to the changes in velocities in agents 1, 2 and 3. Similarly, agent 5 and agent 6 work the same as agent 4.

In order to describe the relationship and movement of these agents, the agents are drawn in a line in Figure 6.6. In reality, they do not need to be in a line when they are flocking.

Given the way acceleration due to chorus-line effect is as described above, we can incorporate it into the standard Cucker-Smale model (2.4). The chorus-line effect

is an additional acceleration component that can be added to \dot{v}_i . Thus the resulting Cucker-Smale model with chorus-line effect, i.e. the CS-CL model, can be expressed as

$$\begin{cases} \dot{p}_i = v_i \\ \dot{v}_i = \frac{1}{N} \sum_{j=1}^N \psi(\|p_j - p_i\|) (v_j - v_i) \\ \quad + \sum_{j \in M_i} \frac{1}{\tau_j} (v_j - v_i) \end{cases} \quad (6.4)$$

The second term on the right-hand-side of \dot{v}_i is to accelerate agent's velocity to realignment inspired by the chorus-line hypothesis. M_i is the set of agents ahead of agent i whose movements it can observe.

The additional acceleration term can also be applied to the augmented Cucker-Smale model (3.10). This will give us

$$\begin{cases} \dot{p}_i = v_i \\ \dot{v}_i = \frac{1}{N} \sum_{j=1}^N \psi(\|p_j - p_i\|) (v_j - v_i) \\ \quad + \sum_{j \neq i} H(\|p_j - p_i\|^2) (p_j - p_i) \\ \quad + \frac{1}{N} \sum_{j \in M_i} \frac{1}{\tau_j} (v_j - v_i) \end{cases} \quad (6.5)$$

We shall refer to this as the augmented CS-CL model.

Figure 6.7 illustrates the field of view of agent i . Agents 1, 2, 3, 4 and 5 are in front of agent i . A limit d could be placed on how far agent i is able to see ahead. In addition, the angle of view $\pm\delta$ in relation to the current heading of agent i could also be defined. Given the constraints as illustrated in Figure 6.7, M_i will include agents 2, 3 and 4.

6.3.2 Performance Evaluation

We shall now consider realignment time of the original Cucker-Smale model and the CS-CL model by computer simulation.

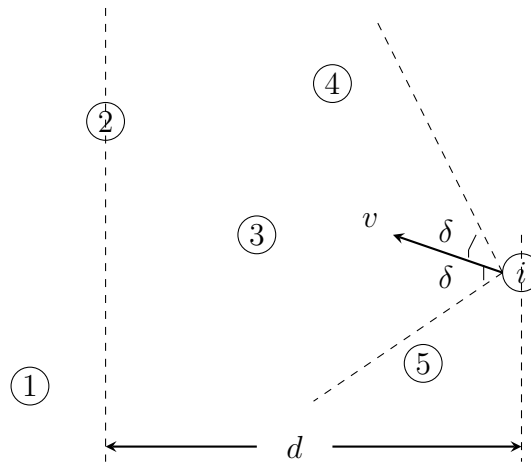


Figure 6.7: Observing range of chorus-line effect

6.3.2.1 Without Finite-time Control

A group of agent is moving in one direction in a 2-dimensional space at the same speed $|v| = 0.3$. The system is in a flocking state with average velocity $v_a \geq 0.99$. Then one agent abruptly changes its heading by an angle of θ and maintain its movement in this new direction throughout the simulation. It is possible to consider the agent who first changes its heading as the leader, and it moves at the fixed heading, with the rest of agents as followers. Any agent can potentially initiate the manoeuver and be the leader. The time it takes the rest of the flock to be realigned in this new direction is referred to as the realignment time. The relaxation time is assumed to be the same for all agents and is set to 0.05. This is reasonable as the flock is assumed to be homogeneous.

Simulation results for $\theta = \pi/6$ is shown in Figure 6.8 for flock sizes N of 5, 10, 15 and 20. This figure compares the realignment times of the original Cucker-Smale model with that of the CS-CL model. It can be observed that the realignment time for the CS-CL model is reduced by approximately 35% for $N = 5$, and by 33% with $N = 20$ compared to the original Cucker-Smale model. In general, realignment time decreases about 30% when applying the model with chorus-line effect.

Next, the effects of varying the values of θ and τ on realignment times are evaluated.

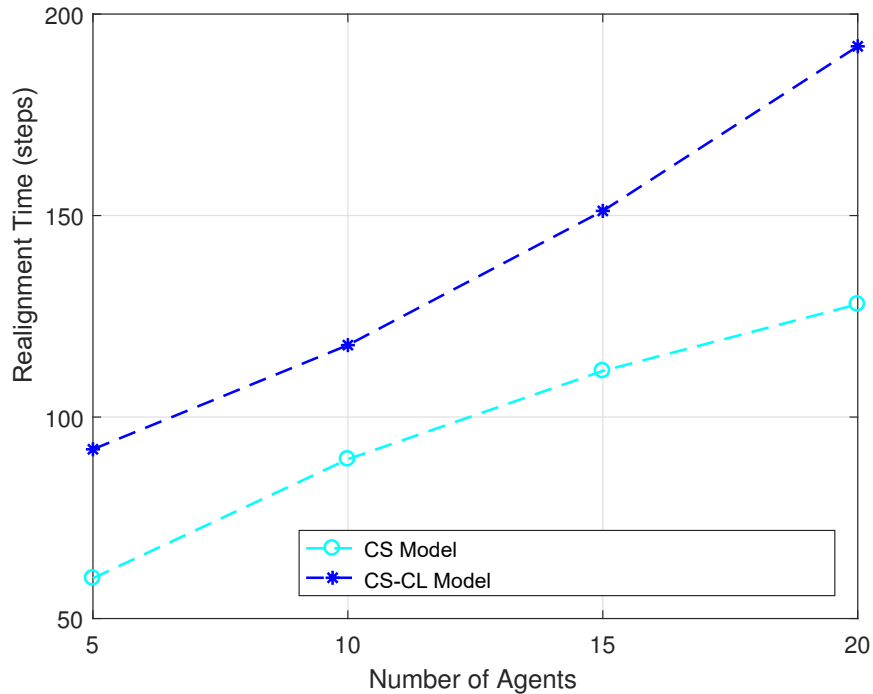


Figure 6.8: Comparison of Realignment Times for CS and CS-CL Models

Figure 6.9 shows the realignment time for $\theta = \pi/6, \pi/3$ and $\pi/2$. It can be seen that doubling the heading change from $\pi/6$ to $\pi/3$ increases the realignment time. The additional realignment time needed for a $\pi/3$ to $\pi/2$ heading change is 45 time steps for $N = 15$ and 51 time steps for $N = 20$. Thus the increase in realignment time is not linear with the amount of heading change.

The effect of the relaxation time on the realignment time is shown in Figure 6.10. These results show that with $N = 5, 10, 15$, the realignment times for $\tau = 0.05$ is roughly 80% of that for $\tau = 0.01$. But for $N = 20$, the improvement is reduced to 10%. This seems to indicate that for larger flocks, the realignment time is less dependent on the relaxation time.

In order to see how the change in velocity propagates through a flock during the realignment process for the CS-CL model, we consider a group of five agents. Agent 1 is in front of agent 2. Agent 2 is in front of agent 3, and so on. Using $\theta = \pi/3$ and a

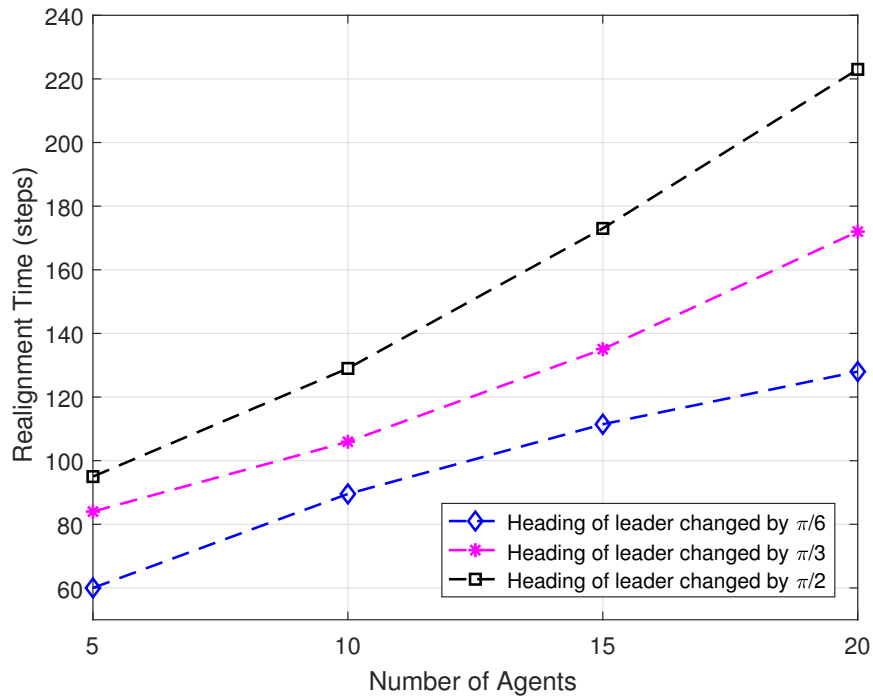


Figure 6.9: Realignment Times with Different Amount of Heading Change

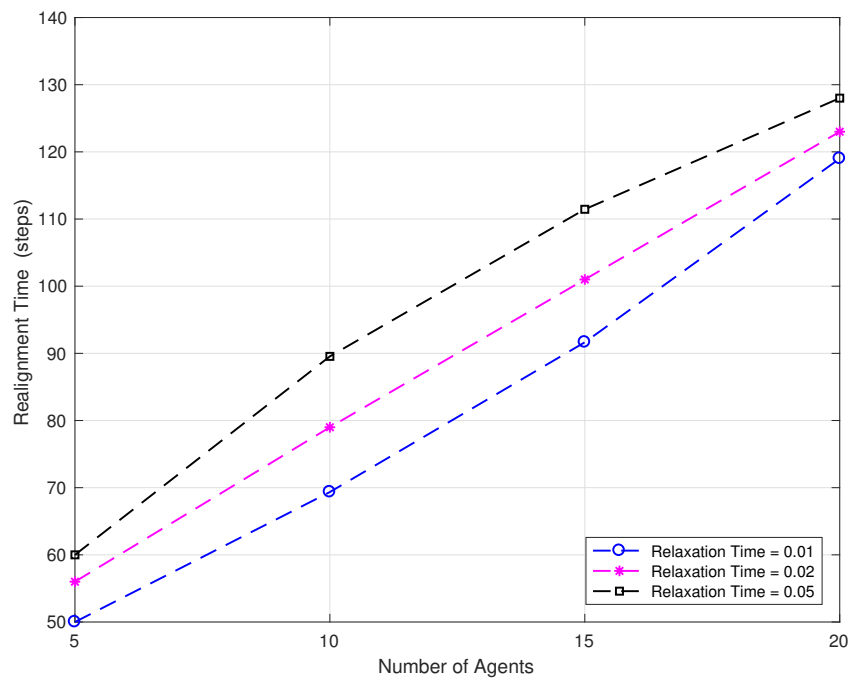


Figure 6.10: Realignment Times with Different Relaxation Times

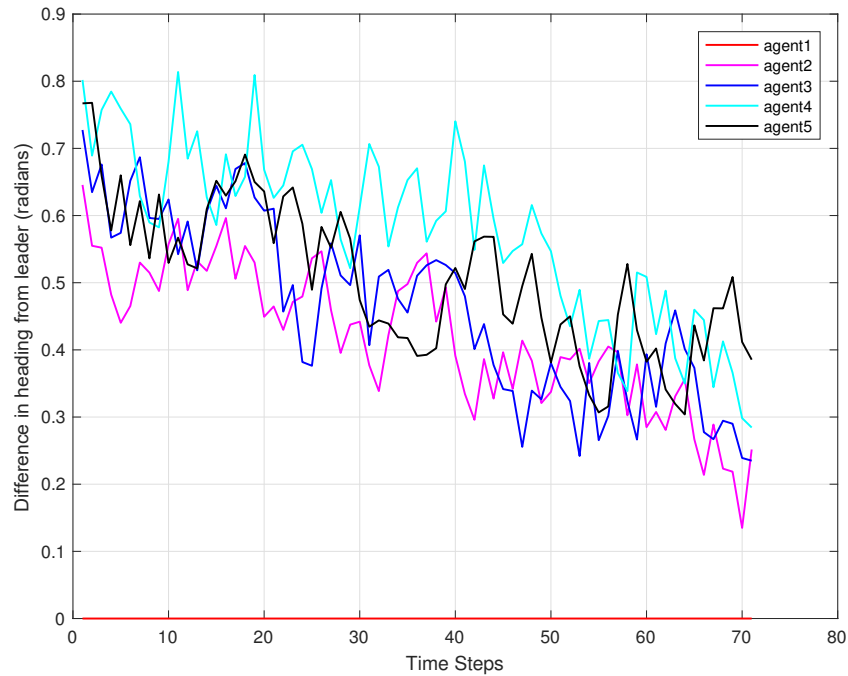


Figure 6.11: Progression of Heading Changes of Individual Agents with CS-CL Model for $N = 5$

relaxation time of 0.01, the heading of each agent relative to the new direction is shown in Figure 6.11. The red line depicts agent 1 which is the leader agent moving with a fixed heading. The change in heading is $\pi/3$ radians after flocking. Agent 2 is the agent closest to the leader, and thus its heading changes the fastest. This is followed by agent 3, 4 and 5. However, the headings of the followers fluctuates even though the trend is to be more in line with the leader. In contrast, the behavior of these agents under the original Cucker-Smale model is shown in Figure 6.12. It shows that these agents realign much more slowly. There is also no apparent propagation of this change through the agents when we observe the first 10 time steps. Furthermore, the heading of agent 2 oscillates and that of agent 3 over-aligns. These results show that the chorus-line model has its intended effect, where the heading of followers are getting closer and closer to that of the leader.

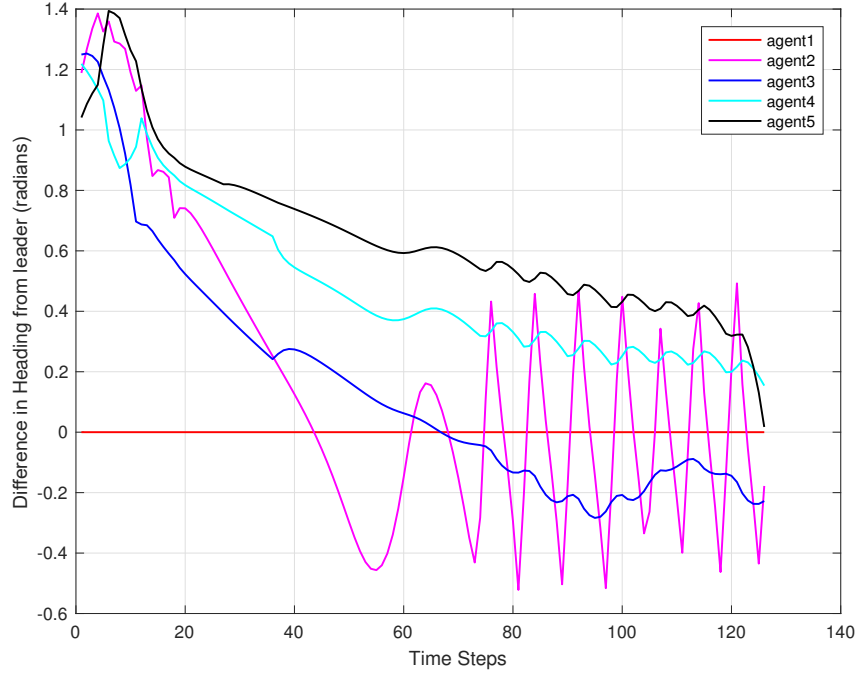


Figure 6.12: Progression of Heading Changes of Individual Agents with CS Model for $N = 5$

6.3.2.2 Applying Finite-time Control

We shall now apply finite-time control to the original Cucker-Smale and the CS-CL model. An upper bound of the realignment time for this model is similar to that given by Theorem 4.7 except for an addition term that is dependent on $(v_j - v_i)$. The parameters used in these simulations are $\theta = 1/2$, $\alpha = 1/2$, and $\psi^* = 1$. L is given by

$$\sum_{i=1}^N \frac{1}{\tau_j} \geq L \quad (6.6)$$

The agents are moving at a constant speed of 0.3 units per time step. The relaxation time is 0.01 and the heading of changing is $\pi/3$ radians. The system is considered to be in a flocking state when the average velocity $v_a \geq 0.99$, same as in previous simulations.

In Figure 6.13, the simulated results for flock sizes of 5, 10, 15 and 20 agents are shown. In order to make comparisons with the simulated results, the time is converted

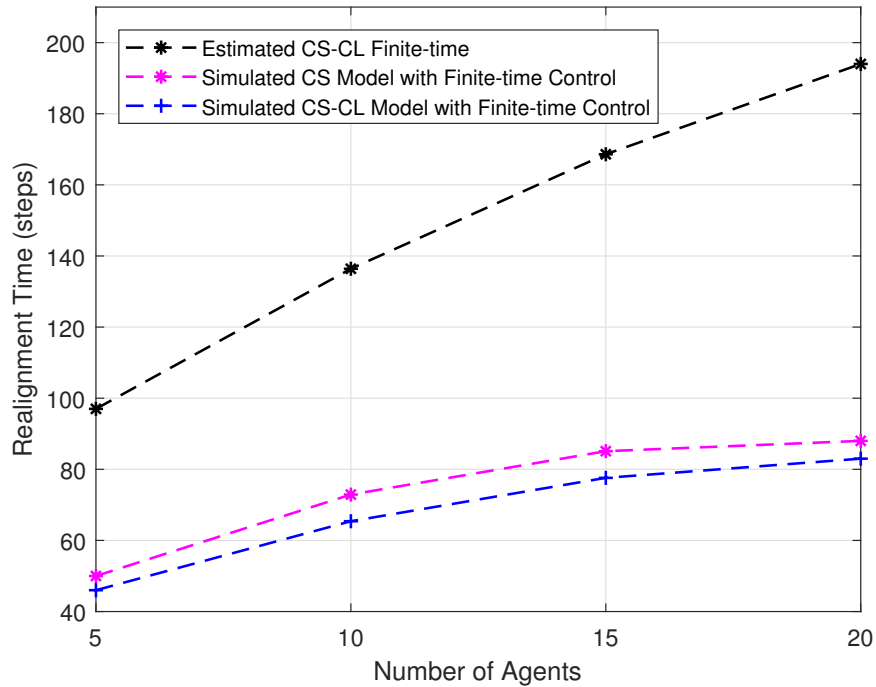


Figure 6.13: Computed and Simulated Finite Realignment Times

to the equivalent number of time steps used in the simulations. The upper bound given by Theorem 4.7 is also plotted here as reference. This figure clearly shows that the simulated realignment times for both models are within the theoretical bounds. It should be pointed out that since the agents move at a constant speed, $W(0)$ is constant for a given number of agents according to (4.7).

Figure 6.14 shows the realignment times with and without finite-time control for both Cucker-Smale and CS-CL models. These results show that while chorus-line effect term in the CS-CL model helps shorten the realignment time compared with the original CS model. Finite-time control has a larger effect for flock sizes larger than 10. It is interesting to note that CS-CL model actually works better than the finite-time controlled Cucker-Smale model for small flock sizes. However, combining finite-time control and the CS-CL model produces the best results.

The way by which the following agents adapt to a heading change by the leader is

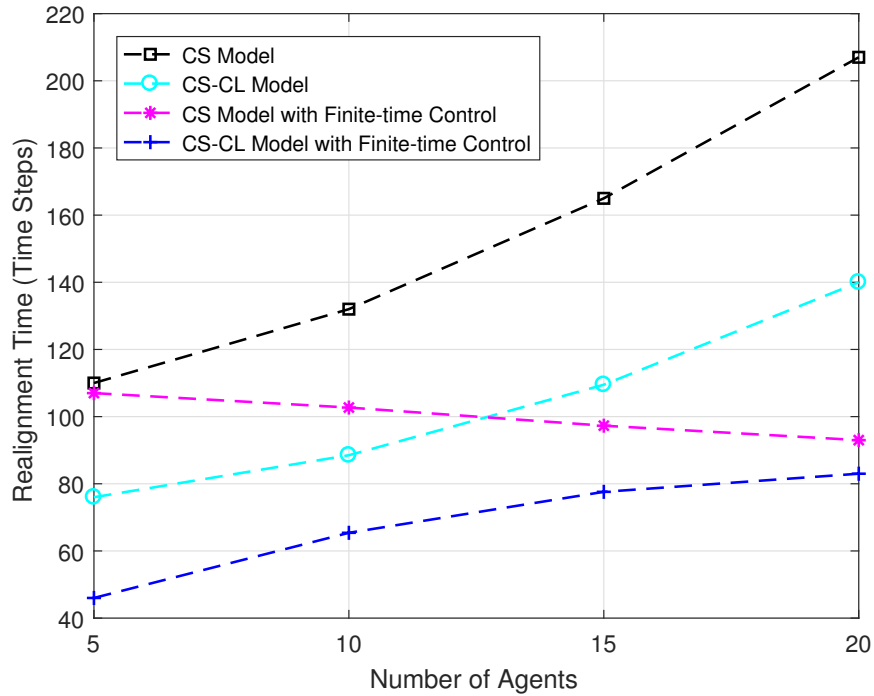
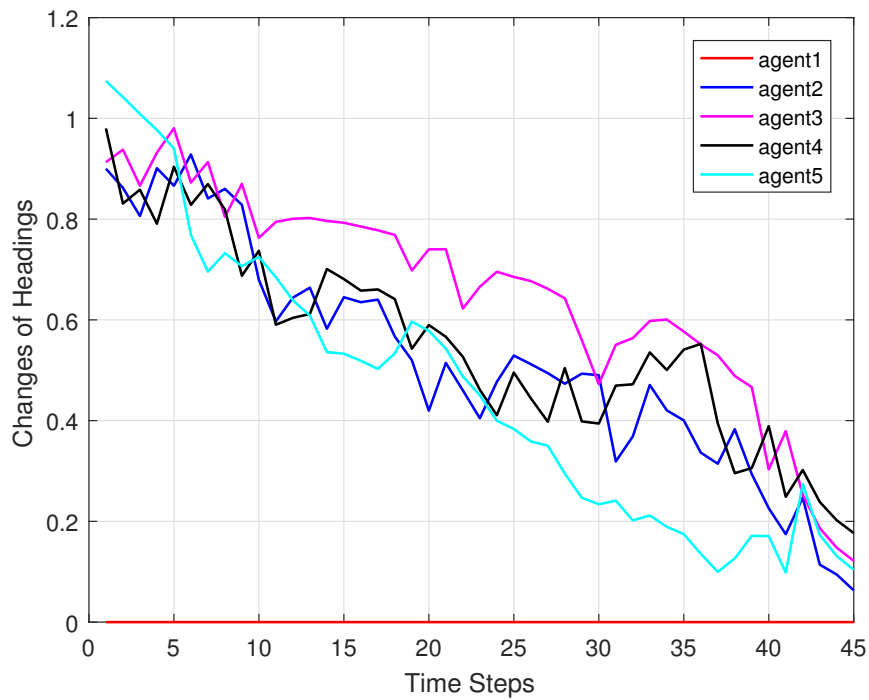


Figure 6.14: Comparisons of Simulated Realignment Times

Figure 6.15: Progression of Heading Changes of Individual Agents with Finite-time Controlled Cucker-Smale Model with $N = 5$

demonstrated in Figure 6.15 for the case of 5 agents with for a finite-time controlled Cucker-Smale model, where leader changed $\pi/3$ and other agents followed by the leader. Other finite-time control parameters remain the same as in previous simulations. When compared with Figures 6.11, the heading changes are much smoother under finite-time control. It is also obvious that the heading of the agents converges much quicker and the agents are more aligned in direction.

6.4 Summary

The effects of three different types of perturbations to Cucker-Smale model based flocking systems have been studied in this chapter. The first is intrinsic noise in the system. A small amount of noise has been shown to reduce the alignment time. However, larger amount of noise will destabilize the system and the system will not flock.

The second type of perturbation happens when commands from a human operator is relied to a single leader in the flock to change direction. Results show that the time interval between commands should be longer than the realignment time for the size of the flock.

The third kind of perturbation relates to a phenomenon known as the chorus-line effect. This effect, observed in nature, enables a flock to react quickly to a sudden change in direction of movement by a single or a few agents in the flock. A way to model this effect and incorporate it into various forms of the Cucker-Smale model has been proposed for the first time. It has been shown that the realignment time is reduced in these models.

Most of the research presented in this chapter has been published in [184–186].

Chapter 7

Conclusions

In this thesis, several issues related to the deployment of a Cucker-Smale based flocking model to real physical agents have been tackled. The research contributions of this thesis are in line with the seven research objectives that have been identified in Section 1.2. In this chapter, we conclude by presenting a summary of these research contributions. Possible directions for future works will also be discussed.

7.1 Summary of Contributions

7.1.1 Concept of Flock Diameter

A technical definition for flocking is proposed in Section 3.1. The concept of flock diameter, which is a measure of the spread of the flock, is introduced. Flocking is then defined as satisfying a constraint on the average velocity and a constraint on the flock diameter. In previous research on flocking with the Cucker-Smale model in the literature, the idea of flock diameter is mostly ignored.

7.1.2 Augmented Cucker-Smale Model

The original Cucker-Smale model has been shown to be inadequate in controlling the flock diameter since it is essentially a velocity alignment model. There is also no guarantee that collisions among agents will not occur. A new augmented Cucker-Smale model is proposed that can potentially be used to control the flock diameter and to prevent collisions. This augmented model is based on the use of cohesive and repulsive forces that have been separately proposed in existing literature to achieve these objectives. Our augmented Cucker-Smale model also has a simpler form compared with similar models in the literature.

7.1.3 Bounded Cohesive and Repulsive Forces

In order to guarantee no collision will occur, previous research has suggested the use of infinite repulsive functions. To allow the forces to be practically implementable, a bounded cohesive and repulsive force is introduced in this thesis. It is based on the logistic function and is symmetric in the sense that the cohesive function is complement to the repulsive function. Therefore there is a crossover point where these two forces cancel each other. Simulation results show that by suitably adjusting this crossover point, tight flocking formations could be achieved. Furthermore, no collisions have been found to occur.

7.1.4 Finite-time Control of the Augmented Cucker-Smale Model

In many practical applications, it is useful to know the upper bound to the flocking time starting from any initial configuration. To obtain this bound, finite-time control is applied to our augmented Cucker-Smale model. We are able to mathematically prove that this finite-time controlled model converges both asymptotically and in a finite time. An upper bound on the flocking time is obtained. Simulation confirmed that the

results are correct although this bound is not tight. It has also been discovered that the finite-time control parameters should be at the lower end of the $(0, 1)$ range in order to obtain the best flocking times.

7.1.5 Effects of Asynchronous Updates

Theoretical work on Cucker-Smale model has always assumed that state updates are computed by all agents at the same time. Previous studies that relax this assumption tend to use random delays between updates. While the internal clocks of the agents are typically not synchronized, each agent's state is updated or computed at regular time intervals according to its own clock. We used a block-sequential approach rather than random delay to model this feature. Using simulation, we discovered that velocity alignment time is longer under asynchronous update with both the original and the augmented Cucker-Smale models. Furthermore, results seem to suggest that this added time is relatively immune to the degree of asynchronicity as the size of the flock becomes larger.

7.1.6 Noise

While the effects of multiplicative noise has been studied in Cucker-Smale models, we studied the effects of additive noise which is more commonly used to model estimation errors. We confirmed the commonly held belief that a small amount of noise reduces the velocity alignment time. However, large noise could destabilize the system.

7.1.7 Neglect Benevolence

The concept of neglect benevolence, in the context of human-swarm interactions, is that if human commands are issued too frequently to a swarm, then its performance

will degrade. We study this in terms of the alignment time in a leader-follower Cucker-Smale system. We showed that the realignment time could be used as a design guide for neglect benevolence. If change-of-direction commands are issued too frequently, the cohesiveness of the flock will be destroyed.

7.1.8 Cucker-Smale Model with Chorus-line Effect

Previous research on the chorus-line effect that has been observed in bird flocks used the wave propagation approach. However, this approach could not be transformed into an agent-based model for implementation. An adaptation of the Cucker-Smale model, called the CS-CL model, to incorporate the chorus-line effect is proposed for the first time. Simulations show that realignment times could be reduced using this model.

7.2 Future Directions of Research

There are limitations in the current study. Many promising directions for future research and applications could be derived. Here, I outline several potential extensions.

Although the symmetric bounded cohesive and repulsive force function is able to avoid collision and cause the final flock diameter to be smaller than its initial value, it is still unable to control the final flock diameter by adjusting the system's parameters explicitly.

A much tighter upper bound on the flocking time of the finite-time controlled augmented Cucker-Smale model is needed. The current bound is too loose as demonstrated in our simulations. A tighter bound could also be used in the design for neglect benevolence, for example.

Noise robustness analysis of the finite-time controlled augmented Cucker-Smale model is an interesting direction for future work. An approach to handling external disturbances and system uncertainty is through terminal sliding mode control which is

a class of robustness control methods. Finite-time sliding mode control will enable us to achieve robustness with finite-time convergence for this system.

In terms of the chorus-line effect, a wave propagation analysis of the CS-CL model would be useful in determining how well the acceleration of the change in movement is incorporated into this model. This may result in a better model that can imitate this effect observed in nature.

References

- [1] T. Vicsek, A. Czirók, E. Ben-Jacob, I. Cohen, and O. Shochet, “Novel type of phase transition in a system of self-driven particles,” *Physical Review Letters*, vol. 75, no. 6, p. 1226, Aug. 1995.
- [2] E. Shaw, “Naturalist at large – fish in schools,” *Natural History*, vol. 84, no. 8, pp. 40–46, Jan. 1975.
- [3] A. Okubo, “Dynamical aspects of animal grouping: swarms, schools, flocks, and herds,” *Advances in Biophysics*, vol. 22, pp. 1–94, 1986.
- [4] I. D. Couzin, J. Krause, R. James, G. D. Ruxton, and N. R. Franks, “Collective memory and spatial sorting in animal groups,” *Journal of Theoretical Biology*, vol. 218, no. 1, pp. 1–11, 2002.
- [5] S. Strogatz, *Sync: How order emerges from chaos in the universe, nature and daily life*. Hachette Books, 2004.
- [6] M. A. Z. Raja, J. Khan, and I. Qureshi, “Swarm intelligent optimized neural networks for solving fractional differential equations,” *International Journal of Innovative Computing, Information and Control*, vol. 7, no. 2, 2011.
- [7] M. Brambilla, E. Ferrante, M. Birattari, and M. Dorigo, “Swarm robotics: a review from the swarm engineering perspective,” *Swarm Intelligence*, vol. 7, no. 1, pp. 1–41, 2013.
- [8] Y. Zhang, F. Tian, B. Song, and X. Du, “Social vehicle swarms: A novel perspective on socially aware vehicular communication architecture,” *IEEE Wireless Communications*, vol. 23, no. 4, pp. 82–89, 2016.
- [9] A. Kushleyev, D. Mellinger, C. Powers, and V. Kumar, “Towards a swarm of agile micro quadrotors,” *Autonomous Robots*, vol. 35, no. 4, pp. 287–300, 2013.
- [10] F. Ducatelle, G. A. Di Caro, C. Pinciroli, and L. M. Gambardella, “Self-organized cooperation between robotic swarms,” *Swarm Intelligence*, vol. 5, no. 2, p. 73, 2011.
- [11] T. W. Z. S. Jiajie Liu, Weiping Wang and X. Li, “A motif-based rescue mission planning method for UAV swarms using an improved PICEA,” *IEEE Access*, vol. 6, pp. 40 778–40 791, 2018.

- [12] M. Bakhshipour, M. J. Ghadi, and F. Namdari, "Swarm robotics search & rescue: A novel artificial intelligence-inspired optimization approach," *Applied Soft Computing*, vol. 57, pp. 708–726, 2017.
- [13] A. Sengupta and R. Sedaghat, "Swarm intelligence driven design space exploration of optimal k-cycle transient fault secured data path during high level synthesis based on user power-delay budget," *Microelectronics Reliability*, vol. 55, no. 6, pp. 990–1004, 2015.
- [14] C. Calderón-Arce, R. Solís-Ortega, and T. Bustillos-Lewis, "Path planning on static environments based on exploration with a swarm robotics and RRG algorithms," in *Proceedings of 38th Central America and Panama Convention (CONCAPAN XXXVIII)*. IEEE, 2018, pp. 1–6.
- [15] X. Liu, P. Chen, X. Tong, S. Liu, S. Liu, Z. Hong, L. Li, and K. Luan, "UAV-based low-altitude aerial photogrammetric application in mine areas measurement," in *Proceedings of Second International Workshop on Earth Observation and Remote Sensing Applications*. IEEE, 2012, pp. 240–242.
- [16] C. Mammides, J. Chen, U. M. Goodale, S. W. Kotagama, S. Sidhu, and E. Goodale, "Does mixed-species flocking influence how birds respond to a gradient of land-use intensity?" *Proceedings of the Royal Society B: Biological Sciences*, vol. 282, no. 1811, pp. 11–18, 2015.
- [17] P. Tokekar, J. Vander Hook, D. Mulla, and V. Isler, "Sensor planning for a symbiotic UAV and UGV system for precision agriculture," *IEEE Transactions on Robotics*, vol. 32, no. 6, pp. 1498–1511, Dec. 2016.
- [18] R. Groß, M. Bonani, F. Mondada, and M. Dorigo, "Autonomous self-assembly in swarm-bots," *IEEE Transactions on Robotics*, vol. 22, no. 6, pp. 1115–1130, 2006.
- [19] V. Trianni and M. Dorigo, "Self-organisation and communication in groups of simulated and physical robots," *Biological Cybernetics*, vol. 95, no. 3, pp. 213–231, 2006.
- [20] M. Dorigo, D. Floreano, L. M. Gambardella, F. Mondada, S. Nolfi, T. Baaboura, M. Birattari, M. Bonani, M. Brambilla, A. Brutschy, D. Burnier, A. Campo, A. L. Christensen, A. Decugniere, G. Di Caro, F. Ducatelle, E. Ferrante, A. Forster, J. M. Gonzales, J. Guzzi, V. Longchamp, S. Magnenat, N. Mathews, M. Montes de Oca, R. O'Grady, C. Pinciroli, G. Pini, P. Retornaz, J. Roberts, V. Sperati, T. Stirling, A. Stranieri, T. Stutzle, V. Trianni, E. Tuci, A. E. Turgut, and F. Vausard, "Swarmanoid: A novel concept for the study of heterogeneous robotic swarms," *IEEE Robotics and Automation Magazine*, vol. 20, no. 4, pp. 60–71, Dec. 2013.

- [21] G. Valentini, H. Hamann, and M. Dorigo, “Self-organized collective decision-making in a 100-robot swarm,” in *Proceedings of the 29th AAAI Conference on Artificial Intelligence*. AAAI Press, 2015, pp. 4216–4217. [Online]. Available: <http://www.aaai.org/ocs/index.php/AAAI/AAAI15/paper/view/9537>
- [22] E. Ferrante, A. E. Turgut, E. A. Duéñez-Guzmán, M. Dorigo, and T. Wenseleers, “Evolution of self-organized task specialization in robot swarms,” *PLoS Computational Biology*, vol. 11, no. 8, 2015.
- [23] T. Vicsek and A. Zafeiris, “Collective motion,” *Physics Reports*, vol. 517, pp. 71–140, 2012.
- [24] J. Toner and Y. Tu, “Flocks, herds, and schools: A quantitative theory of flocking,” *Physical Review E*, vol. 58, no. 4, pp. 4828–4858, Oct. 1998.
- [25] N. Shimoyama, K. Sugawara, T. Mizuguchi, Y. Hayakawa, and M. Sano, “Collective motion in a system of motile elements,” *Physical Review Letters*, vol. 76, no. 20, pp. 3870–3873, May 1996.
- [26] F. Cucker and S. Smale, “Emergent behavior in flocks,” *IEEE Transactions on Automatic Control*, vol. 52, no. 5, pp. 852–862, May 2007.
- [27] F. Cucker and J.-G. Dong, “Avoiding collisions in flocks,” *IEEE Transactions on Automatic Control*, vol. 55, no. 5, pp. 1238–1243, May 2010.
- [28] ———, “A general collision-avoiding flocking framework,” *IEEE Transactions on Automatic Control*, vol. 56, no. 5, pp. 1124–1129, May 2011.
- [29] S. M. Ahn, H. Choi, S.-Y. Ha, and H. Lee, “On collision-avoiding initial configurations to Cucker-Smale type flocking models,” *Communications in Mathematical Sciences*, vol. 10, no. 2, pp. 625–643, 2012.
- [30] J. A. Carrillo, Y.-P. Choi, P. B. Mucha, and J. Peszek, “Sharp conditions to avoid collisions in singular Cucker-Smale interactions,” *Nonlinear Analysis: Real World Applications*, vol. 37, pp. 317–328, 2017.
- [31] W. Yu, G. Chen, and M. Cao, “Some necessary and sufficient conditions for second-order consensus in multi-agent dynamical systems,” *Automatica*, vol. 46, no. 6, pp. 1089–1095, 2010.
- [32] H. Su and X. Wang, *Pinning control of complex networked systems: Synchronization, consensus and flocking of networked systems via pinning*. Springer Science & Business Media, 2013.
- [33] S. Motsch and E. Tadmor, “Heterophilious dynamics enhances consensus,” *SIAM Review*, vol. 56, no. 4, pp. 577–621, 2014.

- [34] H. Pei, S. Chen, and Q. Lai, "Multi-target consensus circle pursuit for multi-agent systems via a distributed multi-flocking method," *International Journal of Systems Science*, vol. 47, no. 16, pp. 3741–3748, 2016.
- [35] V. T. Haimo, "Finite time controllers," *SIAM Journal on Control and Optimization*, vol. 24, no. 4, pp. 760–770, 1986.
- [36] S. P. Bhat and D. S. Bernstein, "Finite-time stability of continuous autonomous systems," *SIAM Journal on Control and Optimization*, vol. 38, no. 3, pp. 751–766, 2000.
- [37] Y. Chen and J. Lü, "Consensus of a modified time-delayed Vicsek model," in *Proceedings of 3rd International Symposium on Optimization and Systems Biology*. APORC, 2009, pp. 57–64.
- [38] F. Xiao and L. Wang, "Asynchronous consensus in continuous-time multi-agent systems with switching topology and time-varying delays," *IEEE Transactions on Automatic Control*, vol. 53, no. 8, pp. 1804–1816, Sep. 2008.
- [39] Y.-P. Choi and J. Haskovec, "Cucker-Smale model with normalized communication weights and time delay," *Kinetic & Related Models*, vol. 10, no. 4, pp. 1011–1033, 2016.
- [40] W. K. Potts, "The chorus-line hypothesis of manoeuvre coordination in avian flocks," *Nature*, vol. 309, no. 5966, pp. 344–345, May 1984.
- [41] C. K. Hemelrijk, L. van Zuidam, and H. Hildenbrandt, "What underlies waves of agitation in starling flocks," *Behavioral Ecology and Sociobiology*, vol. 69, no. 5, pp. 755–764, 2015.
- [42] A. Cavagna, D. Conti, I. Giardina, and T. S. Grigera, "Propagating speed waves in flocks: a mathematical model," *Physical Review E*, vol. 98, no. 5, p. 052404, 2018.
- [43] A. Jadbabaie, J. Lin *et al.*, "Coordination of groups of mobile autonomous agents using nearest neighbour rules," *IEEE Transactions on Automatic Control*, vol. 48, no. 6, pp. 988–1001, 2003.
- [44] R. Olfati-Saber, "Flocking for multi-agent dynamic systems: algorithms and theory," *IEEE Transactions on Automatic Control*, vol. 51, no. 3, pp. 401–420, Mar. 2006.
- [45] T. Li and J.-F. Zhang, "Consensus conditions of multi-agent systems with time-varying topologies and stochastic communication noises," *IEEE Transactions on Automatic Control*, vol. 55, no. 9, pp. 2043–2057, Sep. 2010.

- [46] Y. Chen, D. W. Ho, J. Lü, and Z. Lin, “Convergence rate for discrete-time multiagent systems with time-varying delays and general coupling coefficients,” *IEEE Transactions on Neural Networks and Learning Systems*, vol. 27, no. 1, pp. 178–189, Jan. 2016.
- [47] Y. Zhao, Z. Duan, G. Wen, and Y. Zhang, “Distributed finite-time tracking control for multi-agent systems: an observer-based approach,” *Systems & Control Letters*, vol. 62, no. 1, pp. 22–28, 2013.
- [48] Z. Zuo, “Nonsingular fixed-time consensus tracking for second-order multi-agent networks,” *Automatica*, vol. 54, pp. 305–309, 2015.
- [49] S. Hauert, S. Leven, M. Varga, F. Ruini, A. Cangelosi, J.-C. Zufferey, and D. Floreano, “Reynolds flocking in reality with fixed-wing robots: communication range vs. maximum turning rate,” in *IEEE/RSJ International Conference on Intelligent Robots and Systems (IROS)*. IEEE, 2011, pp. 5015–5020.
- [50] F. Jiang and L. Wang, “Finite-time information consensus for multi-agent systems with fixed and switching topologies,” *Physica D: Nonlinear Phenomena*, vol. 238, no. 16, pp. 1550–1560, 2009.
- [51] F. Xiao, L. Wang, J. Chen, and Y. Gao, “Finite-time formation control for multi-agent systems,” *Automatica*, vol. 45, no. 11, pp. 2605–2611, 2009.
- [52] C. W. Reynolds, “Flocks, herds and schools: A distributed behavioral model,” *ACM SIGGRAPH Computer Graphics*, vol. 21, no. 4, pp. 25–34, 1987.
- [53] J. Welsby and C. Melhuish, “Autonomous minimalist following in three dimensions: A study with small-scale dirigibles,” Department of Computer Science, University of Manchester, Tech. Rep. UMCS-01-4-1, Jan. 2001.
- [54] B. Crowther and X. Riviere, “Flocking of autonomous unmanned air vehicles,” *Aeronautical Journal*, vol. 107, no. 1068, pp. 99–109, Feb. 2003.
- [55] J. B. Clark and D. R. Jacques, “Flight test results for UAVs using boid guidance algorithms,” *Procedia Computer Science*, vol. 8, pp. 232–238, 2012.
- [56] B. Beneš and C. Hartman, “Autonomous boids,” *Computer Animation and Virtual Worlds*, vol. 17, no. 3-4, pp. 199–206, 2006.
- [57] A. V. Moere, “Information flocking: Time-varying data visualization using boid behaviors,” in *Proceedings of Eighth International Conference on Information Visualisation IV*. IEEE, 2004, pp. 409–414.
- [58] C. Yates, R. Baker, R. Erban, and P. Maini, “Refining self-propelled particle models for collective behaviour,” *Canadian Applied Mathematics Quarterly*, vol. 18, no. 3, pp. 299–350, Fall 2010.

- [59] A. V. Savkin, "Coordinated collective motion of groups of autonomous mobile robots: Analysis of Vicsek's model," *IEEE Transactions on Automatic Control*, vol. 49, no. 6, pp. 981–983, Jun. 2004.
- [60] Z. Liu and L. Guo, "Connectivity and synchronization of Vicsek model," *Science in China Series F: Information Sciences*, vol. 51, no. 7, pp. 848–858, 2008.
- [61] G. Chen, Z. Liu, and L. Guo, "The smallest possible interaction radius for flock synchronization," *SIAM Journal of Control and Optimization*, vol. 50, no. 4, pp. 1950–1970, 2012.
- [62] J. Zheng, J.-G. Dong, and L. Xie, "Synchronization of the delayed Vicsek model," *IEEE Transactions on Automatic Control*, vol. 62, no. 11, pp. 5866–5872, Nov. 2017.
- [63] M. Huang, "Stochastic approximation for consensus: A new approach via ergodic backward products," *IEEE Transactions on Automatic Control*, vol. 57, no. 12, pp. 2994–3008, Dec. 2012.
- [64] L. Cheng, Z.-G. Hou, and M. Tan, "A mean square consensus protocol for linear multi-agent systems with communication noises and fixed topologies," *IEEE Transactions on Automatic Control*, vol. 59, no. 1, pp. 261–267, Jan. 2014.
- [65] G. Chen, L. Y. Wang, C. Chen, and G. Yin, "Critical connectivity and fastest convergence rates of distributed consensus with switching topologies and additive noises," *IEEE Transactions on Automatic Control*, vol. 62, no. 12, pp. 6152–6167, Dec. 2017.
- [66] S.-Y. Ha, J.-G. Liu *et al.*, "A simple proof of the Cucker-Smale flocking dynamics and mean-field limit," *Communications in Mathematical Sciences*, vol. 7, no. 2, pp. 297–325, 2009.
- [67] J.-G. Dong and L. Qiu, "Flocking of the Cucker-Smale model on general digraphs," *IEEE Transactions on Automatic Control*, vol. 62, no. 10, pp. 5234–5239, Oct. 2017.
- [68] S. Ha and E. Tadmor, "From particle to kinetic and hydrodynamic descriptions of flocking," *Kinetic and Related Models*, vol. 1, no. 3, pp. 415–435, Sep. 2008.
- [69] J. Carrillo, M. Fornesier, J. Rosado, and G. Toscani, "Asymptotic flocking dynamics for the kinetic Cucker-Smale model," *SIAM Journal on Mathematical Analysis*, vol. 42, no. 1, pp. 218–236, May 2010.
- [70] R. Bailo, M. Bongini, J. A. Carrillo, and D. Kalise, "Optimal consensus control of the Cucker-Smale model," *IFAC-PapersOnLine*, vol. 51, no. 13, pp. 1–6, 2018.

- [71] W. H. Fleming, “Generalized solutions in optimal stochastic control,” in *Differential Games and Control Theory 2*, ser. Lecture Notes on Pure and Applied Mathematics 30. Marcel Dekker, 1977, pp. 147–165.
- [72] J. J. Florentin, “Optimal control of continuous time, Markov, stochastic systems,” *International Journal of Electronics*, vol. 10, no. 6, pp. 473–488, 1961.
- [73] D. Lacker, “Limit theory for controlled McKean-Vlasov dynamics,” *SIAM Journal on Control and Optimization*, vol. 55, no. 3, pp. 1641–1672, 2017.
- [74] G. Albi, M. Bongini, E. Cristiani, and D. Kalise, “Invisible control of self-organizing agents leaving unknown environments,” *SIAM Journal on Applied Mathematics*, vol. 76, no. 4, pp. 1683–1710, 2016.
- [75] M. Bongini, M. Fornasier, F. Rossi, and F. Solombrino, “Mean-field Pontryagin maximum principle,” *Journal of Optimization Theory and Applications*, vol. 175, no. 1, pp. 1–38, 2017.
- [76] M. Fornasier, B. Piccoli, and F. Rossi, “Mean-field sparse optimal control,” *Philosophical Transactions of the Royal Society A: Mathematical, Physical and Engineering Sciences*, vol. 372, no. 2028, p. 20130400, 2014.
- [77] M. Fornasier, S. Lisini, C. Orrieri, and G. Savaré, “Mean-field optimal control as Gamma-limit of finite agent controls,” *arXiv preprint arXiv:1803.04689*, 2018.
- [78] S.-Y. Ha and X. Zhang, “Uniform-in-time transition from discrete dynamics to continuous dynamics in the Cucker-Smale flocking,” *Mathematical Models and Methods in Applied Sciences*, vol. 28, no. 09, pp. 1699–1735, 2018.
- [79] A. B. Barbaro, J. A. Canizo, J. A. Carrillo, and P. Degond, “Phase transitions in a kinetic flocking model of Cucker-Smale type,” *Multiscale Modeling & Simulation*, vol. 14, no. 3, pp. 1063–1088, 2016.
- [80] F. Cucker and E. Mordecki, “Flocking in noisy environments,” *Journal de mathématiques pures et appliquées*, vol. 89, no. 3, pp. 278–296, 2008.
- [81] P. Cattiaux, F. Delebecque, L. Pédèches *et al.*, “Stochastic Cucker-Smale models: Old and new,” *The Annals of Applied Probability*, vol. 28, no. 5, pp. 3239–3286, 2018.
- [82] J. Haskovec and I. Markou, “Delayed Cucker-Smale model with and without noise revisited,” *arXiv preprint arXiv:1810.01084*, 2018.
- [83] R. Erban, J. Haskovec, and Y. Sun, “A Cucker-Smale model with noise and delay,” *SIAM Journal on Applied Mathematics*, vol. 76, no. 4, pp. 1535–1557, 2016.
- [84] C. Pignotti and E. Trélat, “Convergence to consensus of the general finite-dimensional Cucker-Smale model with time-varying delays,” *Communication in Mathematical Sciences*, vol. 16, no. 8, pp. 2053–2076, 2018.

- [85] J. Park, H. J. Kim, and S.-Y. Ha, "Cucker-Smale flocking with inter-particle bonding forces," *IEEE Transactions on Automatic Control*, vol. 55, no. 11, pp. 2617–2623, Nov. 2010.
- [86] L. Perea, P. Elosegui, and G. Gómez, "Extension of the Cucker-Smale control law to space flight formations," *Journal of Guidance, Control, and Dynamics*, vol. 32, no. 2, pp. 527–537, 2009.
- [87] V. Gazi and K. M. Passino, "A class of attractions/repulsion functions for stable swarm aggregations," *International Journal of Control*, vol. 77, no. 18, pp. 1567–1579, 2004.
- [88] Q. Song, F. Liu, J. Cao, and J. Qiu, "Cucker-Smale flocking with bounded cohesive and repulsive forces," in *Abstract and Applied Analysis*, vol. 2013, no. 783279. Hindawi, 2013, p. 9 pages.
- [89] P. B. Mucha and J. Peszek, "The Cucker-Smale equation: Singular communication weight, measure-valued solutions and weak-atomic uniqueness," *Archive for Rational Mechanics and Analysis*, vol. 227, no. 1, pp. 273–308, 2018.
- [90] P. Minakowski, P. B. Mucha, J. Peszek, and E. Zatorska, "Singular Cucker-Smale dynamics," *arXiv preprint arXiv:1807.08617*, 2018.
- [91] H. Dong, Y. Zhao, J. Wu, and S. Gao, "A velocity-adaptive Couzin model and its performance," *Physica A: Statistical Mechanics and its Applications*, vol. 391, no. 5, pp. 2145–2153, 2012.
- [92] H. Dong, Y. Zhao, and S. Gao, "A fuzzy-rule-based couzin model," *Journal of Control Theory and Applications*, vol. 11, no. 2, pp. 311–315, 2013.
- [93] M. Zhao, H. Su, M. Wang, L. Wang, and M. Z. Chen, "A weighted adaptive-velocity self-organizing model and its high-speed performance," *Neurocomputing*, vol. 216, pp. 402–408, 2016.
- [94] R. C. Arkin, *Behavior-based robotics*. MIT press, 1998.
- [95] A. Sadowska, H. Huijberts, D. Kostic, N. van de Wouw, and H. Nijmeijer, "Formation control of unicycle robots using the virtual structure approach," in *Proceedings of 15th International Conference on Advanced Robotics (ICAR)*, 2011, pp. 365–370.
- [96] B. Sharma, J. Vanualailai, and J. Raj, "Motion planning and control of a swarm of boids in a 3-dimensional space," *International Journal of Mathematical, Computational, Physical, Electrical and Computer Engineering*, vol. 8, no. 2, pp. 247–252, 2014.

- [97] X. Luo, S. Li, and X. Guan, "Flocking algorithm with multi-target tracking for multi-agent systems," *Pattern Recognition Letters*, vol. 31, no. 9, pp. 800–805, Jul. 2010.
- [98] S. H. Semnani, O. A. Basir, and P. Van Beek, "Constrained clustering for flocking-based tracking in maneuvering target environment," *Robotics and Autonomous Systems*, vol. 83, pp. 243–250, Sep. 2016.
- [99] Y. Cao, W. Yu, W. Ren, and G. Chen, "An overview of recent progress in the study of distributed multi-agent coordination," *IEEE Transactions on Industrial Informatics*, vol. 9, no. 1, pp. 427–438, Feb. 2013.
- [100] Y. Liang and H.-H. Lee, "Decentralized formation control and obstacle avoidance for multiple robots with nonholonomic constraints," in *Proceedings of the American Control Conference*. IEEE, 2006, pp. 5596–5601.
- [101] H.-T. Zhang, Z. Cheng, G. Chen, and C. Li, "Model predictive flocking control for second-order multi-agent systems with input constraints," *IEEE Transactions on Circuits and Systems—Part I: Regular Papers*, vol. 62, no. 6, pp. 1599–1606, Jun. 2015.
- [102] A. T. Hayes and P. Dormiani-Tabatabaei, "Self-organized flocking with agent failure: Off-line optimization and demonstration with real robots," in *Proceedings of IEEE International Conference on Robotics and Automation*, vol. 4. IEEE, 2002, pp. 3900–3905.
- [103] N. Chopra, D. M. Stipanovic, and M. W. Spong, "On synchronization and collision avoidance for mechanical systems," in *2008 American Control Conference*. IEEE, 2008, pp. 3713–3718.
- [104] W. Ren, "Distributed leaderless consensus algorithms for networked Euler-Lagrange systems," *International Journal of Control*, vol. 82, no. 11, pp. 2137–2149, 2009.
- [105] M. J. Mataric, "Interaction and intelligent behavior," Artificial Intelligence Laboratory, Massachusetts Institute of Technology, Tech. Rep. AITR-1495, 1994.
- [106] I. Kelly and D. Keating, "Flocking by the fusion of sonar and active infrared sensors on physical autonomous mobile robots," in *Proceedings of The Third Int. Conf. on Mechatronics and Machine Vision in Practice*, vol. 1, 1996, pp. 1–4.
- [107] T. Nguyen, T.-T. Han, and H. M. La, "Distributed flocking control of mobile robots by bounded feedback," in *54th Annual Allerton Conference on Communication, Control, and Computing*. IEEE, 2016, pp. 563–568.
- [108] D. Xu, X. Zhang, Z. Zhu, C. Chen, and P. Yang, "Behaviour-based Formation Control of Swarm Robots," *Mathematical Problems in Engineering*, vol. 2014, 2014.

- [109] K.-H. Tan and M. A. Lewis, "Virtual structures for high-precision cooperative mobile robotic control," in *Proceedings of the 1996 IEEE/RSJ International Conference on Intelligent Robots and Systems*, vol. 1. IEEE, 1996, pp. 132–139.
- [110] P. Wang, "Navigation strategies for multiple autonomous mobile robots moving in formation," *Journal of Robotic Systems*, vol. 8, no. 2, pp. 177–195, 1991.
- [111] J. P. Desai, J. Ostrowski, and V. Kumar, "Controlling formations of multiple mobile robots," in *Proceedings of IEEE International Conference on Robotics and Automation*, vol. 4. IEEE, 1998, pp. 2864–2869.
- [112] B. Anderson, S. Dasgupta, and C. Yu, "Control of directed formations with a leader-first follower structure," in *Proceedings of IEEE Conference on Decision and Control*. IEEE, Dec. 2007, pp. 2882–2887.
- [113] L. Consolini, F. Morbidi, D. Prattichizzo, and M. Tosques, "Leader-follower formation control of nonholonomic mobile robots with input constraints," *Automatica*, vol. 44, no. 5, pp. 1343–1349, 2008.
- [114] S. Ghapani, J. Mei, W. Ren, and Y. Song, "Fully distributed flocking with a moving leader for Lagrange networks with parametric uncertainties," *Automatica*, vol. 67, pp. 67–76, 2016.
- [115] Z. Wang and D. Gu, "Distributed cohesion control for leader-follower flocking," in *IEEE International Fuzzy Systems Conference*. IEEE, Jul. 2007, pp. 1–6.
- [116] W. Yu, G. Chen, and M. Cao, "Distributed leader-follower flocking control for multi-agent dynamical systems with time-varying velocities," *Systems & Control Letters*, vol. 59, no. 9, pp. 543–552, 2010.
- [117] H. Su, X. Wang, and Z. Lin, "Flocking of multi-agents with a virtual leader," *IEEE Transactions on Automatic Control*, vol. 54, no. 2, pp. 293–307, 2009.
- [118] J. Ghommam, H. Mehrjerdi, and M. Saad, "Leader-follower based formation control of nonholonomic robots using the virtual vehicle approach," in *IEEE International Conference on Mechatronics*. IEEE, 2011, pp. 516–521.
- [119] J. Shao, G. Xie, and L. Wang, "Leader-following formation control of multiple mobile vehicles," *IET Control Theory & Applications*, vol. 1, no. 2, pp. 545–552, 2007.
- [120] S. Hou-Sheng, "Flocking in multi-agent systems with multiple virtual leaders based only on position measurements," *Communications in Theoretical Physics*, vol. 57, no. 5, p. 801, 2012.
- [121] G. L. Mariottini, F. Morbidi, D. Prattichizzo, N. V. Valk, N. Michael, G. Pappas, and K. Daniilidis, "Vision-based localization for leader-follower formation control," *IEEE Transactions on Robotics*, vol. 25, no. 6, pp. 1431–1438, Dec. 2009.

- [122] W. Wang and J.-J. Slotine, "A theoretical study of different leader roles in networks," *IEEE Transactions on Automatic Control*, vol. 51, no. 7, pp. 1156–1161, Jul. 2006.
- [123] Y. Hong, G. Chen, and L. Bushnell, "Distributed observers design for leader-following control of multi-agent networks," *Automatica*, vol. 44, no. 3, pp. 846–850, 2008.
- [124] W. Ren and R. W. Beard, *Distributed consensus in multi-vehicle cooperative control*. Springer, 2008.
- [125] A. Procaccini, A. Orlandi, A. Cavagna, I. Giardina, F. Zoratto, D. Santucci, F. Chiarotti, C. K. Hemelrijk, E. Alleva, G. Parisi *et al.*, "Propagating waves in starling, *sturnus vulgaris*, flocks under predation," *Animal behaviour*, vol. 82, no. 4, pp. 759–765, 2011.
- [126] D. M. Kitchen and C. Packer, "Complexity in vertebrate societies," in *Levels of Selection in Evolution*, L. Keller, Ed. Princeton University Press, 1999, pp. 176–196.
- [127] C. K. Hemelrijk and H. Hildenbrandt, "Scale-free correlations, influential neighbours and speed control in flocks of birds," *Journal of Statistical Physics*, vol. 158, no. 3, pp. 563–578, 2015.
- [128] Q. Lu, Q.-L. Han, X. Xie, and S. Liu, "A finite-time motion control strategy for odor source localization," *IEEE Transactions on Industrial Electronics*, vol. 61, no. 10, pp. 5419–5430, 2014.
- [129] A. Polyakov, D. Efimov, and W. Perruquetti, "Finite-time and fixed-time stabilization: Implicit lyapunov function approach," *Automatica*, vol. 51, pp. 332–340, 2015.
- [130] S. Parsegov, A. Polyakov, and P. Shcherbakov, "Nonlinear fixed-time control protocol for uniform allocation of agents on a segment," in *Proceedings of IEEE Conference on Decision and Control*. IEEE, Dec. 2012, pp. 7732–7737.
- [131] X. Yang, J. Lam, D. W. Ho, and Z. Feng, "Fixed-time synchronization of complex networks with impulsive effects via nonchattering control," *IEEE Transactions on Automatic Control*, vol. 62, no. 11, pp. 5511–5521, 2017.
- [132] A. Bryson and Y. Ho, *Applied Optimal Control*. Wiley, 1975.
- [133] I. Flugge-Lotz, *Discontinuous and Optimal Control*. McGraw-Hill, 1968.
- [134] Z. Zuo and L. Tie, "A new class of finite-time nonlinear consensus protocols for multi-agent systems," *International Journal of Control*, vol. 87, no. 2, pp. 363–370, 2014.

- [135] H. Wang, Z.-z. Han, Q.-y. Xie, and W. Zhang, "Finite-time synchronization of uncertain unified chaotic systems based on CLF," *Nonlinear Analysis: Real World Applications*, vol. 10, no. 5, pp. 2842–2849, 2009.
- [136] J. Cortés, "Finite-time convergent gradient flows with applications to network consensus," *Automatica*, vol. 42, no. 11, pp. 1993–2000, 2006.
- [137] J. Ma and E. M.-K. Lai, "Finite-time flocking control of a swarm of Cucker-Smale agents with collision avoidance," in *Proceedings of 24th International Conference on Mechatronics and Machine Vision in Practice (M2VIP)*, May 2017, pp. 1–6.
- [138] Y. Cao, W. Ren, F. Chen, and G. Zong, "Finite-time consensus of multi-agent networks with inherent nonlinear dynamics under an undirected interaction graph," in *Proceedings of the American Control Conference*. IEEE, 2011, pp. 4020–4025.
- [139] J. Fu, R. Ma, and T. Chai, "Global finite-time stabilization of a class of switched nonlinear systems with the powers of positive odd rational numbers," *Automatica*, vol. 54, pp. 360–373, 2015.
- [140] Z. Zuo and L. Tie, "Distributed robust finite-time nonlinear consensus protocols for multi-agent systems," *International Journal of System Science*, vol. 47, no. 6, pp. 1366–1375, 2016.
- [141] Z.-Y. Sun, L.-R. Xue, and K. Zhang, "A new approach to finite-time adaptive stabilization of high-order uncertain nonlinear system," *Automatica*, vol. 58, pp. 60–66, 2015.
- [142] S. Khoo, L. Xie, and Z. Man, "Robust finite-time consensus tracking algorithm for multirobot systems," *IEEE/ASME Transactions on Mechatronics*, vol. 14, no. 2, pp. 219–228, 2009.
- [143] L. Wang and F. Xiao, "Finite-time consensus problems for networks of dynamic agents," *IEEE Transactions on Automatic Control*, vol. 55, no. 4, pp. 950–955, Apr. 2010.
- [144] S. Yongzheng, L. Feng, L. Wang, and S. Hongjun, "Finite-time flocking of Cucker-Smale systems," in *Proceedings of 34th Chinese Control Conference (CCC)*. IEEE, 2015, pp. 7016–7020.
- [145] Y. Han, D. Zhao, and Y. Sun, "Finite-time flocking problem of a Cucker-Smale-type self-propelled particle model," *Complexity*, vol. 21, no. S1, pp. 354–361, 2016.
- [146] S. Parsegov, A. Polyakov, and P. Shcherbakov, "Fixed-time consensus algorithm for multi-agent systems with integrator dynamics," in *Proceedings of 4th IFAC*

- Workshop on Distributed Estimation and Control in Networked Systems*, 2013, pp. 110–115.
- [147] Z. Zuo, W. Yang, L. Tie, and D. Meng, “Fixed-time consensus for multi-agent systems under directed and switching interaction topology,” in *Proceedings of the American Control Conference*. IEEE, 2014, pp. 5133–5138.
- [148] M. Defoort, A. Polyakov, G. Demesure, M. Djemai, and K. Veluvolu, “Leader-follower fixed-time consensus for multi-agent systems with unknown non-linear inherent dynamics,” *IET Control Theory & Applications*, vol. 9, no. 14, pp. 2165–2170, 2015.
- [149] Z. Zuo, B. Tian, M. Defoort, and Z. Ding, “Fixed-time consensus tracking for multiagent systems with high-order integrator dynamics,” *IEEE Transactions on Automatic Control*, vol. 63, no. 2, pp. 563–570, 2017.
- [150] B. Ning, J. Jin, J. Zheng, and Z. Man, “Finite-time and fixed-time leader-following consensus for multi-agent systems with discontinuous inherent dynamics,” *International Journal of Control*, vol. 91, no. 6, pp. 1259–1270, 2018.
- [151] F. Cucker and S. Smale, “On the mathematics of emergence,” *Japanese Journal of Mathematics*, vol. 2, no. 1, pp. 197–227, March 2007.
- [152] J. Ma and E. M.-K. Lai, “Flock diameter control in a collision-avoiding Cucker-Smale flocking model,” in *Advances in Swarm Intelligence. ICSI 2017. Lecture Notes in Computer Science*, 2017, vol. LNCS 10385, pp. 31–39.
- [153] G. H. Hardy, J. E. Littlewood, and G. Pólya, “Inequalities cambridge university press,” *Cambridge, England*, p. 89, 1952.
- [154] V. Borkar and P. Varaiya, “Asymptotic agreement in distributed estimation,” *IEEE Transactions on Automatic Control*, vol. 27, no. 3, pp. 650–655, Jun. 1982.
- [155] J. Tsitsiklis and M. Athans, “Convergence and asymptotic agreement in distributed decision problems,” *IEEE Transactions on Automatic Control*, vol. 29, no. 1, pp. 42–50, Jan. 1984.
- [156] G. A. De Castro and F. Paganini, “Convex synthesis of controllers for consensus,” in *Proceedings of the American Control Conference*, vol. 6. IEEE, Jul. 2004, pp. 4933–4938.
- [157] L. Fang and P. J. Antsaklis, “Information consensus of asynchronous discrete-time multi-agent systems,” in *Proceedings of the American Control Conference*. IEEE, Jun. 2005, pp. 1883–1888.
- [158] M. Cao, A. S. Morse, B. D. Anderson *et al.*, “Agreeing asynchronously,” *IEEE Transactions on Automatic Control*, vol. 53, no. 8, p. 1826, Sep. 2008.

- [159] J. M. Bahi and S. Contassot-Vivier, “Stability of fully asynchronous discrete-time discrete-state dynamic networks,” *IEEE Transactions on Neural Networks*, vol. 13, no. 6, pp. 1353–1363, Nov. 2002.
- [160] A. V. Herz and C. M. Marcus, “Distributed dynamics in neural networks,” *Physical Review E*, vol. 47, no. 3, p. 2155, 1993.
- [161] E. Goles-Chacc, F. Fogelman-Soulié, and D. Pellegrin, “Decreasing energy functions as a tool for studying threshold networks,” *Discrete Applied Mathematics*, vol. 12, no. 3, pp. 261–277, 1985.
- [162] J. Ma and E. M.-K. Lai, “Cucker-Smale flocking under asynchronous update dynamics,” in *Proceedings of International Conference on Agents (ICA)*, Jul. 2017, pp. 50–54.
- [163] G. Chen *et al.*, “Small noise may diversify collective motion in Vicsek model,” *IEEE Transactions on Automatic Control*, vol. 62, no. 2, pp. 636–651, Feb. 2017.
- [164] B. Liu and H.-x. Peng, “Robot flocking with communication noise,” in *Proceedings of International Conference on Electronic Science and Automation Control*. Atlantis Press, Aug. 2015, pp. 308–311.
- [165] S. M. Ahn and S.-Y. Ha, “Stochastic flocking dynamics of the Cucker-Smale model with multiplicative white noises,” *Journal of Mathematical Physics*, vol. 51, no. 10, p. 103301, 2010.
- [166] T. Hatanaka, N. Chopra, and M. Fujita, “Passivity-based bilateral human-swarm-interactions for cooperative robotic networks and human passivity analysis,” in *Proceedings of IEEE 54th Annual Conference on Decision and Control*, Dec. 2015, pp. 1033–1039.
- [167] A. Kolling, P. Walker, N. Chakraborty, K. Sycara, and M. Lewis, “Human interaction with robot swarms,” *IEEE Transactions on Human-Machine Systems*, vol. 46, no. 1, pp. 9–26, Jan. 2016.
- [168] P. Walker, S. Nunnally, M. Lewis, A. Kolling, N. Chakraborty, and K. Sycara, “Neglect benevolence in human control of swarms in the presence of latency,” in *Proceedings of IEEE International Conference on Systems, Man, and Cybernetics*, Oct. 2012, pp. 3009–3014.
- [169] J. P. de la Croix and M. Egerstedt, “Controllability characterizations of leader-based swarm interactions,” in *Proceedings of AAAI Symposium on Human Control of Bio-inspired Swarms*, Nov. 2012, p. 6 pages.
- [170] S. Bashyal and G. Venayagamoorthy, “Human swarm interaction for radiation source search and localization,” in *IEEE Swarm Intelligence Symposium*, 2008, pp. 1–8.

- [171] G. Kapellmann-Zafra, N. Salomons, A. Kolling, and R. Groß, “Human-robot swarm interaction with limited situational awareness,” in *Proceedings of 7th International Conference on Swarm Intelligence*, Jun. 2016, pp. 125–136.
- [172] M. A. Goodrich, B. Pendleton, P. Sujit, and J. Pinto, “Toward human interaction with bio-inspired robot teams,” in *Proceedings of IEEE International Conference on Systems, Man, and Cybernetics*. IEEE, Oct. 2011, pp. 2859–2864.
- [173] P. Walker, M. Lewis, and K. Sycara, “The effect of display type on operator prediction of future swarm states,” in *Proceedings of IEEE International Conference on Systems, Man, and Cybernetics*. IEEE, Oct. 2011, pp. 2521–2526.
- [174] S. Nagavalli, L. Luo, N. Chakraborty, and K. Sycara, “Neglect benevolence in human control of robotic swarms,” in *Proceedings of IEEE International Conference on Robotics and Automation (ICRA)*, Jun. 2014, pp. 6047–6053.
- [175] S. Nagavalli, S. Y. Chien, M. Lewis, N. Chakraborty, and K. Sycara, “Bounds of neglect benevolence in input timing for human interaction with robotic swarms,” in *Proceedings of the 10th Annual ACM/IEEE International Conference on Human-Robot Interaction*, Mar. 2015, pp. 197–204.
- [176] T. Nguyen, M. Doi, T. Hatanaka, E. Garone, and M. Fujita, “A passivity-based approach for constrained mobile robotic networks,” in *Proceedings of IEEE 55th Conference on Decision and Control (CDC)*, Dec. 2016, pp. 4352–4357.
- [177] D. Brown and M. Goodrich, “Limited bandwidth recognition of collective behaviors in bio-inspired swarms,” in *Proceedings of the 2014 International Conference on Autonomous Agents and Multi-agent Systems*, May 2014, pp. 405–412.
- [178] P. Walker, S. A. Amraii, N. Chakraborty, M. Lewis, and K. Sycara, “Human control of robot swarms with dynamic leaders,” in *Proceedings of IEEE/RSJ International Conference on Intelligent Robots and Systems (IROS)*, Sep. 2014, pp. 1109–1113.
- [179] S. L. Lima, “Collective detection of predatory attack by social foragers: fraught with ambiguity?” *Animal Behaviour*, vol. 50, no. 4, pp. 1097–1108, 1995.
- [180] S. L. Lima and P. A. Zollner, “Towards a behavioral ecology of ecological landscapes,” *Trends in Ecology & Evolution*, vol. 11, no. 3, pp. 131–135, 1996.
- [181] D. Helbing and P. Molnar, “Social force model for pedestrian dynamics,” *Physical Review E*, vol. 51, no. 5, p. 4282, 1995.
- [182] H. Hildenbrandt, C. Carere, and C. K. Hemelrijk, “Self-organized aerial displays of thousands of starlings: A model,” *Behavioral Ecology*, vol. 21, no. 6, pp. 1349–1359, 2010.

-
- [183] C. K. Hemelrijk and H. Hildenbrandt, “Self-organized shape and frontal density of fish schools,” *Ethology*, vol. 114, no. 3, pp. 245–254, 2008.
- [184] J. Ma, E. M.-K. Lai, and W. Pang, “CS-CL: A flocking model that incorporates the bio-inspired chorus-line effect,” in *Proceedings of IEEE International Joint Conference on Neural Networks (IJCNN)*, Jul. 2018.
- [185] J. Ma and E. M.-K. Lai, “Incorporating chorus-line effect into a Cucker-Smale system for fast manoeuvre tracking,” in *Proceedings of 17th IEEE International Conference on Autonomous Agents and MultiAgent Systems (AAMAS)*, Jul. 2018, pp. 2007–2009.
- [186] J. Ma, E. M.-K. Lai, and J. Ren, “On the timing of operator commands for the navigation of robot swarms,” in *Proceedings of 15th IEEE International Conference on Control, Automation, Robotics and Vision (ICARCV)*, Nov. 2018, pp. 1634–1639.
- [187] H. K. Khalil and J. W. Grizzle, *Nonlinear Systems*. Prentice Hall, 2002.

Appendix A

Proof of Lemmas

The original proofs of these two lemmas can be found in [135]. They are included here for completeness.

A.1 Proof of Lemma 4.3

By the plus-minis technique, we have

$$\begin{aligned}\sum_{i=1}^N \sum_{j=1}^N y_i \phi(x_j, x_i) &= \sum_{i=1}^N \sum_{j=1}^N (y_i - y_j) \phi(x_j, x_i) \\ &+ \sum_{i=1}^N \sum_{j=1}^N y_j \phi(x_j, x_i) \\ &= - \sum_{i=1}^N \sum_{j=1}^N (y_j - y_i) \phi(x_j - x_i) \\ &- \sum_{i=1}^N \sum_{j=1}^N y_j \phi(x_i, x_j)\end{aligned}$$

Which induces

$$\sum_{i=1}^N \sum_{j=1}^N y_i \phi(x_j, x_i) = -\frac{1}{2} \sum_{i=1}^N \sum_{j=1}^N (y_j - y_i) \phi(x_j - x_i) \quad (\text{A.1})$$

A.2 Proof of Lemma 4.2

Consider the following differential equation:

$$\dot{X}(t) = -cX^\eta(t), \quad X(t_0) = V(t_0). \quad (\text{A.2})$$

Although this differential equation does not satisfy the global Lipschitz condition, the unique solution to this equation is given by

$$X^{1-\eta}(t) = X^{1-\eta}(t_0) - c(1-\eta)(t-t_0) \quad (\text{A.3})$$

and

$$x(t) \equiv 0, \quad \forall t \geq t_1.$$

It is direct to prove that $x(t)$ is differential for $t > t_0$. From the comparion lemma [187], one obtains

$$X^{1-\eta}(t) \leq X^{1-\eta}(t_0) - c(1-\eta)(t-t_0), \quad t_0 \leq t \leq t_1$$

and

$$V(t) = 0, \quad \forall t \geq t_1$$

WITH t_1 given in $t_1 = t_0 + [V(t_0)^{1-\eta}]/k(1-\eta)$.